Reliability Analysis of the Distribution Network Due to the Integration of Distributed Generations

By

Zanele Zamalunga Lunga

Student No: 21116780

A dissertation submitted in fulfilment of the requirements for the **Master of Engineering Degree** in the Department of Electrical Power Engineering, Faculty of Engineering and the Built Environment

Durban University of Technology

Supervisor: Prof Evans Eshiemogie Ojo

Co-supervisor: Dr Nelson Dhanpal Chetty

March 2025

Declaration

I hereby declare that this dissertation is my work, and each text has been correctly referenced or cited. Moreover, this work has not been previously published in part or whole for another degree at any other university.

This research was duly supervised by Prof. Evans E. Ojo and Dr Nelson Chetty at the Durban University of Technology.

Submitted by:

23-03-2025

Zanele Zamalunga Lunga — Date

Student Number: 21116780

Approved for Final Submission by:

29-03-2025

……. Supervisor: Prof. Evans E. Ojo — Date

02-04-2025

. Co-Supervisor: Dr Nelson Chetty — Date

Acknowledgments

I am deeply grateful to God Almighty for His strength and guidance in bringing me this far.

I sincerely appreciate my research supervisor, Professor Evans E. Ojo, for his invaluable encouragement, guidance, cooperation, and involvement throughout this project. His support was instrumental in making this work possible.

My heartfelt thanks to my co-supervisor, Dr. Nelson D. Chetty, for his valuable input and contributions that enriched this research.

To my colleagues, Mr. Sandile Dlamini and Ms. Luyanda Sbahle Zulu, I am deeply grateful for your encouraging feedback and unwavering support, which kept me motivated during the most challenging phases of this journey. Your belief in me helped me realise my potential.

Finally, I express my profound appreciation to the National Research Foundation (NRF) for their financial support, which made this study possible.

Dedication

This work is dedicated to:

My parents, Mr. M. S. Lunga and Mrs. K. M. Lunga, and my siblings.

I appreciate your exceptional support throughout the duration of this study.

Ngiyabonga boMthiyane!

Abstract

Reliability analysis is critical to power system design and planning, ensuring that electrical networks operate efficiently under defined conditions over a specified period. The growing integration of Distributed Generation (DG) units, driven by advancements in renewable energy technologies such as solar photovoltaic (PV) and wind energy systems, has significantly impacted power distribution networks. DG units, which are small-scale power generation sources, can be connected at distribution substations or dispersed throughout the network. Their implementation influences voltage profiles and reduces power losses, but their increasing penetration levels also affect overall system operation.

This study evaluates the reliability of a distribution network with and without DG integration. A numerical model is developed to analyse the impact of DG integration on network performance. The IEEE 30-bus system is the test network, incorporating solar PV and wind energy conversion systems as DG sources. Numeral Simulations are conducted, implemented on the MATLAB/Simulink software. The Newton-Raphson method is employed for load flow analysis, determining the network's voltage magnitudes and phase angles. Additionally, the Particle Swarm Optimization (PSO) algorithm is utilised to determine the optimal placement of DGs, aiming to minimise power losses, reduce operational costs, and improve voltage stability under various conditions. A reliability assessment is performed using Monte Carlo simulation, which calculates key reliability indices to evaluate system performance.

The results confirm that the location and capacity of DG units significantly influence network reliability. The study establishes that integrating optimally placed DGs enhances power system reliability by improving voltage stability and reducing power losses. These findings highlight the potential benefits of renewable energy-based DGs in strengthening distribution networks and ensuring a more stable and resilient power supply.

Table of Contents

Declaration ..... **Error! Bookmark not defined.**

Acknowledgments iii

Dedication iv

Abstract v

Table of Contents vi

List of Figures ix

List of Tables xi

List of Abbreviations xii

Chapter 1 1

Introduction 1

1.1 General Background 1

1.2 Problem Statement 2

1.3 Motivation 2

1.4 Aim and Objectives 3

1.5 Scope of Study 4

1.6 Dissertation Outline 4

1.7 Publication 5

Chapter 2 6

Literature Review 6

2.1 Introduction 6

2.2 Non-Renewable 7

2.3 Renewable Energy Sources 8

2.3.1 Wind Power 9

2.3.2 Solar Power 10

2.3.3 Tidal Power 16

2.3.4 Biomass 19
2.3.5 Hydropower 21
2.3.6 Geothermal Power 22
2.4 Hybrid Renewable Energy System 24
2.5. Traditional Power Systems 25
2.6 Distribution Network Configuration 27
2.8 Distributed Generation 31
2.8.1 Integration of DGs into the Distribution Network 33
2.9 Power Quality 34
2.9.1 Frequency Variations 35
2.9.2 Harmonics 35
2.9.3 Voltage Fluctuations 36
2.10 Grid Code for Renewable Energy Integration 37
2.11 Reliability of Distribution Systems Integrated with DGs 41
2.12 Conclusion 43
Chapter 3 45
Numerical Modelling 45
3.1 Power System Reliability 45
3.2 Reliability Indices 46
3.3 Reliability Evaluation Techniques 49
3.3.2 Reliability Evaluation Techniques: Simulation 51
3.4 Failure Mode and Effect Analysis (FMEA) 52
3.5 Load Flow Analysis: Newton-Rapson Technique 53
3.6 Modelling Distribution Generations 58
3.6.2 Wind Energy Conversion System (WECS) Modeling 59
3.7 Distribution Network: IEEE 30 Bus System 64
3.8 Reliability Evaluation of Distribution Networks with Distributed Generation 65

3.8.1 Particle Swarm Optimization Method 65
3.9 System Configuration and Simulation Model 69
Chapter 4 71
Simulations, Results and Analysis 71
4.1 Computer Simulations 71
4.2 System Specifications 71
4.3 Simulation Results 75
4.5 Simulation Result for Solar PV System 76
4.6 Simulation Result for WECS 77
4.7 Computer Simulation Result for Load Flow 79
Phase Angle Variations and Reactive Power Demand 82
Power Injection and Load Distribution 82
4.8 Simulation Results for Placement and Sizing of DGs Using PSO 84
4.9 Simulation Results for Reliability Analysis: Monte-Carlo Simulation 88
4.11 Conclusion 92
Chapter 5 94
Conclusion and Recommendations 94
5.1 Summary of Key Findings 94
5.2 Contributions of the Study 95
5.3 Limitations of the Study 95
5.4 Recommendations for Future Work 96
References 98
Appendices 103

List of Figures

Figure 1.1: South African Energy Mix for 2019 [2] 1
Figure 1.2: Energy trilemma diagram [4]. 3
Figure 2.1: Energy sources for renewable energy and conventional fossil fuel [8]. 8
Figure 2.2: Block diagram for wind energy conversion system (WECS) [11]. 10
Figure 2.3: Diagram for solar radiation [12]. 11
Figure 2.4: Illustration of sun energy as thermal energy or solar-PV systems [13]. 12
Figure 2.5: Solar-PV cell [14]. 12
Figure 2.6: Configuration for the formation of Solar PV array [14]. 13
Figure 2.7: The different forms of solar thermal systems [17]. 15
Figure 2.8: Diagram of tidal barrage [18]. 17
Figure 2.9: The significant components of tidal stream technologies [20]. 18
Figure 2.10: Tidal energy conversion system [19]. 18
Figure 2.11: Biomass energy sources [22]. 20
Figure 2.12: The hydropower plant [25]. 22
Figure 2.13: Geothermal energy power plant [27]. 23
Figure 2.14: The schematic diagram of the solar and wind hybrid energy system [33]. 24
Figure 2.15: Shows the schematic diagram of a traditional power system. 25
Figure 2.16: An example of a substation, feeder, distributor, and service primary connection [31]. 26
Figure 2.17: The structure of a typical distribution network [32]. 28
Figure 2.18: Diagram illustrating a typical Loop distribution system [32] 29
Figure 2.19: Diagram illustrating a radial distribution system [32]. 30
Figure 2.20: Diagram illustrating a parallel feeder distribution system [32]. 31
Figure 2.21: Distributed Generation Technologies [36]. 31
Figure 2.22: Classification of distributed generation technologies [38]. 33
Figure 2.23: The acceptable frequency ranges of DG units during a frequency disturbance [52]. 39
Figure 2.24: Voltage-ride-through capability of DGs in category A1 and A2 [52]. 39
Figure 2.25: Voltage-ride-through capabilities for the DG technologies of category A3, B and C [52]. 40
Figure 2.26: Classification of potential challenges in integration of Res [53]. 41

Figure 3.1: Typical power system [61]. 45
Figure 3.3: Newton-Raphson characteristic graph [70] 53
Figure 3.4: Utility connected Solar PV systems. 58
Figure 3.5: Equivalent circuit of the solar cell with the load connected [75]. 59
Figure 3.6: Modern utility-scale wind diagram [76]. 60
Figure 3.7: Power coefficient curve [78]. 62
Figure 3.9: The IEEE 30 bus system 64
Figure 3.12: The designed simulation model. 69
Figure 4.1: MATLAB/Simulink simulation model for Solar PV. 75
Figure 4.2: MATLAB/Simulink simulation model for WECS. 75
Figure 4.3: The I-V characteristic for the solar PV array 76
Figure 4.4: The inverter output voltage from the solar PV system 77
Figure 4.5: The inverter output current from the solar PV system 77
Figure 4.6: The diagram of the turbine power characteristics 78
Figure 4.7: The inverter output voltage from the WECS 78
Figure 4.8: The inverter output current from the WECS 79
Figure 4.9: Result showing the voltage profile for the IEEE 30-bus without DGs. 85
Figure 4.10: Result showing the voltage profile for the IEEE 30-bus with DG1 86
Figure 4.11: Result showing the voltage profile for the IEEE 30-bus with DG1 and DG2. 87
Figure 4.12: Comparison graph of DG systems. 92

List of Tables

Table 2.1 Comparison of solar panel types.....14
Table 2.2: Comparison of solar thermal and solar PV Systems 15
Table 2.3: Sections on distribution system. 26
Table 2.4: Analysis of the types of distribution system [32]. 28
Table 2.5: The summary of grid code requirements for each DG category [40]. 38
Table 3.1: Markov model approach 50
Table: 3.2 Comparison of the Load Flow Methods 53
Table 4.1: The solar PV specifications 71
Table 4.2: The Specifications for the WECS 72
Table 4.3: Line Data for IEEE 30-Bus System .....**Error! Bookmark not defined.**
Table 4.4: MW Limits for Branches in IEEE 30-Bus System .**Error! Bookmark not defined.**
Table 4.5: Results for load flow 80
Table 4.6: Results for load flow in terms line flow and losses 81
Table 4.7: Reliability indices values for IEEE 30 bus without and with DGs.....89
Table 4.8: Comparison of outcomes for three scenarios: with no DG, DG1, and DG2 91

List of Abbreviations

AC	Alternating Current
CHP	Combined Heat Power
CAES	Compressed Air Energy Storage
CSP	Concentrating Solar Power
CO_2	Carbon Dioxide
DC	Direct Current
DC-DC	Direct Current to Direct Converter
DG	Distributed Generation
DER	Distributed Energy Resources
DS	Distribution System
FOR	Forced Outage Rate
GHG	Greenhouse Gas
HV	High Voltage
IEEE	Institute of Electrical Electronics Engineers
IEA	International Energy Agency
LV	Low Voltage
MW	Mega Watt
MV	Medium Voltage
PV	Photovoltaic
PCC	Point Common Coupling
PQ	Power Quality
PSO	Particle Smart Optimization
PSH	Peak Sun Hours
RPP	Renewable Power Plant
RE	Renewable Energy
TS	Transmission System
WECS	Wind Energy Conversion System

Chapter 1

Introduction

1.1 General Background

The increasing global demand for electrical energy, driven by population growth and industrial expansion, has necessitated the need for more reliable and efficient power generation. Traditionally, most electricity is produced from fossil fuels such as coal, diesel, and natural gas. However, these conventional energy sources contribute significantly to environmental issues, including greenhouse gas emissions and climate change.

In South Africa, electricity is primarily generated and transmitted by Eskom, with local municipalities responsible for distribution [1]. However, the country faces a persistent energy crisis due to a generation capacity that falls short of demand. This has led to frequent load shedding and power rationing, negatively impacting both the economy and consumers. There is a growing focus on integrating renewable energy sources such as solar photovoltaic (PV) and wind energy into the national grid to address these challenges. Figure 1.1 shows the energy mix for South Africa in 2019. These sources offer a sustainable solution by reducing dependency on fossil fuels and mitigating environmental concerns.

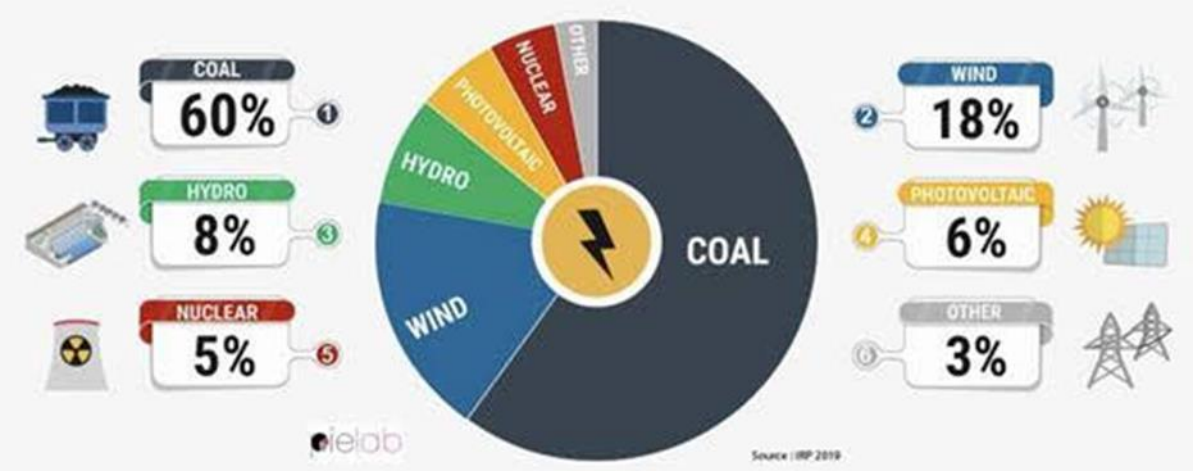

Figure 1.1: South African Energy Mix for 2019 [2]

Large-scale power plants are typically located far from load centres in a traditional power system, requiring extensive transmission infrastructure. The construction of new transmission lines is both costly and logistically complex. These challenges have increased interest in employing the concept of Distributed Generation (DG) which is small-scale power generation systems installed closer to consumption points. DG units can be connected at distribution

substations or dispersed throughout the power network, offering improved voltage stability, reduced transmission losses, and enhanced system reliability. However, integrating DGs into an existing power grid presents technical challenges, including potential power quality issues, voltage fluctuations, and system protection concerns. The effects of distributed generation are short circuit levels are increased, load losses change, voltage profiles change along the network, voltage transients will appear, congestions can appear in system branches, power quality and reliability may be affected, and the networks protections may not function properly [3].

This study examines the impact of DG integration on the reliability of distribution networks. By developing a numerical model and conducting simulations, the research evaluates how optimally placed DG units can enhance network performance while minimising losses.

1.2 Problem Statement

The growing demand for electricity and concerns over greenhouse gas emissions and climate change present a significant challenge for power systems worldwide. In South Africa, reliance on fossil fuels has contributed to energy shortages, forcing the implementation of load shedding. To mitigate this crisis, renewable energy sources such as solar PV and wind power are increasingly considered viable alternatives. The integration of DGs into distribution networks can improve power system efficiency, but it also introduces complexities. These include increased short-circuit levels, voltage fluctuations, power quality concerns, and potential disruptions to existing protection schemes. Therefore, it is essential to investigate the technical impact of DG integration on power distribution reliability.

1.3 Motivation

The conventional centralised power system, where electricity is generated at large-scale plants and transmitted over long distances, faces multiple challenges, including transmission losses, high infrastructure costs, and environmental concerns. As a result, decentralised power generation using Distributed Generation (DG) has emerged as a promising alternative.

However, the intermittent nature of renewable energy sources like solar PV and wind presents operational challenges. Properly integrating these DGs into the distribution network requires careful planning to optimise their placement and sizing while ensuring grid stability. By doing so, DGs can enhance voltage support, minimise losses, and improve overall network reliability.

Integrating wind and solar energy into the electrical grid can significantly increase the available power supply, addressing the growing electricity demand. Furthermore, their utilisation is crucial in solving the energy trilemma, the balance between energy security, environmental sustainability, and economic affordability, as illustrated in Figure 1.2. This study aims to model, analyse, and optimise the integration of DG units into the distribution network to ensure a more resilient and efficient energy supply, particularly in regions experiencing electricity shortages.

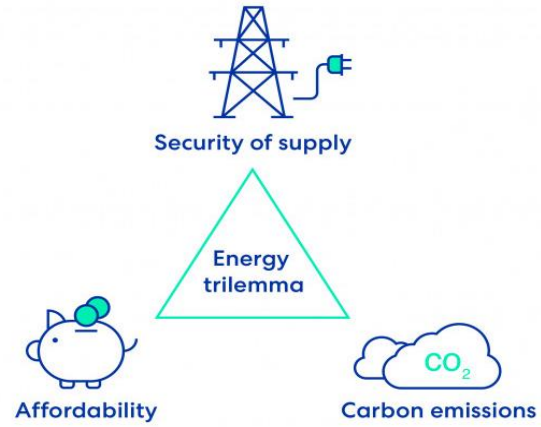

Figure 1.2: Energy trilemma diagram [4].

1.4 Aim and Objectives

The aim of this study is to evaluate the impact of integrating Distributed Generation (DG) units from renewable energy sources into a distribution network. This includes developing a numerical model, optimising DG placement and sizing, and assessing the network's reliability to enhance system performance.

To achieve this aim, the study sets out the following objectives:

1. Develop a numerical model to simulate a distribution network integrated with DG units, specifically solar photovoltaic (PV) and wind energy conversion systems.
2. Perform load flow analysis to evaluate the power distribution characteristics of the network.
3. Optimize the allocation and sizing of DG units using the Particle Swarm Optimization (PSO) algorithm to minimise network losses and enhance voltage stability.

4. Assess the reliability of the distribution network by calculating key reliability indices and comparing system performance with and without DG integration.
5. Evaluate the technical impact of DGs on the power system, focusing on voltage support, power availability, and overall network performance.

1.5 Scope of Study

The potential of renewable energy in South Africa has not yet been fully harnessed despite increasing government and private sector efforts. Renewable energy sources solve the country's electricity crisis by improving grid stability and enhancing power system reliability. This study focuses on the technical aspects of DG integration, particularly regarding reliability analysis. The research evaluates how the introduction of DGs affects voltage stability and system performance, using reliability indices to determine optimal placement strategies. The Particle Swarm Optimization (PSO) algorithm optimises DG locations and minimises network losses.

Areas not covered in this study include fault analysis of the distribution network and real-time control of DG systems. The study also does not address economic aspects such as investment costs and policy

1.6 Dissertation Outline

The thesis is structured into five chapters:

- Chapter 1: This chapter presents the background of the study and the potential of DGs. It includes motivation, the problem statement, aim and objectives of the research and the scope of the study.
- Chapter 2: This chapter focuses on reviewing literature with regards to DGs integration into the power systems. The review for the research which includes the concept theory, perspectives, and the concept of the integration of DGs.
- Chapter 3: This chapter presents the modeling and design consideration of DGs and the development of the numerical models that were used in the research to carry out the computer simulations.
- Chapter 4: This chapter was used for simulation, presentation of resents and analysis of simulation results.

- Chapter 5: This chapter was used to summarize the study by providing the appropriate conclusion based on the various aspects of this study. Also, the recommendations for possible areas for future study were provided based on the findings of this study.

1.7 Publication

Ndumiso Gwala, Zanele Lunga and Evans Ojo. 2025 “Simulation and Analysis of the Integration of Power from Mini Hydroelectric Power Plant into Microgrid”. Accepted and presented at the 2025 SAUPEC Conference, Johannesburg, South Africa, January 29-30, 2025.

Chapter 2

Literature Review

2.1 Introduction

This chapter comprehensively reviews existing literature relevant to the reliability analysis of distribution networks integrated with Distributed Generation (DG). The review covers fundamental concepts, theoretical perspectives, and methodologies for assessing power system reliability. A country's energy consumption is often an indicator of its level of development, as economic, industrial, and educational activities rely heavily on a stable and sufficient power supply. However, the depletion of conventional energy resources, such as coal, oil, and natural gas, combined with the environmental damage caused by their combustion, has significantly increased global interest in renewable energy sources. Reliability assessment of electrical distribution systems has become a critical area of research, given its direct impact on end users.

Reliability assessment becomes even more crucial for distribution networks incorporating intermittent renewable energy sources (RESs). Integrating RESs into the grid presents various challenges, including power stability issues, voltage and frequency fluctuations, phase imbalance, and power quality concerns [5]. The primary goal of power system reliability assessment is to evaluate a system's ability to meet customer demand under different operating conditions. The increasing penetration of RESs into power grids is driven by several factors, including the rising cost of fossil fuels, heightened concerns over greenhouse gas emissions, and the need for energy security. As a result, many countries are promoting using renewable energy for electricity generation. Wind and solar PV systems have gained significant attention as viable alternatives to traditional power generation. These technologies can enhance power system reliability and provide an uninterrupted energy supply for residential and industrial applications.

Reliability analysis plays a key role in power system planning and operation. A thorough understanding of system performance under different scenarios enables utilities and operators to implement strategies that maintain acceptable reliability. Given South Africa's increasing energy demand and constrained power generation capacity, assessing the reliability of distribution networks integrated with DG is particularly relevant. This chapter provides a detailed review of the reliability assessment of distribution networks. It examines conventional

distribution networks (without RESs) and modern networks that incorporate RESs, highlighting the critical challenges and opportunities associated with DG integration.

2.2 Non-Renewable

Non-renewable energy refers to natural resources that exist in finite quantities and cannot be replenished at the rate at which they are consumed. These energy sources, including fossil fuels such as crude oil, coal, natural gas, and nuclear energy, have been the backbone of global power generation for decades. However, their long-term sustainability is increasingly questioned due to their environmental impact and diminishing reserves [6].

Fossil fuels are formed from the remains of ancient organic matter subjected to heat and pressure over millions of years beneath the Earth's surface. At the same time, they have historically provided a reliable and concentrated energy source; their extraction, processing, and combustion result in significant environmental degradation. The primary concern associated with fossil fuel consumption is the emission of greenhouse gases (GHGs), particularly carbon dioxide (CO_2), contributing to global warming and climate change. Additionally, fossil fuel extraction often leads to deforestation, water pollution, and habitat destruction, further exacerbating environmental issues [6].

In South Africa, coal-fired power stations dominate electricity generation, contributing significantly to the national energy mix. Despite coal's abundance and affordability in the region, its environmental consequences, such as high carbon emissions and air pollution, pose severe challenges [7]. The continued reliance on coal has also led to increasing international pressure for South Africa to transition towards cleaner energy sources in line with global sustainability goals. Figure 2.1 illustrates the various energy sources used for electricity generation, including conventional fossil fuels and renewable energy.

Nuclear energy, another non-renewable energy, offers a low-carbon alternative to fossil fuels. It relies on nuclear fission to produce large amounts of electricity with minimal greenhouse gas emissions. However, nuclear power comes with challenges, including high capital costs, concerns over radioactive waste disposal, and the potential risks associated with nuclear accidents. Although nuclear energy presents a viable option for reducing carbon emissions, public perception and safety concerns continue to limit its widespread adoption [6].

While non-renewable energy sources have historically ensured a stable and continuous power supply, their long-term viability is uncertain. The depletion of fossil fuel reserves, rising energy demand, and environmental concerns have highlighted the urgent need for energy diversification. Many countries, including South Africa, are exploring strategies to integrate renewable energy sources to enhance energy security and sustainability. Transitioning to cleaner energy alternatives mitigates environmental damage and reduces dependence on finite resources, making it a critical step toward a resilient and future-proof energy system.

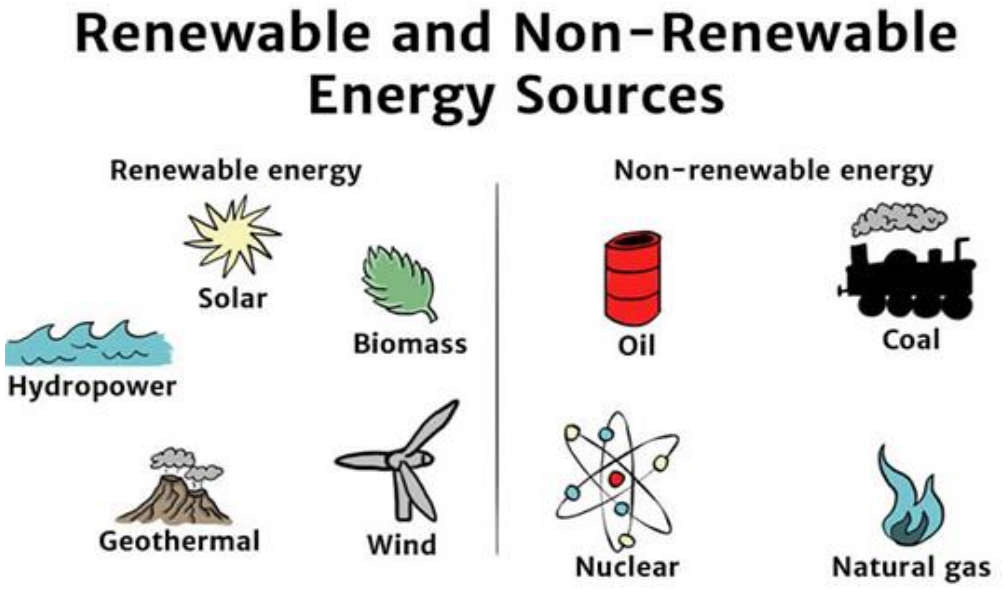

Figure 2.1: Energy sources for renewable energy and conventional fossil fuel [8].

2.3 Renewable Energy Sources

Renewable energy refers to energy derived from naturally replenishing sources that are sustainable over the long term. Unlike fossil fuels, which are finite and environmentally harmful, renewable energy sources such as solar, wind, hydropower, biomass, geothermal, tidal, and ocean wave energy offer a cleaner and more sustainable alternative for electricity generation. As global energy demand continues to rise, renewable energy has gained increasing attention as a viable solution to energy security and climate change mitigation [9]. Renewable energy sources are characterised by their ability to regenerate naturally and their minimal environmental impact. These sources are key to reducing greenhouse gas emissions and mitigating the adverse effects of fossil fuel consumption. As illustrated in Figure 2.1, renewable energy technologies are being adopted globally to diversify energy production and decrease dependence on non-renewable resources.

In South Africa, despite abundant renewable energy potential, the country still relies heavily on fossil fuels for electricity generation. However, initiatives to promote the use of renewable energy are gaining momentum, driven by policy interventions, international commitments to reduce carbon emissions, and the need to address ongoing energy supply challenges. The Renewable Energy Independent Power Producer Procurement Programme (REIPPPP) exemplifies South Africa's commitment to increasing renewable energy capacity [9]. Each renewable energy source has unique characteristics and advantages, making them suitable for different applications. The following subsections provide an overview of the key renewable energy sources and their role in electricity generation.

2.3.1 Wind Power

Wind energy is one of the fastest-growing renewable energy sources worldwide. Wind results from atmospheric pressure gradients that cause air movement from high-pressure to low-pressure areas. Wind turbines convert this kinetic energy into mechanical energy, which is then transformed into electrical energy using a generator [10]. A typical Wind Energy Conversion System (WECS) consists of turbine blades, a gearbox, a generator, a power electronic converter, and a transformer. The turbine blades capture wind energy, transferring mechanical power through the gearbox to the generator, which is converted into electrical power. The efficiency of wind energy generation depends on wind speed, turbine design, and site selection. Figure 2.2 illustrates a simplified block diagram of a WECS.

Wind energy is a clean, renewable, and cost-effective power source but also presents challenges such as intermittency, land use constraints, and noise concerns. Modern wind farms incorporate advanced forecasting techniques and energy storage systems to mitigate these issues. South Africa has considerable wind energy potential, particularly along its coastal regions, where consistent wind patterns allow large-scale wind farm deployment [10].

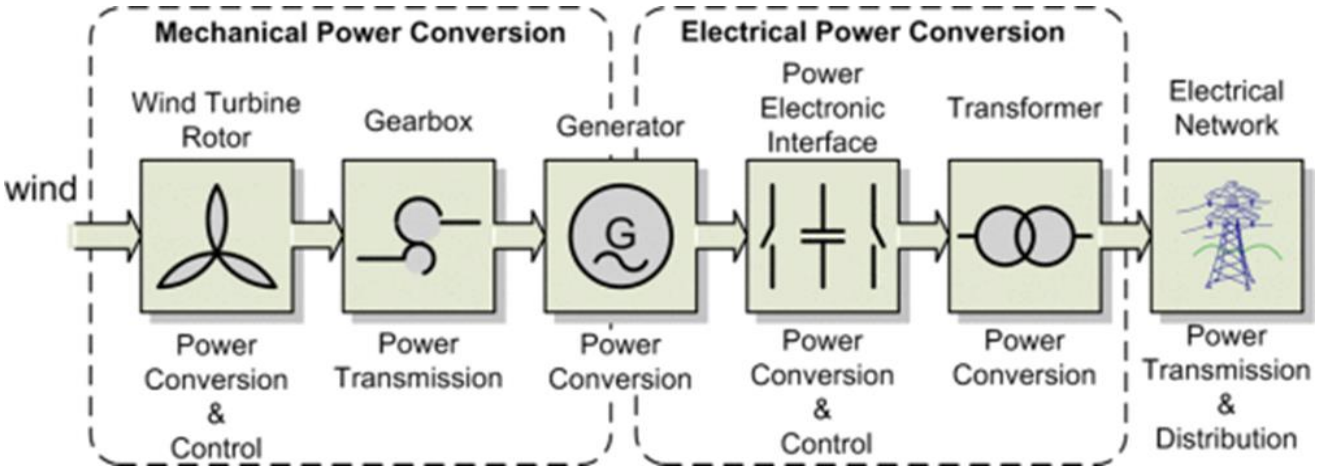

Figure 2.2: Block diagram for wind energy conversion system (WECS) [11].

2.3.2 Solar Power

Solar power harnesses energy from the sun to generate electricity. It is one of the most abundant renewable energy sources available. Solar energy can be utilised through two primary technologies: solar photovoltaic (PV) systems and concentrated solar power (CSP) systems. Solar PV technology converts sunlight directly into electricity using semiconductor materials such as silicon. When photons from sunlight strike a PV cell, they excite electrons, generating an electric current. The efficiency of solar PV systems depends on factors such as solar irradiance, temperature, panel orientation, and shading. Figure 2.3 illustrates how solar radiation reaches the Earth's surface.

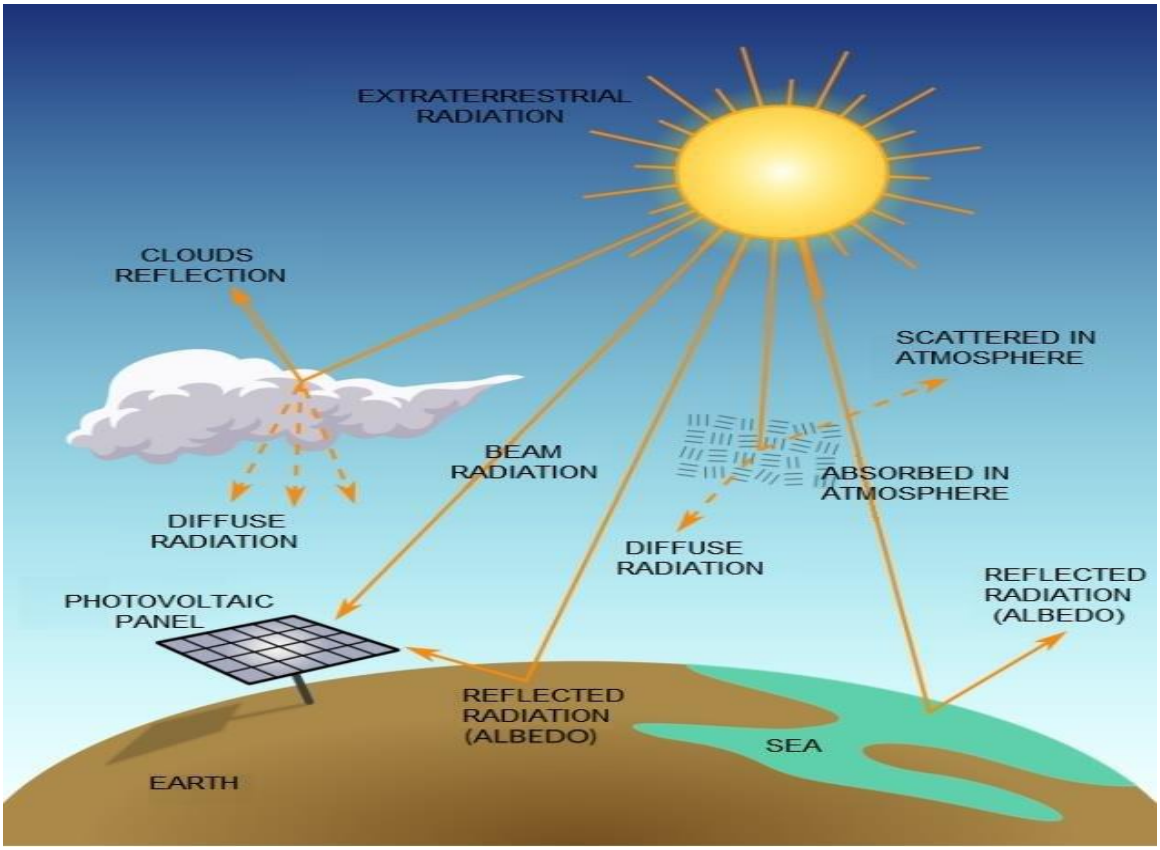

Figure 2.3: Diagram for solar radiation [12].

CSP systems, on the other hand, use mirrors or lenses to concentrate solar energy onto a small area, generating high temperatures that drive steam turbines for electricity production. While CSP systems are adequate for large-scale power generation, they require significant land and infrastructure investments. Figure 2.4 illustrates the difference between solar PV and thermal systems. South Africa has excellent solar energy potential due to its high solar radiation levels. The country has already as the Northern Cape. The continued expansion of solar energy could significantly reduce reliance on fossil fuels and improve energy security [13].

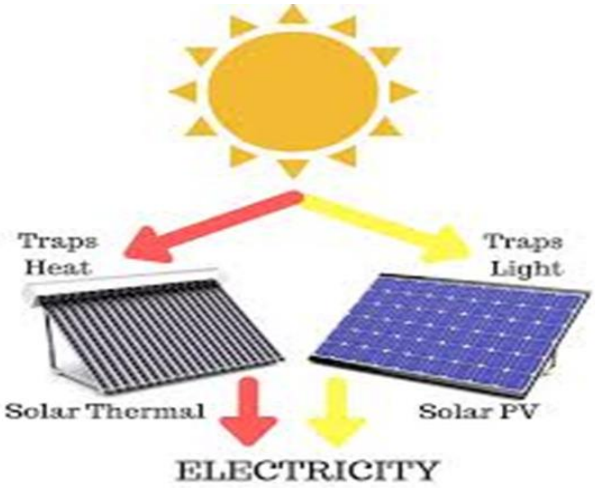

Figure 2.4: Illustration of sun energy as thermal energy or solar-PV systems [13].

2.3.2.1 Solar PV Systems

Solar PV technology converts sunlight directly into electricity through the photovoltaic effect. A solar panel consists of multiple photovoltaic (PV) cells made from semiconductor materials, primarily silicon. When sunlight strikes these cells, the energy from photons excites electrons, creating an electric current. Figure 2.5 illustrates the photovoltaic effect, showing how electrons are transferred between the semiconductor layers, generating a continuous flow of electricity.

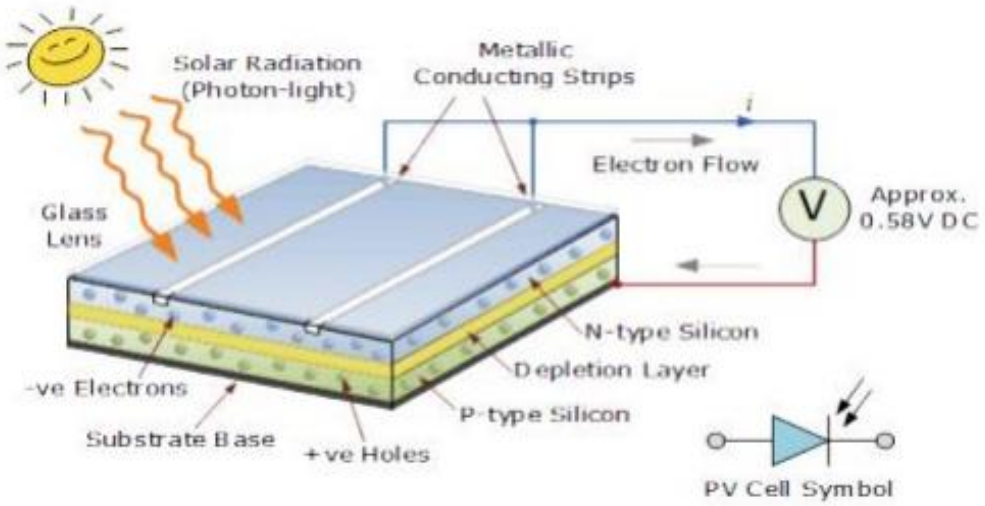

Figure 2.5: Solar-PV cell [14].

A solar PV system consists of multiple photovoltaic cells combined to form a solar panel, and a group of solar panels arranged together creates a solar array. This hierarchical structure enables scalability, allowing PV systems to be tailored for residential, commercial, or large-

scale utility applications. Figure 2.6 illustrates the transformation from individual solar cells to complete solar arrays.

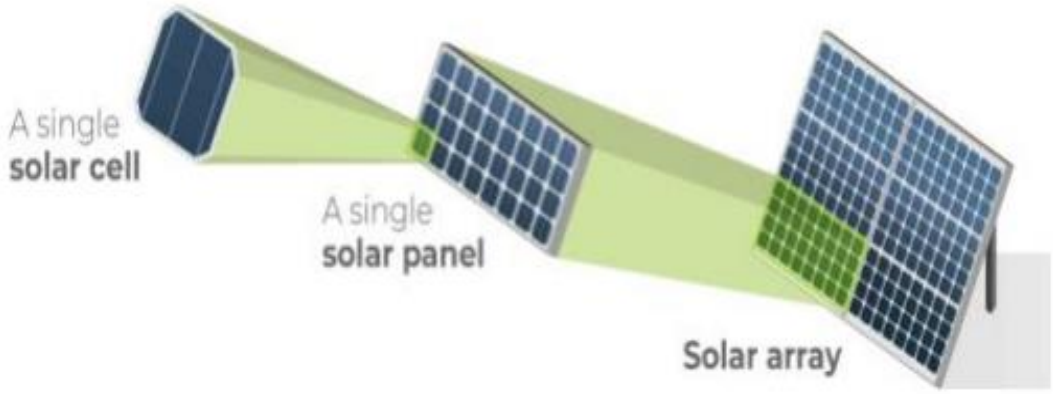

Figure 2.6: Configuration for the formation of Solar PV array [14].

Solar panels produce direct current (DC) electricity, which can be configured in series or parallel connections to achieve the desired voltage and current levels. The efficiency of a solar PV system depends on several external factors, including:

- **Climate and weather conditions** – Rain, clouds, mist, dust, and fog can reduce solar radiation reaching the panels
- **Panel orientation and tilt angle** – The angle and positioning of panels affect the amount of sunlight captured.
- **Shading effects** – Shadows from buildings, trees, or other obstructions can significantly reduce panel output.
- **Solar radiation intensity** – Higher solar irradiance leads to more significant power generation.
- **Ambient temperature** – Excessive heat can decrease the efficiency of PV cells.

There are three primary types of solar panels, each with distinct advantages and disadvantages. Table 2.1 presents a detailed comparison of these solar panel types. The choice of panel type depends on factors such as budget, space availability, and energy requirements.

Solar PV systems can be categorised into two primary configurations:

- Off-grid (standalone) systems: used in locations without access to the utility grid. These systems typically include battery storage to ensure continuous power availability.
- Grid-tied systems: connected to the electrical grid, allowing users to export excess electricity while drawing power from the grid when needed.

Grid-tied systems are more common in urban areas due to their cost-effectiveness, whereas off-grid systems are suitable for remote locations with limited grid access.

Table 2.1 Comparison of solar panel types.

Solar panel type	Advantages	Disadvantages
Monocrystalline	• High efficiency/performance • Aesthetics	• Higher costs
Polycrystalline	• Low cost	• Lower efficiency/performance
Thin-film	• Portable and flexible • Lightweight • Aesthetics	• Lowest efficiency/performance

2.3.2.2 Solar Thermal Systems

Unlike PV systems, solar thermal technology captures sunlight and converts it into heat energy. This heat is then used for various applications, including:

- Electricity generation – By converting solar heat into steam to drive turbines.
- Water heating – For residential and industrial use.
- Space heating – For warming buildings and other thermal applications.

Solar thermal systems utilise mirrors or lenses to concentrate sunlight onto a collector, which absorbs and transfers the heat. Figure 2.7 illustrates different solar thermal configurations used for power generation.

The most common large-scale solar thermal power plants use Concentrating Solar Power (CSP) technology. These systems focus sunlight onto a central receiver, such as a tower or an array of pipes, where a heat-transfer fluid is heated to generate steam that drives a turbine. CSP systems are typically deployed in regions with high solar radiation and require substantial land area for installation [15].CSP plants are significantly larger than residential solar PV systems, with capacities exceeding 100 megawatts—over 10,000 times the output of a typical household solar panel installation [16].

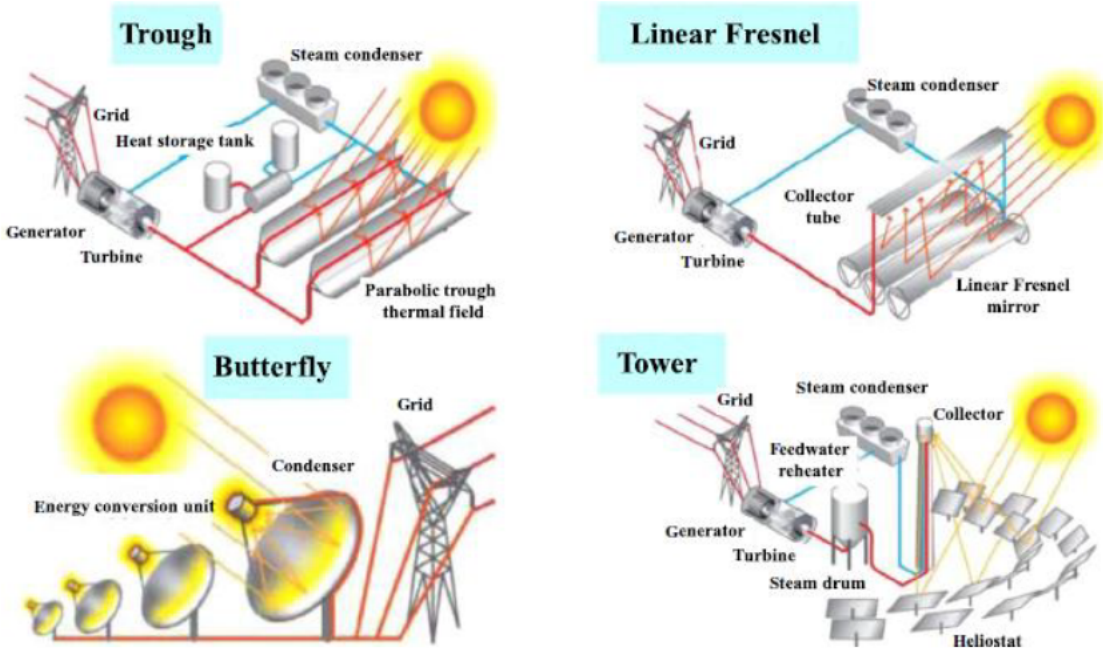

Figure 2.7: The different forms of solar thermal systems [17].

While both solar PV and solar thermal systems provide clean energy, they differ in efficiency, cost, and application. Table 2.2 presents a comparison of these two solar technologies.

Table 2.2: Comparison of solar thermal and solar PV Systems

Thermal Solar System		**Solar-PV System**	
Advantages	**Challenges**	**Advantages**	**Challenges**
• High efficiencies in converting sunlight into usable heat. • Reduces energy bills and can have a quick payback period in sunny regions. • Various applications ranging from residential to industrial scale	• Can require much space for collectors and storage tanks. • High-temperature systems can be complex and expensive. • May require backup heating during periods of low solar radiation.	• Produces electricity without emitting pollutants. • Can last 25 years or more with minimal maintenance. • Systems can be scaled up or down	• Upfront costs can be significant. • It varies with the weather and time of the day. • Large installations may require a large area or rooftop space.

Solar PV systems are generally more affordable and easier to install, making them suitable for residential and commercial use. However, solar thermal systems are highly efficient for large-scale energy production, particularly for industrial applications requiring heat energy. Solar energy is a critical component of the transition to renewable energy. The choice between solar PV and solar thermal depends on specific energy needs, space availability, and budget constraints. With its abundant sunshine in South Africa, the expansion of solar energy projects presents a significant opportunity to reduce fossil fuel dependence, enhance energy security, and create a more sustainable power system.

2.3.3 Tidal Power

Tidal power is a form of renewable energy that harnesses the movement of ocean tides to generate electricity. This energy source is highly predictable and reliable since the gravitational interactions between the Earth, Moon, and Sun drive tides. Unlike wind and solar power, which are subject to weather variations, tidal energy benefits from consistent and cyclical tidal patterns, making it a promising renewable energy solution [18].

Tidal energy can be harnessed through two primary methods:

- Tidal Barrages use dams or barriers to capture the potential energy of tides.
- Tidal Stream Generators extract kinetic energy from moving tidal currents.

These technologies have advantages and challenges, as discussed below.

2.3.3.1 Tidal Barrage

Tidal barrages are large dam-like structures built across the mouth of an estuary. They work by trapping seawater during high tide and releasing it through turbines during low tide, converting water movement into electricity. The process is similar to conventional hydroelectric power generation. Figure 2.8 illustrates a typical tidal barrage system.

The electricity generation potential of a tidal barrage system depends on the tidal range the vertical difference between high and low tide. Locations with large tidal ranges are more suitable for tidal barrage power plants. The total energy that can be extracted from a tidal barrage is given by the (2.1)

$$p = \frac{1}{2} A \rho g H^2 \tag{2.1}$$

Where,

A is the surface area of the barrage,

ρ is the specific density of ocean water,

g is the gravitational acceleration, and

H is the tidal range at the site.

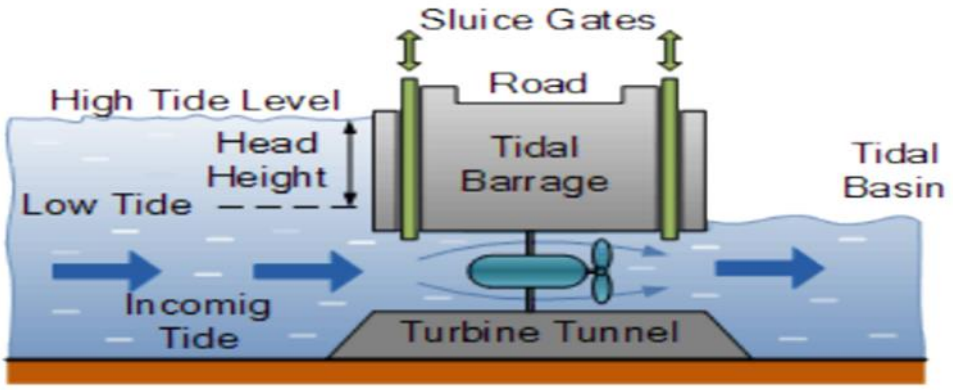

Figure 2.8: Diagram of tidal barrage [18].

One of the key advantages of tidal barrages is their ability to generate significant amounts of electricity. However, they also have environmental and economic drawbacks, including:

- High construction costs: building tidal barrages requires large-scale infrastructure investments.
- Ecological disruption: barrages can alter estuarine ecosystems by changing water flow, sediment transport, and marine habitats.
- Limited suitable sites: only locations with large tidal ranges and appropriate geography can support tidal barrages.

Despite these challenges, some of the world's most successful tidal barrage plants, such as the La Rance Tidal Power Station in France, have demonstrated the long-term viability of this technology.

2.3.3.2 Tidal Stream Generators

Tidal stream generators, known as tidal turbines, function similarly to underwater wind turbines. They are placed in fast-moving tidal currents, where the kinetic energy of flowing water turns turbine blades, generating electricity. These turbines are anchored to the seabed and do not require considerable barriers or dams, making them a more environmentally friendly alternative to tidal barrages [19]. Tidal stream generators consist of the following key components, as illustrated in Figure 2.9:

- Turbine rotor: Captures energy from moving water.

- Gearbox: Increases rotational speed for electricity generation.
- Generator: Converts mechanical energy into electrical energy.
- Underwater cable: Transmits power to the electrical grid.

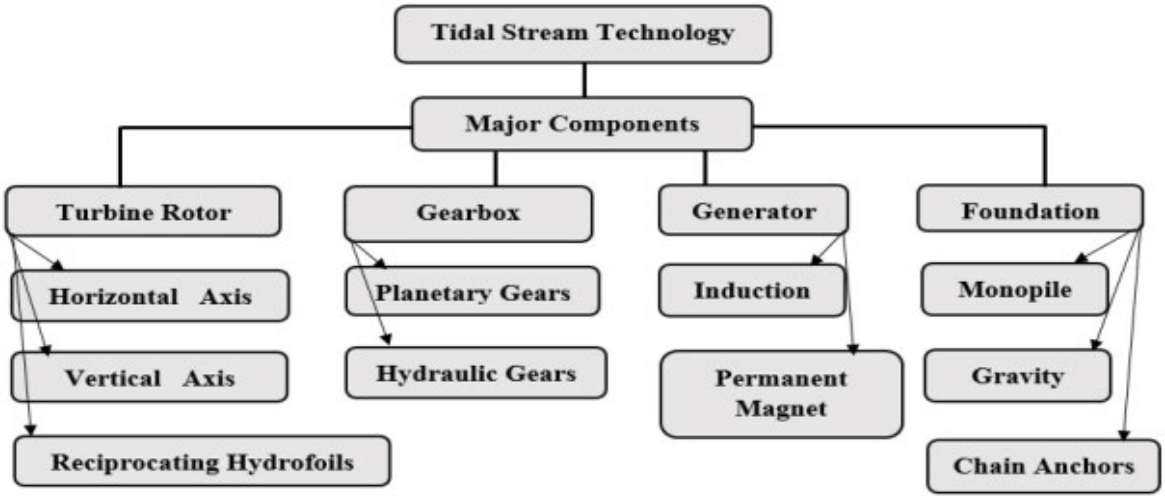

Figure 2.9: The significant components of tidal stream technologies [20].

Figure 2.10 illustrates a tidal stream generator, an energy conversion system that harnesses power from moving water masses, particularly tidal currents. The turbine rotor captures kinetic energy from the flowing water, with lower stream velocities resulting in reduced turbine speeds. The turbine shaft is connected to a gearbox to enhance efficiency, which increases rotational speed to optimise power generation. The gear train is linked to an electric generator, which converts mechanical energy into electrical energy. The generated electricity is transmitted to the power grid via an underwater cable, ensuring integration into the existing electrical infrastructure.

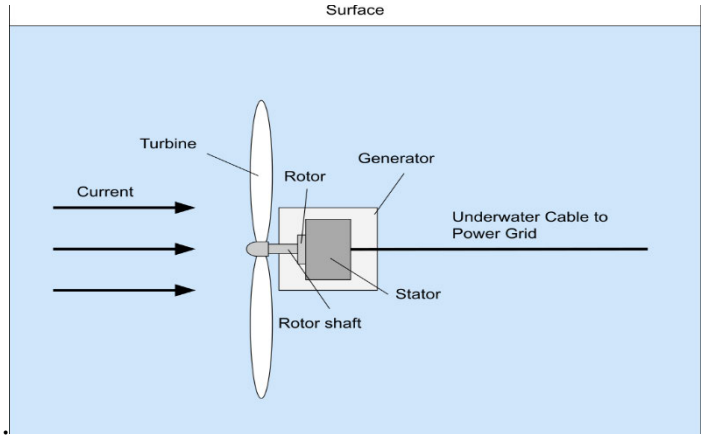

Figure 2.10: Tidal energy conversion system [19].

Unlike tidal barrages, tidal stream systems take advantage of the kinetic energy of tidal currents rather than the potential energy of tidal height differences. Their energy output is determined by the velocity of water flow and the efficiency of the turbine blades. The power output of a tidal turbine can be calculated using (2.2).

$$P = \frac{1}{2} C_p \rho A V^3 \tag{2.2}$$

where:

P is the power generated,

C_p is the power coefficient of the turbine,

ρ is the density of seawater,

A is the swept area of the turbine blades,

V is the velocity of the tidal current.

Tidal energy is one of the most predictable and reliable renewable energy sources. While tidal barrages offer high power output, they have significant environmental and economic challenges. Tidal stream generators, on the other hand, provide a more sustainable solution but require strong tidal currents for effective operation. In South Africa, tidal power remains largely unexplored, but with ongoing research and technological advancements, it could play a role in the country's future energy strategy. Investing in feasibility studies, pilot projects, and technology development could unlock the potential of tidal energy as part of a diversified renewable energy portfolio.

2.3.4 Biomass

Biomass energy is derived from organic materials, including plant matter, agricultural residues, forestry waste, and biodegradable municipal waste. It is one of the oldest energy sources used by humans, with applications ranging from traditional combustion for heating and cooking to modern biofuel production and electricity generation. Unlike fossil fuels, biomass is considered renewable, as it can be replenished through sustainable agricultural and forestry practices. However, its sustainability depends on responsible resource management and emissions control measures [21]. Biomass can be converted into energy through direct combustion, biochemical, or thermochemical processes. The conversion method choice depends on the biomass feedstock type and the desired energy output. Figure 2.11 illustrates various biomass energy sources.

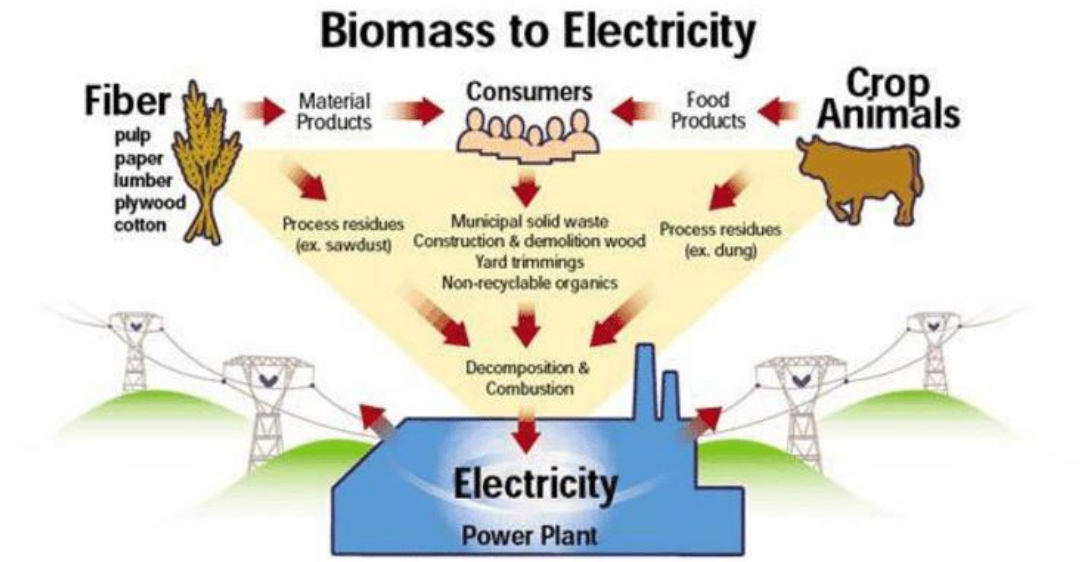

Figure 2.11: Biomass energy sources [22].

There are both advantages and challenges of biomass energy, which are highlighted below:

- **Advantages**
- Renewable and carbon-neutral: Biomass absorbs CO_2 during growth, offsetting emissions from combustion.
- Versatile energy applications: Biomass can be used for electricity, heating, transportation fuels, and industrial applications.
- Reduces waste: Organic waste materials are repurposed for energy production, reducing landfill use.
- Energy security: Biomass provides a local and sustainable alternative to fossil fuels, reducing dependence on imported energy.
- **Challenges**
- Land use and food security: Large-scale biomass production may compete with food crops, leading to deforestation and rising food prices.
- Air pollution: Uncontrolled biomass combustion can release particulate matter and harmful pollutants.
- Supply chain limitations: Biomass collection, processing, and transportation require infrastructure and investment.

South Africa has significant biomass energy potential, with feedstocks including sugarcane waste, forestry residues, and agricultural by-products. The country has been exploring biomass-to-electricity projects, particularly in rural areas where biogas digesters and waste-to-energy

plants can improve access to clean energy [23]. However, large-scale deployment remains limited due to high capital costs and policy uncertainties.

2.3.5 Hydropower

Hydropower, also known as hydroelectric power, is one of the oldest and most widely used renewable energy sources. It harnesses the energy of flowing or falling water to generate electricity. This process is achieved through hydroelectric power plants, which use turbines and generators to convert the kinetic energy of moving water into electrical energy. Hydropower is considered a clean, renewable, and reliable source of electricity, contributing significantly to global energy production [24, 25].

Hydropower plants are classified based on their design and how they utilise water resources. The main types include:

1. Conventional Dams and Reservoirs

These hydropower plants store water in a reservoir behind a dam. When electricity is needed, water is released from the reservoir and directed through turbines, generating power. This type of hydropower provides stable and consistent electricity generation. However, large-scale dams can have significant environmental and social impacts, such as disrupting ecosystems and displacing communities. Figure 2.12 illustrates a typical hydroelectric power plant.

2. Run-of-River (ROR) Systems

Run-of-river systems do not require large reservoirs. Instead, they divert a portion of a river's flow through a turbine before returning it to the river downstream. These systems are considered more environmentally friendly than conventional dams because they do not involve large-scale water storage. However, their power generation depends on river flow, making them susceptible to seasonal variations.

3. Pumped Storage Hydropower

Pumped storage hydropower (PSH) operates as a grid energy storage system, helping to balance electricity supply and demand. During periods of low electricity demand, excess energy is used to pump water from a lower reservoir to an upper reservoir. When demand increases, the stored water is released to generate electricity. This system improves grid stability and integrates well with variable renewable energy sources such as solar and wind.

4. Micro and Small Hydropower

Micro and small hydropower plants generate power on a smaller scale, typically below 10 MW. They are often used for rural electrification in off-grid areas. These systems are cost-effective

and have minimal environmental impact, making them suitable for remote communities and small industries.

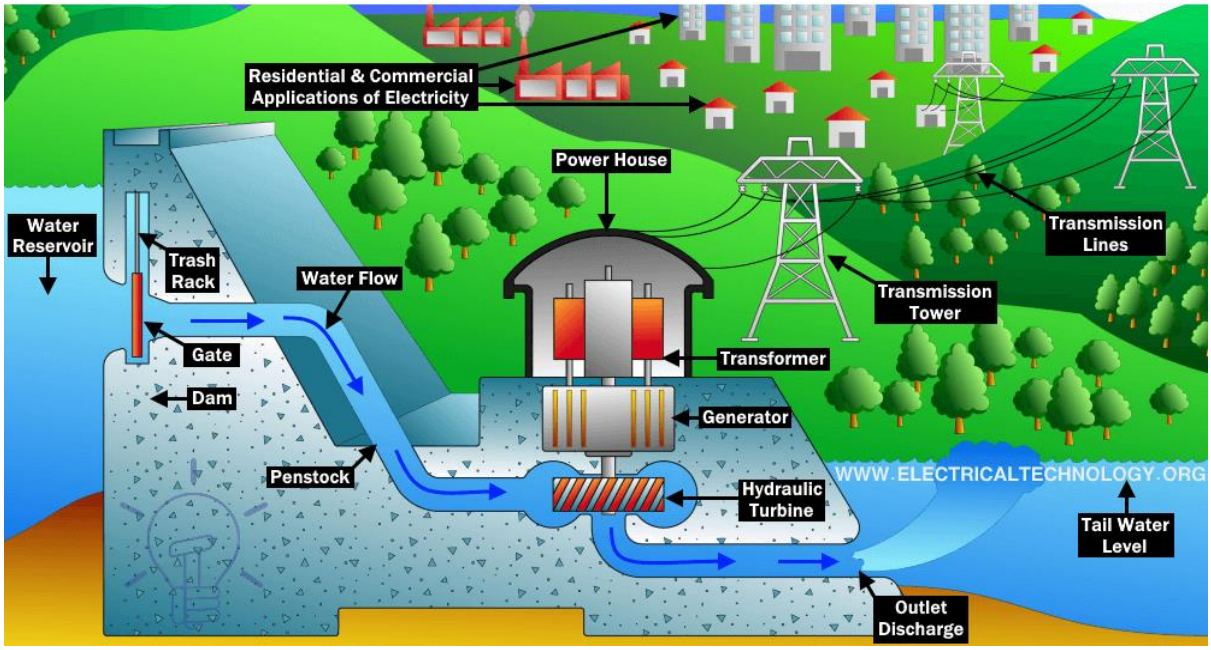

Figure 2.12: The hydropower plant [25].

South Africa has limited large-scale hydropower resources due to its relatively low annual rainfall and few major rivers suitable for hydroelectric dams. However, small-scale and pumped storage hydropower is essential to the country's energy mix. Some of the notable hydropower projects in South Africa include:

- Gariep Dam (360 MW) – The largest hydroelectric plant in the country.
- Vanderkloof Dam (240 MW) – Another central hydropower station supplying electricity to the national grid.
- Drakensberg and Ingula Pumped Storage Schemes – Used to store energy and balance grid demand.

With increasing focus on renewable energy diversification, South Africa is exploring the potential of micro-hydropower systems for rural electrification. These systems could provide sustainable energy solutions for off-grid communities, supporting economic development in remote areas [26].

2.3.6 Geothermal Power

Geothermal power harnesses heat from the Earth's interior to generate electricity or provide direct heating. This energy originates from radioactive decay and residual heat from the planet's formation. Figure 2.13. is an illustration of a geothermal power plant. Unlike solar and

wind, geothermal energy offers a stable, continuous power supply with minimal carbon emissions. There are three types of geothermal power plants [27]:

- **Dry Steam Plants:** Use naturally occurring steam from underground reservoirs to drive turbines.
- **Flash Steam Plants:** Extract high-pressure hot water, which flashes into steam to generate power.
- **Binary Cycle Plants:** Use moderate-temperature geothermal fluids to heat a secondary working fluid, which evaporates to drive a turbine [25].

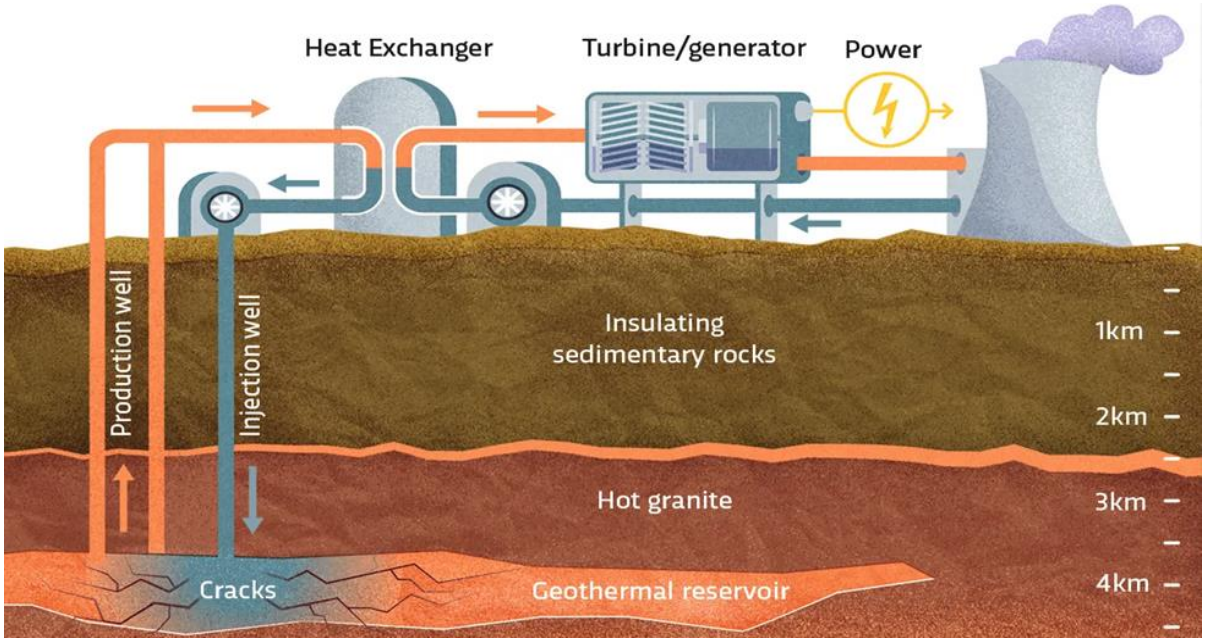

Figure 2.13: Geothermal energy power plant [27].

Geothermal energy has the following advantages and challenges:

- **Advantages**
  - **Reliable & low emissions:** Provides baseload power with minimal environmental impact.
  - **Efficient land use**: Requires less space than wind or solar.
- **Challenges**
  - **Geographic limitations**: High-temperature reservoirs are needed for electricity generation.
  - **High upfront costs:** Drilling and exploration require significant investment [27].

South Africa has limited geothermal potential due to its geological conditions. However, hot springs in Limpopo, KwaZulu-Natal, and the Western Cape could support direct-use applications such as space heating and industrial processes. While large-scale electricity

generation is unlikely, further research and technological advancements could expand its role in the country's renewable energy mix [27].

2.4 Hybrid Renewable Energy System

A Hybrid Renewable Energy System (HRES) combines two or more renewable energy sources to enhance reliability, efficiency, and energy security. By integrating different energy sources, hybrid systems mitigate the intermittency of renewables such as solar and wind, ensuring a stable power supply [28]. HRES typically integrates solar, wind, biomass, hydro, or geothermal energy with energy storage or backup power sources. Standard configurations include [29]:

- **Solar-Wind Hybrid System:** Utilizes solar PV during the day and wind power at night or in high-wind conditions.
- **Solar-Biomass Hybrid System:** Solar PV supplies electricity, while biomass provides backup power during low solar availability.
- **Solar-Hydro Hybrid System:** Hydropower compensates for solar energy fluctuations, ensuring continuous power generation.
- **Renewable-Diesel Hybrid System:** Diesel generators are a backup when renewable sources are insufficient, commonly used in remote areas.

The schematic diagram to illustrate hybrid renewable sources is shown in Figure 2.14.

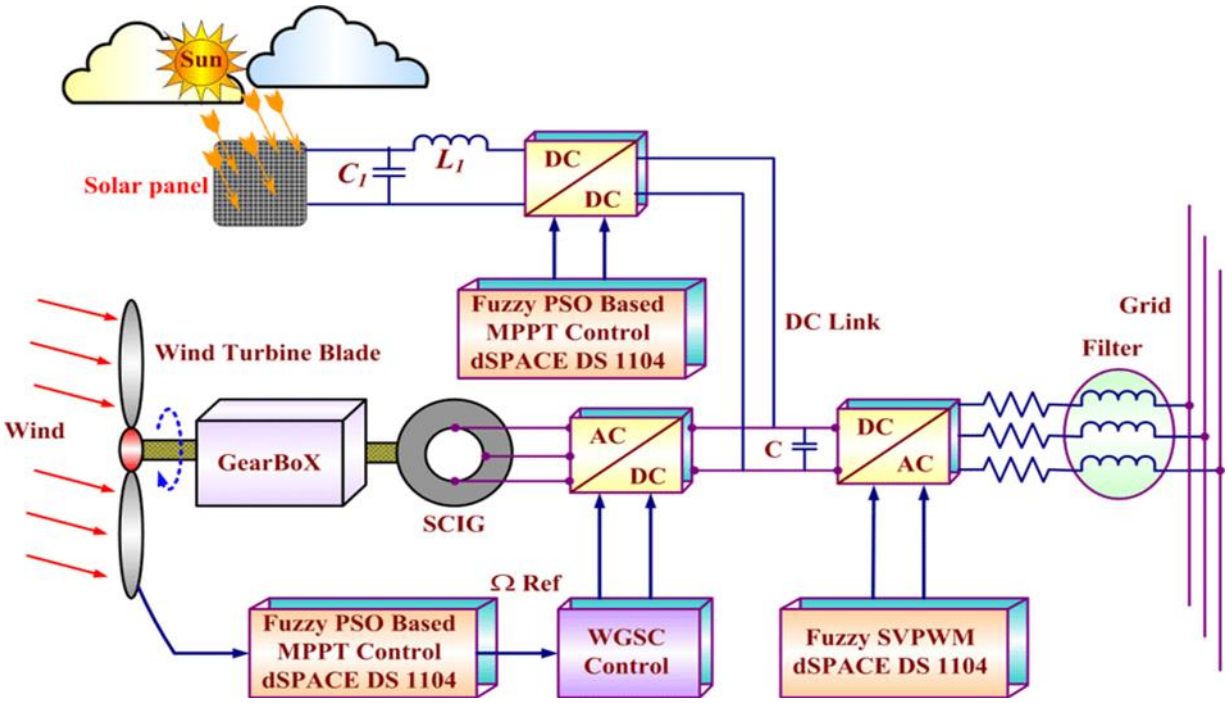

Figure 2.14: The schematic diagram of the solar and wind hybrid energy system [33].

HRES has the following advantages and challenges [30]:

- **Advantages**
    - **Enhanced Reliability:** Reduces dependence on a single energy source.
    - **Higher Efficiency:** Optimizes power generation by complementing variable resources.
    - **Lower Carbon Emissions:** Reduces reliance on fossil fuels.
- **Challenges**
    - **High Initial Cost:** Requires advanced energy management and storage systems.
    - **Complexity**: Requires integration planning and grid compatibility.

Given South Africa's abundant solar and wind resources, HRES offers a viable solution for off-grid electrification and reducing reliance on coal-fired power. Integrating solar, wind, and pumped hydro storage could significantly improve the country's energy security and grid stability.

2.5. Traditional Power Systems

Traditional power systems are centralised energy networks that generate electricity at large-scale power plants and distribute it to consumers via high-voltage transmission and distribution networks. These systems primarily rely on fossil fuels (coal, oil, natural gas), nuclear power, and hydropower, with coal being the dominant source in many countries, including South Africa [31]. Figure 2.15 illustrates a schematic diagram of a traditional power system, showing its key components from generation to end-user delivery.

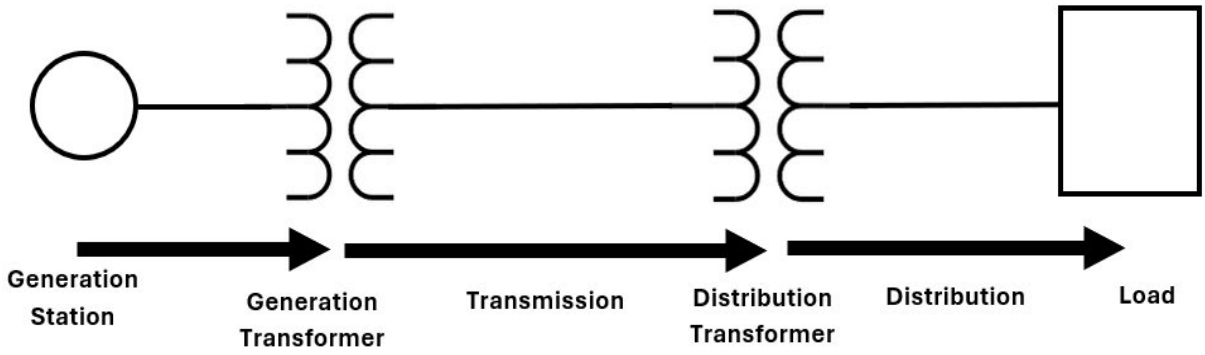

Figure 2.15: Shows the schematic diagram of a traditional power system.

A conventional power system consists of three main sections [31]:

- **Generation**: Electricity is produced in thermal, nuclear, hydro, or gas power stations at high voltages.

- **Transmission** – High-voltage electricity (typically 132 kV – 765 kV) is transported over long distances through transmission lines to substations.
- **Distribution** – Power is stepped down to lower voltages for consumer use.

The distribution system is responsible for delivering electricity from substations to consumers. Table 2.3 outlines the different sections of the distribution system:

Table 2.3: Sections on distribution system.

Feeder	Distributor	Service main
The conductor connects the substation with the distributor. No tapping takes place within a feeder.	Conductor through which tapping takes place to supply to the consumer.	Cable connecting distributor and consumer utility.

Figure 2.16 shows a primary connection between the substation, feeder, distributor, and service, demonstrating how power flows from the grid to consumers.

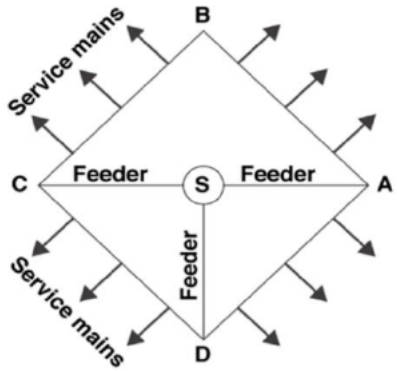

Figure 2.16: An example of a substation, feeder, distributor, and service primary connection [31].

Traditional power systems have the following advantages and challenges [31].

Advantages

- Reliable & Well-Established – Provides consistent power supply using proven infrastructure.
- High Power Output – Capable of meeting national industrial and residential demands.

Challenges

- High Carbon Emissions – Fossil fuel-based generation contributes to climate change.
- Transmission Losses – Energy losses occur over long-distance power transmission.

- Limited Flexibility – Traditional grids are not optimised for integrating renewable energy sources

Many countries, including South Africa, are transitioning from traditional centralised grids to modern, decentralised energy systems to address climate change, energy security, and grid inefficiencies. Integrating renewables, smart grids, and energy storage is helping to create more flexible, sustainable, and efficient power networks [31].

2.6 Distribution Network Configuration

The distribution network delivers electricity from substations to end users, ensuring a reliable and efficient power supply. It is a critical part of the power system, bridging the gap between high-voltage transmission networks and consumers. The design and configuration of a distribution network influence power quality, system reliability, and operational efficiency [32]. A typical distribution network consists of the following components [32]:

- **Primary Distribution Network:** Operates at 11 kV – 33 kV, transporting electricity from substations to feeders.
- **Feeders:** Main lines that carry power to different locations within the network.
- **Distributors:** Branch out from feeders to supply electricity to different areas.
- **Service Mains:** Provide the final connection to residential, commercial, and industrial consumers.

Figure 2.17 illustrates a schematic distribution network diagram showing how power is delivered from the substation to end-users.

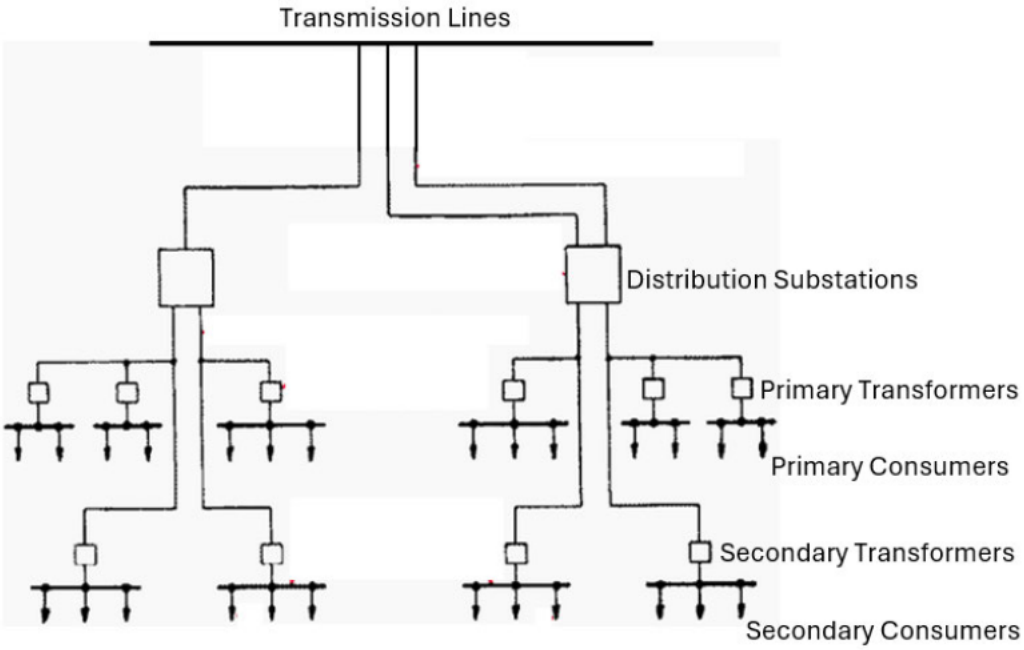

Figure 2.17: The structure of a typical distribution network [32].

Distribution networks can be classified into configurations based on their topology and power flow characteristics. The most common types are tabulated in Table 2.4.

Table 2.4: Analysis of the types of distribution system [32].

Characteristics	**Radial system**	**Ring Main System**	**Inter-connected system**
Substation quantity	A single substation feeds each feeder	Consist of a single substation	Consist of more than one substation
Feeder connection	No connection of any feeder with its adjacent feeder	Feeders are connected in the form of a loop	The feeder forms a ring
Supply to distributor	Each feeder is connected to a single distributor	Due to loop formation, each distributor will be fed by two feeders	Ring formation and supply from more than two substations leads to an uninterrupted power supply
Advantages	Cost-effective but less reliable.	Improve reliability but require additional investment.	They offer the highest reliability but are complex to manage.
Challenges	Less reliable, if a fault occurs, downstream consumers lose power	More expensive due to additional infrastructure requirements	Complex operation and higher costs. Used mainly in urban and industrial areas.

The choice of distribution network configuration depends on cost, reliability requirements, and load demand. While radial systems are the most common due to their simplicity, ring and mesh

networks offer better redundancy and fault tolerance. As South Africa modernises its power grid, transitioning to more resilient configurations will enhance system stability and efficiency. South Africa primarily uses a radial distribution network in rural areas due to its low cost and more straightforward design. In urban and industrial areas, a ring or interconnected system enhances reliability and minimises outages [32].

2.7.1 Loop Distribution Network

A loop (ring) distribution network is an electrical distribution system where power flows in a closed-loop configuration. This design allows electricity to be supplied from multiple directions, enhancing reliability and fault tolerance compared to radial systems. Figure 2.18 illustrates the structure of a loop distribution network, showing how power can be rerouted in case of a fault.

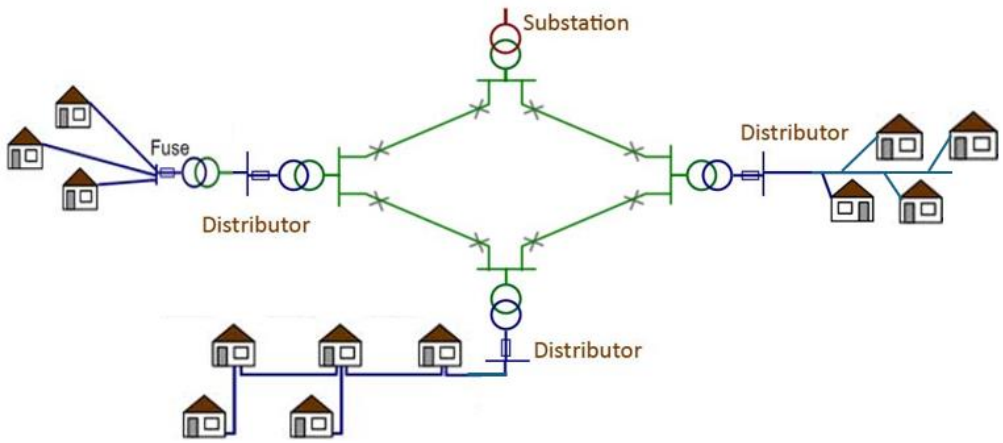

Figure 2.18: Diagram illustrating a typical Loop distribution system [32] .

From Figure 2.17, it is observed that the network consists of a continuous loop connecting substations and loads. Each consumer or distribution point can receive power from two or more directions. If a fault occurs at any point, the affected section can be isolated, and power can still be supplied from the alternate path.

A loop distribution network offers enhanced reliability, load balancing, and fault management, making it ideal for densely populated and high-demand areas. While it comes with higher costs and operational complexity, its benefits outweigh these challenges in regions requiring uninterrupted power supply. Loop distribution networks are commonly used in urban and industrial areas, where high power reliability and quality are essential. In South Africa, loop networks are employed in business districts, industrial zones, and regions with critical power demands, ensuring uninterrupted supply in case of localised faults [33].

2.7.2 Radial Distribution Network

A radial distribution network is the most straightforward and commonly used electrical distribution system, particularly in rural and suburban areas. In this configuration, power flows in one direction from the substation to consumers, with each feeder supplying electricity to multiple distribution points. Figure 2.19 illustrates a typical radial distribution network, showing its straightforward structure and power flow.

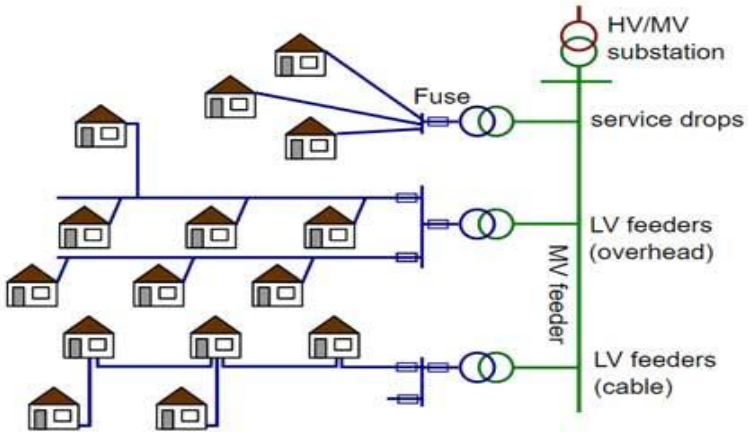

Figure 2.19: Diagram illustrating a radial distribution system [32].

Figure 2.18 shows that power originates from a single substation and is distributed through main feeders to different loads. Each consumer or distribution point is connected to only one power source, meaning a fault on a feeder affects all downstream customers. Power flow is unidirectional, simplifying control and protection compared to loop or mesh systems [34]. Radial distribution networks require fewer components, making them cheaper to install and maintain. The network can be easily extended to accommodate new loads. It is efficient for low-density areas with lower power demand. However, a fault on a feeder cuts off supply to all consumers downstream, making the network less reliable. The Power quality decreases over long distances, affecting end users, and there are no alternative supply routes in case of failures, requiring longer repair times [35].

2.7.3 Parallel Feeders Distribution System

A Parallel Feeders Distribution System is a configuration where multiple feeders run in parallel from the substation to the load centres, ensuring higher reliability and improved power supply capacity. This system is commonly used in areas with high power demand, such as industrial zones, commercial districts, and metropolitan areas. Figure 2.20 illustrates a typical parallel feeder distribution system. Multiple feeders originate from the same or different substations

and supply power to the same area or critical loads. If one feeder fails, power can be rerouted through an alternate feeder, minimising outages. The network is used to balance load distribution and prevent overloading of a single feeder.

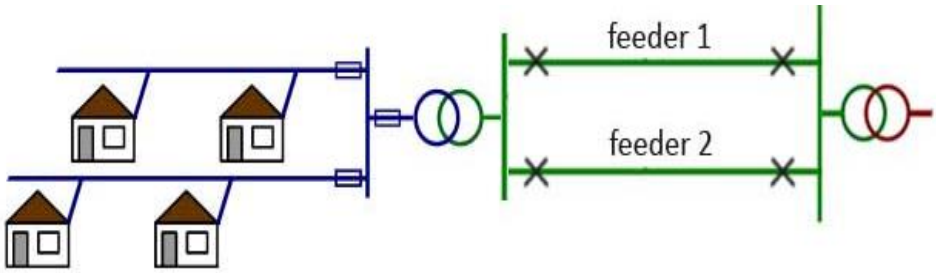

Figure 2.20: Diagram illustrating a parallel feeder distribution system [32].

A parallel feeder distribution system provides enhanced reliability, load balancing, and redundancy, making it ideal for high-demand areas. While it requires higher investment and operational complexity, its ability to minimise power disruptions makes it a valuable solution for critical infrastructure and economic hubs. Major cities like Johannesburg and Cape Town in South Africa utilise parallel feeders to ensure continuous power supply to essential services and businesses.

2.8 Distributed Generation

Distributed Generation (DG) refers to small-scale electricity generation that occurs near the point of consumption, reducing the need for long-distance power transmission. Unlike centralised power plants, which generate electricity at a large scale and distribute it via high-voltage transmission lines, DG systems are typically connected to the distribution network or serve individual consumers directly. Figure 2.21 illustrates the concept of distributed generation and its integration into the grid.

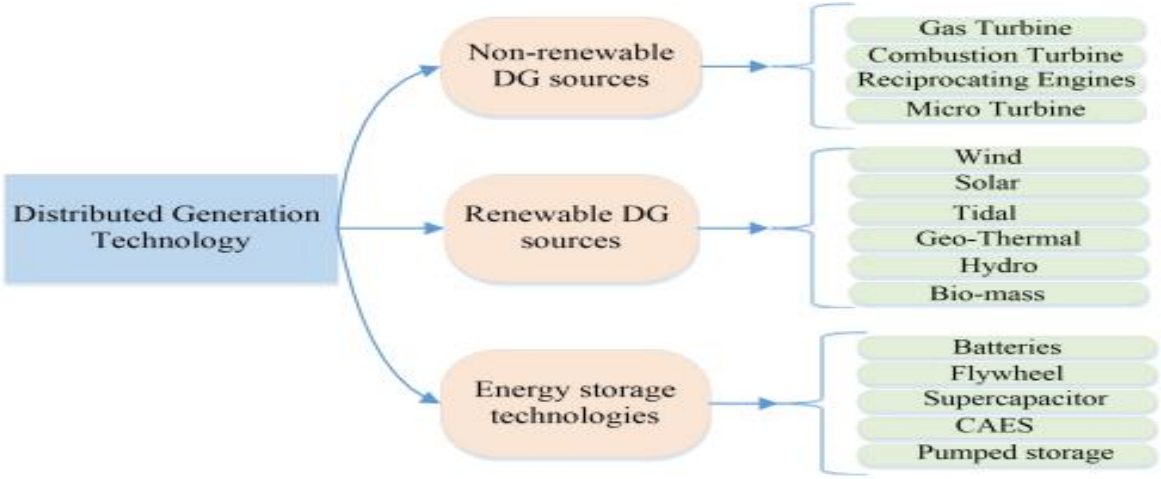

Figure 2.21: Distributed Generation Technologies [36].

Various professional organisations define DG based on size, location, and grid integration. The International Energy Agency (IEA) defines DG as generating plants supplying a customer on-site or supporting the network at distribution voltage levels [32]. The Institute of Electrical and Electronics Engineers (IEEE) describes DG as electricity generation from smaller units than centralised plants, capable of interconnection at almost any point in a network [37]. Despite differences, all definitions emphasise DG's decentralised nature and proximity to consumers. The characteristics and structure of DG systems are [37, 38]

- **Location:** DG units are positioned close to end-users, reducing transmission losses and enhancing grid efficiency.
- **Grid Connection:** Can operate grid-tied (integrated with the primary grid) or off-grid (standalone systems).
- **Scale:** Typically ranges from a few kilowatts (kW) to several megawatts (MW), serving residential, commercial, or industrial consumers.
- **Energy Sources**: Can be powered by renewables (solar PV, wind, biomass, small hydro) or conventional sources (gas turbines, diesel generators).

DG technologies can be classified into three categories, as shown in Figure 2.22:

- **Renewable DG Sources:** These include wind turbines, solar photovoltaic (PV), small hydropower, and biomass systems.
- **Non-renewable DG Sources:** Include diesel generators and fuel cells.
- **Energy Storage Systems (ESS):** Batteries and other storage technologies that enhance grid stability and reliability.

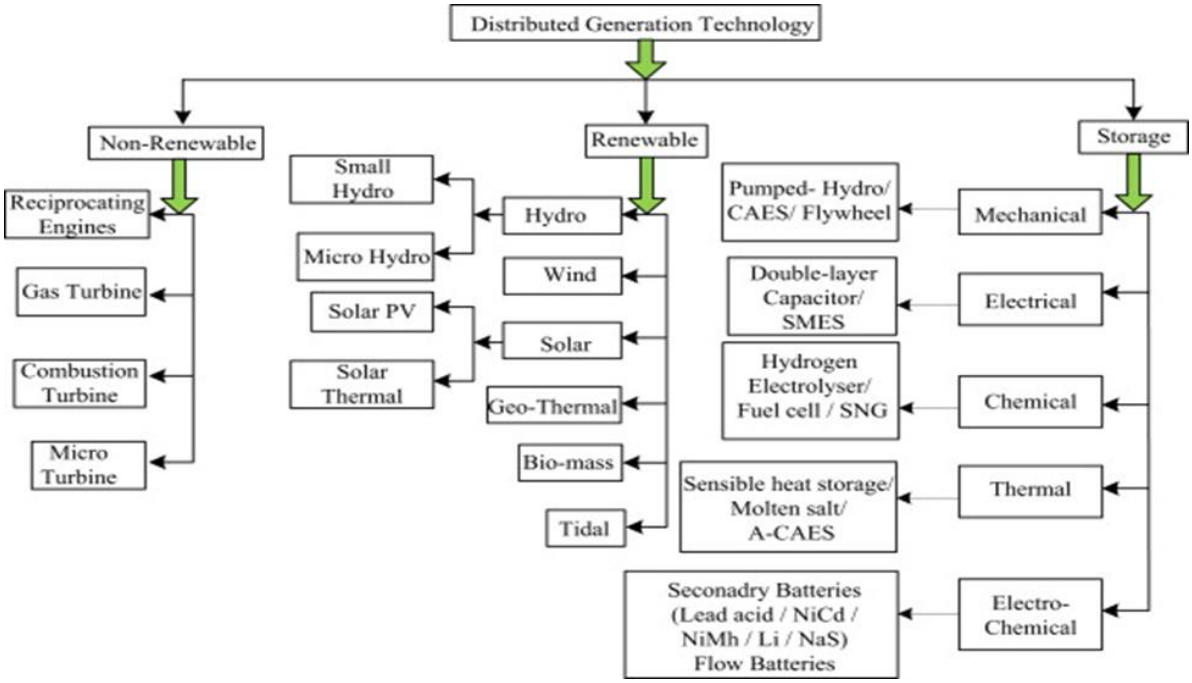

Figure 2.22: Classification of distributed generation technologies [38].

DG units can operate in two main configurations [38, 39]:

- **Islanded Mode:** The DG unit functions independently, supplying off-grid power to a specific site or community.
- **Grid-Connected Mode:** The DG unit is integrated with the primary grid at sub-transmission or distribution levels, allowing surplus power to be exported

2.8.1 Integration of DGs into the Distribution Network

Due to advancements in various DG technologies, DG technologies are expected to play a vital role in future energy generation. The International Energy Agency (IEA) highlights several key factors driving the increased adoption of distributed generation (DG) [40]:

- Technological advancements in DG systems.
- Growing demand for reliable electricity from consumers.
- Liberalization of electricity markets, allowing more competition.
- Climate change concerns, prompting a shift away from fossil fuels.
- Restrictions on new transmission line construction due to costs and land-use constraints.
- Uncertainty in fuel costs, increasing interest in energy diversification.

Solar PV and wind power deployment have grown significantly, making their optimal integration into the grid a key focus in the renewable energy industry. Besides their role as

clean energy sources, grid-connected solar and wind DG systems offer the following benefits [41]:

- **Improved Power Quality (PQ):** Enhances voltage stability and reduces network disturbances.
- **Reduced Active Power Losses:** Minimizes energy dissipation in the system.
- **Enhanced Reliability:** Provides additional power sources to support the grid during peak demand.

Among DG technologies, solar PV has a significant global footprint due to its inexhaustible energy source and environmental benefits. Similarly, wind energy has experienced rapid growth due to its potential to alleviate energy crises and its clean, renewable nature [42]. However, integrating DG into existing power networks introduces several challenges; existing grids may need upgrades to accommodate DG connections. Voltage regulation, frequency control, and system stability must be managed, and poor Power Quality (PQ) can negatively affect network loads, leading to voltage fluctuations, harmonic distortion, and grid instability [43]. Despite these challenges, DG is transforming modern power systems, enhancing energy security, reducing transmission losses, and promoting renewable energy adoption. While technical and regulatory challenges exist, DG remains a key solution for a more resilient, decentralised, and sustainable energy future in South Africa and globally.

2.9 Power Quality

The increasing demand for electricity and technological advancements have made power quality (PQ) a critical concern for modern electrical systems [44]. Utilities face significant challenges in ensuring a stable and high-quality power supply due to various factors, many of which are influenced by integrating new technologies. Several key aspects drive the importance of PQ. As society becomes more dependent on electrical power, even minor disruptions can have severe economic consequences, particularly for industrial customers where a short outage may result in substantial financial losses. Prolonged interruptions can affect nearly all aspects of modern society, emphasising the need for a stable and reliable power supply.

Furthermore, most industrial and residential processes now rely on electrical equipment that is highly sensitive to variations in power quality. The increasing use of sophisticated electronic devices, including those used in continuous-process industries and information technology systems, has heightened the demand for high-quality electrical power. Poor PQ can

significantly impact these devices' efficiency and operational life, leading to costly downtime and maintenance [44]. Additionally, the widespread adoption of power electronic devices such as variable speed drives, inverters, and computers has necessitated stricter compliance with PQ standards outlined in grid codes to prevent adverse effects on network performance.

The growing penetration of distributed generation (DG) systems, particularly those based on wind and solar energy, has also contributed to PQ challenges. The intermittent nature of these renewable energy sources results in fluctuating power outputs, which can introduce voltage and current disturbances in the grid. DG technologies utilise power electronic devices to ensure effective integration, which, while improving grid compatibility, also increases the likelihood of voltage and current harmonic distortions [45].

2.9.1 Frequency Variations

Frequency stability is a fundamental requirement for maintaining PQ in power systems. While frequency variations are relatively rare in well-regulated utility grids, they can occur in systems with inadequate infrastructure, high penetration of power electronics, or overloaded generation sources. Voltage source converters, commonly used in power systems, can cause frequency deviations due to their harmonic emissions. In weak power networks, frequency variations can become more pronounced, mainly when generators operate under high loads [46].

The permissible frequency ranges vary depending on regional grid codes and standards. According to the IEEE Standard 1547, the acceptable frequency range for electrical distribution systems is between 59.3 Hz and 60.5 Hz [47]. However, the South African grid code specifies an operating frequency range of 49 Hz to 51 Hz for all DG categories, with the nominal system frequency set at 50 Hz. This slight difference reflects regional operational standards tailored to local grid conditions [48]. Addressing frequency variation issues requires identifying sources of instability, upgrading power infrastructure, and implementing advanced frequency control mechanisms within DG systems [46].

2.9.2 Harmonics

The increased use of power electronic converters in modern electrical networks has increased harmonic distortions, negatively impacting PQ. Harmonics refer to voltage and current waveforms that deviate from their ideal sinusoidal shape due to multiple frequencies of the fundamental system frequency. In the case of South Africa, where the fundamental frequency

is 50 Hz, harmonics manifest as unwanted components that alter the waveform, reducing system efficiency and increasing losses [49].

Power electronic converters used in DG systems, particularly those interfacing wind and solar PV generators with the grid, are significant sources of harmonics. Other contributors include semiconductor-based switching devices and nonlinear loads such as motor drives, LED lighting, and uninterruptible power supply (UPS) systems [49]. The adverse effects of harmonics extend across the entire power network, from generation and transmission to distribution and end-user equipment. These effects include increased transformer and motor heating, waveform distortion leading to inefficient energy usage, and overloading of neutral conductors [49].

Regulatory bodies have established limits on harmonic distortion levels to mitigate their impact on power systems. According to IEEE Standard 1250, the maximum allowable Total Harmonic Distortion (THD) varies by voltage level [49].
$\leq$ 5% at 2.3 kV - 69 kV
$\leq$ 2.5% at 69 kV - 138 kV
$\leq$ 1.5% above 138 kV
Harmonic mitigation strategies include passive and active filters, optimised power electronic designs, and network-wide compensation techniques to improve PQ [50].

2.9.3 Voltage Fluctuations

Voltage fluctuations occur due to continuous or intermittent variations in voltage levels, often resulting from sudden changes in power demand or the integration of renewable energy sources. These fluctuations can degrade PQ by affecting the stability and efficiency of electrical networks. The variability of wind speeds directly impacts the voltage output of wind energy conversion systems (WECS), while solar PV systems experience fluctuations based on changes in solar irradiance. Such inconsistencies can lead to voltage profile instability, negatively affecting network operators and end-users [42, 51].

Voltage fluctuations are classified based on their duration. Long-duration variations persist for over one minute and may manifest as over or undervoltage. Overvoltage occurs when the root mean square (RMS) AC voltage exceeds 110% of the nominal system voltage for an extended period. In comparison, undervoltage occurs when RMS AC voltage drops below 90% of the

nominal voltage [42]. Common causes of long-duration variations include excessive load demand, system overloading, and switching operations within the network [46].

Short-duration voltage variations, on the other hand, last between 0.5 AC cycles and one minute. The energisation of large electrical loads with high starting currents, transformer inrush currents, or loose conductor connections often causes these. Unlike harmonics and steady-state waveform distortions, which persist for each cycle, short-duration variations typically result from transient disturbances in the system [46].

Mitigating voltage fluctuations requires deploying voltage regulation devices such as tap-changing transformers, automatic voltage regulators, and static VAR compensators. Advanced power system monitoring techniques, including innovative grid technologies, enable real-time voltage control and improve network stability. Proper system planning, incorporating robust network design and renewable energy forecasting, can further enhance voltage stability and reduce PQ issues associated with DG integration [46].

The increasing reliance on DG and power electronic devices has introduced new challenges in maintaining PQ. Frequency variations, harmonic distortions, and voltage fluctuations present challenges to grid stability, equipment performance, and energy efficiency. Effective regulatory compliance, system upgrades, and advanced PQ monitoring technologies are essential for maintaining a stable and reliable power system [42, 51].

2.10 Grid Code for Renewable Energy Integration

The grid code establishes a comprehensive set of technical, operational, and safety requirements for integrating renewable energy sources into the power system. As DG penetration increases, ensuring compatibility between intermittent renewable energy sources, such as solar PV and wind energy, and the existing grid infrastructure becomes critical in maintaining power system stability and reliability. The grid code defines the conditions under which renewable energy plants connect, operate, and interact with the utility grid, ensuring that these systems do not negatively impact power quality, grid security, or overall system stability [52].

The primary objectives of the grid code for renewable energy integration include [53]:

- Ensuring the safe and stable operation of the power system when integrating renewable energy sources.

- Defining the technical requirements for connecting DG units to the grid, including voltage and frequency regulations.
- Establishing performance standards for renewable energy generation, such as reactive power control and fault ride-through capability.
- Protecting grid infrastructure from disturbances caused by variable renewable energy generation.
- Facilitating fair and transparent market participation for renewable energy generators [53].

The grid code classifies DG units into different categories, each with specific requirements for grid integration. Table 2.5 summarizes the grid code requirements for each DG category. Grid-connected renewable energy systems must comply with technical and operational requirements outlined in national and international grid codes. These requirements cover voltage and frequency control, power factor regulation, fault ride-through capability, and power quality standards.

Table 2.5: The summary of grid code requirements for each DG category [40].

Category	**A1**	**A2**	**A3**	**B**		**C**
Output power [KVA]	0 – 13.8	13.8 - 100	100 -1000	>1000 - 20000		>20000
Voltage level	LV			MV		MV/HV
Operating frequency		49-51Hz				
Operating voltage range	-15 to + 10%				±5%	
Operating power range		20 -100%				
Low voltage ride through	60% for 0.15s				0% for 0.15s	
High voltage ride through	N/A				120% for 2s	
Power factor operating range (leading and lagging)	0.95			0.975		0.95

Renewable energy sources must operate within specified frequency limits to prevent instability in the power network. In South Africa, the nominal system frequency is 50 Hz, with grid code regulations requiring DG units to remain operational within an allowable range depending on their category. Figure 2.23 illustrates the acceptable frequency ranges of DG units during a frequency disturbance. The frequency tolerance requirements ensure that DG units remain

connected during minor frequency deviations while disconnecting safely during major disturbances to prevent cascading failures in the grid [54].

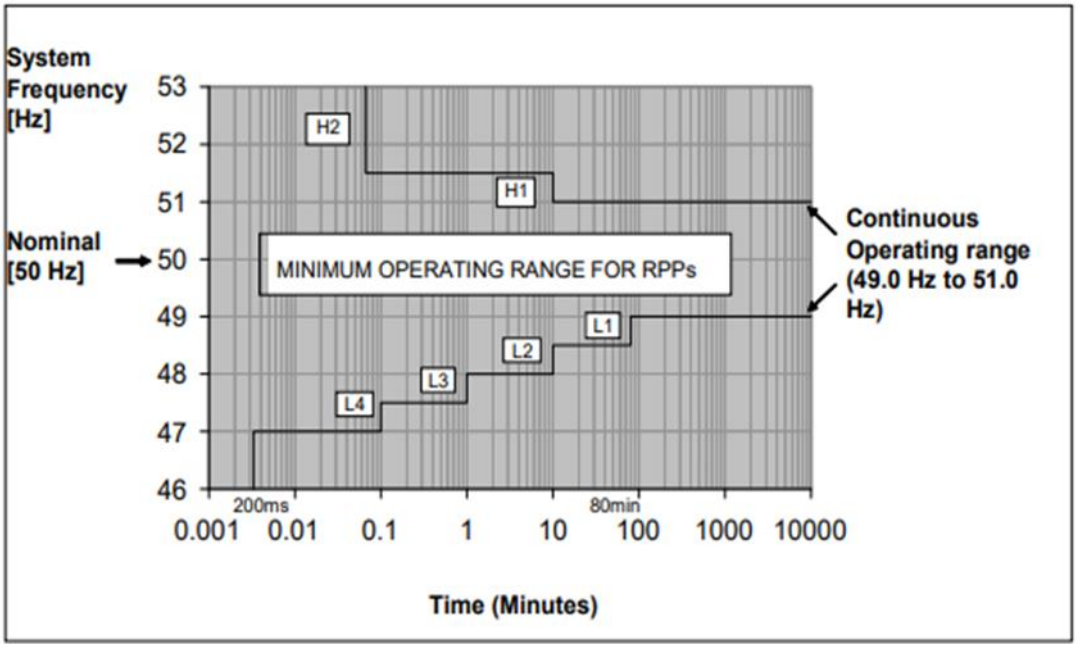

Figure 2.23: The acceptable frequency ranges of DG units during a frequency disturbance [52].

Voltage ride-through (VRT) capability ensures that DG units can withstand temporary voltage disturbances without immediate disconnection. The grid code defines specific VRT requirements based on the category of the DG unit. For low and medium voltage DG units (Categories A1 and A2), the ride-through capability is limited, meaning they may disconnect sooner during significant voltage disturbances. Figure 2.24 illustrates the VRT capability for these DG units.

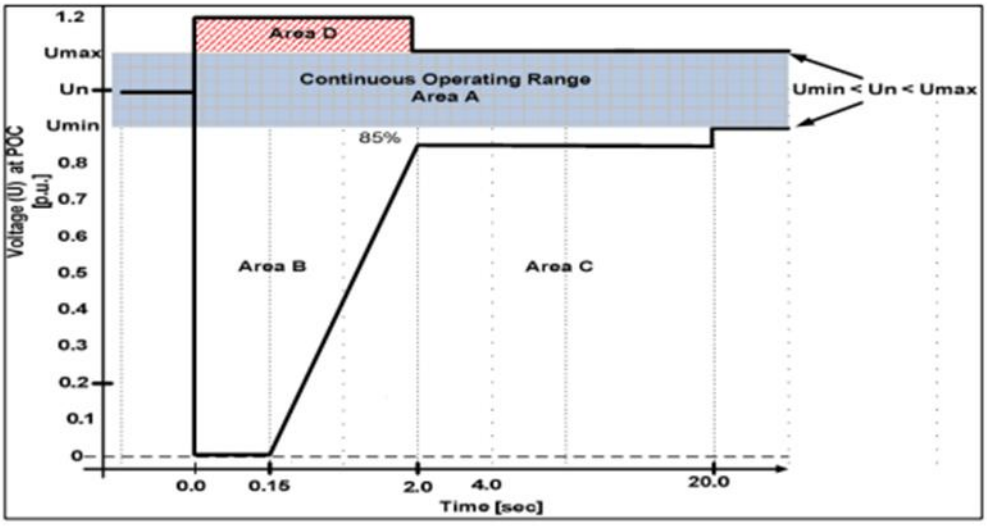

Figure 2.24: Voltage-ride-through capability of DGs in category A1 and A2 [52].

For high voltage and extra-high voltage DG units (Categories A3, B, and C), the grid code mandates stricter VRT requirements. These DGs must remain connected during transient voltage dips and support system recovery. Figure 2.25 depicts the VRT capability of these DG technologies [52].

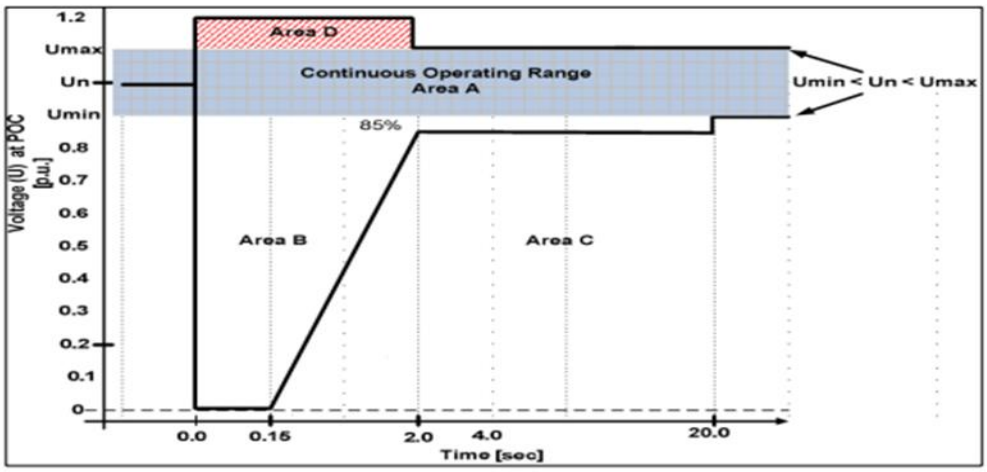

Figure 2.25: Voltage-ride-through capabilities for the DG technologies of category A3, B and C [52].

By enforcing VRT requirements, the grid code ensures that DG units contribute to system stability rather than exacerbating voltage disturbances [55]. To maintain grid voltage stability, renewable energy generators must support reactive power compensation. The grid code specifies that DG units must operate at a power factor close to unity (1.0) or within a prescribed range (e.g., 0.95 lagging to 0.95 leading). Larger DG plants are also required to participate in voltage regulation by adjusting reactive power output [56].

Renewable energy generators must adhere to harmonic distortion limits, flicker levels, and voltage fluctuation constraints to prevent PQ issues. The grid code mandates compliance with IEEE Standard 519, which specifies maximum allowable total harmonic distortion (THD) based on voltage level. Excessive harmonics from power electronic converters used in wind and solar systems can lead to waveform distortions, negatively impacting both grid stability and end-user equipment [57].

In South Africa, the Grid Connection Code for Renewable Power Plants (RPPs) defines the technical and operational standards for renewable energy integration. This grid code applies to all wind, solar PV, biomass, and hydroelectric plants connected to the national grid at transmission or distribution voltage levels. Key compliance requirements include:

- Voltage and frequency regulation to maintain grid stability.
- Reactive power and power factor control to support voltage regulation.

- Fault ride-through capabilities to prevent widespread system instability.
- Harmonic distortion limits to maintain power quality.

Grid codes for renewable energy integration play a crucial role in ensuring the stability, reliability, and efficiency of modern power networks. By defining requirements for frequency tolerance, voltage ride-through, reactive power control, and power quality compliance, these codes help maintain grid security and accommodate increasing levels of distributed generation.

2.11 Reliability of Distribution Systems Integrated with DGs

The reliability of a distribution system refers to its ability to deliver continuous and stable power to consumers while minimizing outages and disruptions. With the increasing integration of DG, assessing and improving the reliability performance of modern distribution networks has become a critical concern. DGs, particularly solar PV and wind power, offer advantages such as reducing transmission losses, supporting peak demand, and enhancing energy security. However, their intermittent nature and grid integration challenges necessitate careful planning and system reliability analysis [53].

The integration of REs introduces several technical, operational, and economic challenges to distribution system reliability. These challenges can be categorized into four key areas, as illustrated in Figure 2.26.

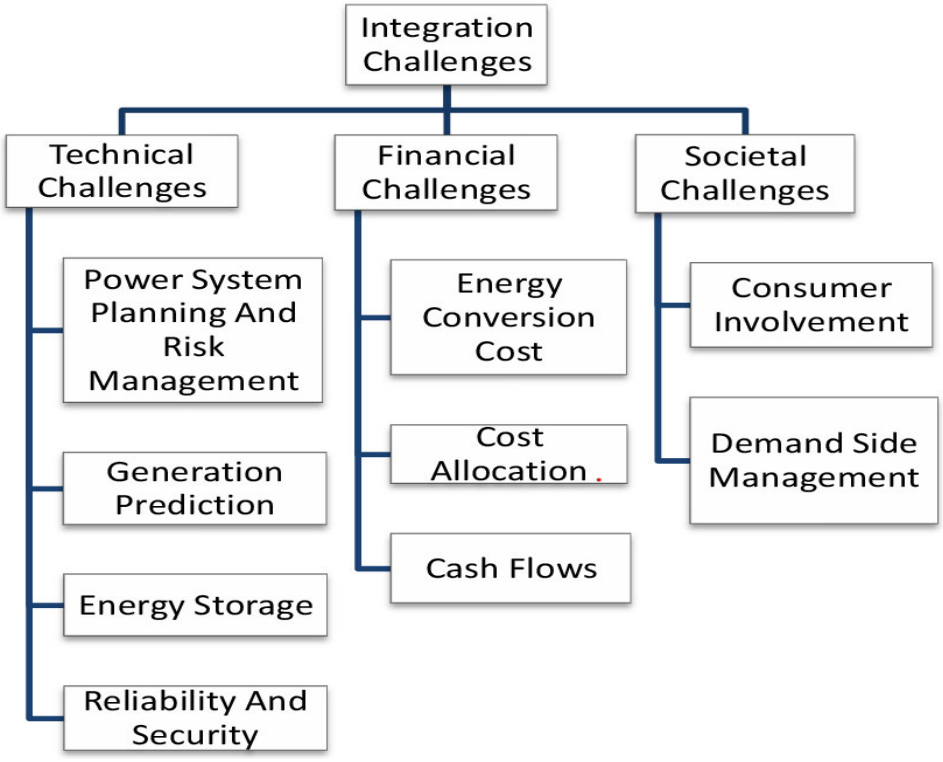

Figure 2.26: Classification of potential challenges in integration of Res [53].

The major challenges affecting reliability include power quality issues, protection system coordination, grid stability concerns, and operational uncertainties [58]. Addressing these challenges is essential to ensure that DG-integrated networks maintain high reliability levels while accommodating increasing shares of renewable energy. Integrating DG into a distribution network significantly affects reliability metrics by influencing power availability, fault response, and system performance. The effects of DG penetration on system reliability can be categorized into positive and negative impacts:

- **Positive Impact:**
- DG integration enhances reliability by reducing transmission constraints and improving voltage stability, especially in remote areas with weak grid infrastructure.
- By supplying power closer to the demand centers, DGs help reduce dependency on long-distance transmission lines, thereby minimizing transmission losses and voltage drops.
- Additionally, during grid outages, DGs operating in island mode can maintain power supply to critical loads, improving system resilience.
- **Negative Impact:**
- DG integration also presents challenges that may compromise reliability.
- The variability of solar and wind power leads to fluctuating power outputs, which can cause voltage instability, frequency deviations, and power quality disturbances.
- Moreover, uncoordinated DG penetration may lead to reverse power flow issues, requiring advanced protection and control strategies.

The reliability of a distribution network is typically evaluated using quantitative reliability indices. The commonly used indices include:

- **System Average Interruption Frequency Index (SAIFI):** Measures the average number of power interruptions per consumer per year. A lower SAIFI indicates better reliability.
- **System Average Interruption Duration Index (SAIDI):** Represents the total duration of power interruptions per consumer per year. It highlights the severity of outages.
- **Customer Average Interruption Duration Index (CAIDI):** Provides the average duration of an outage experienced by consumers.
- **Average Service Availability Index (ASAI):** Measures the percentage of time the system is available to consumers.

- **Expected Energy Not Supplied (EENS):** Quantifies the amount of energy lost due to system failures.

The presence of DGs can influence these indices positively or negatively, depending on their location, dispatchability, and reliability. Proper DG placement can reduce SAIFI and SAIDI values, whereas poor DG integration may lead to frequent voltage violations and system instability [59]. To improve reliability in DG-integrated distribution networks, the following strategies can be adopted:

1. Optimized DG Placement and Sizing

Proper placement and sizing of DG units ensures they provide maximum reliability benefits by reducing feeder congestion and enhancing voltage profiles.

2. Energy Storage Systems (ESS)

Integrating battery energy storage systems (BESS) with DGs mitigates the intermittency of solar and wind power, thereby ensuring continuous power supply during low-generation periods.

3. Advanced Protection Schemes

Traditional overcurrent protection devices may not function effectively in bidirectional power flow scenarios. Upgrading to adaptive protection systems helps mitigate false tripping and miscoordination issues.

4. Microgrid Implementation

The formation of microgrids, where DG units operate autonomously during main grid failures, enhances the self-sufficiency and resilience of distribution networks.

5. Smart Grid Technologies

Deploying real-time monitoring, automated fault detection, and intelligent switching systems allows proactive fault prevention and faster restoration of supply.

2.12 Conclusion

In South Africa, the reliability of distribution systems is a major concern due to aging infrastructure, load shedding, and increasing renewable energy penetration. The reliability of distribution networks integrated with DGs depends on various factors, including DG placement, power output stability, and system protection coordination. While DGs can enhance reliability by reducing transmission losses and providing backup power, they also introduce challenges such as voltage instability and intermittent generation. Implementing advanced control strategies, energy storage solutions, and smart grid technologies can significantly

improve system reliability, ensuring a stable and resilient power supply, particularly in regions with high renewable energy penetration.

Chapter 3

Numerical Modelling

This chapter presents an in-depth discussion on power system reliability, emphasizing the impact of distributed generation (DG) integration. The chapter outlines reliability indices, evaluation techniques, modelling approaches, and optimization techniques for DG placement. Various methodologies, including Markov models, Monte Carlo simulations, Failure Mode and Effect Analysis (FMEA), and Newton-Raphson load flow analysis, are explored. Furthermore, the modelling of solar PV and wind energy conversion systems is presented, along with Particle Swarm Optimization (PSO) for optimal DG placement.

3.1 Power System Reliability

Power system reliability refers to the ability of an electrical network to consistently deliver power without unexpected failures or service interruptions. As energy demand grows, distribution networks face increasing challenges in maintaining stable power supply, particularly with the integration of renewable energy-based DG. Ensuring a reliable distribution network requires proper DG planning, grid reinforcement, and advanced optimization techniques [60]. Figure 3.1 illustrates a typical power system network from the point of generation to the end-user.

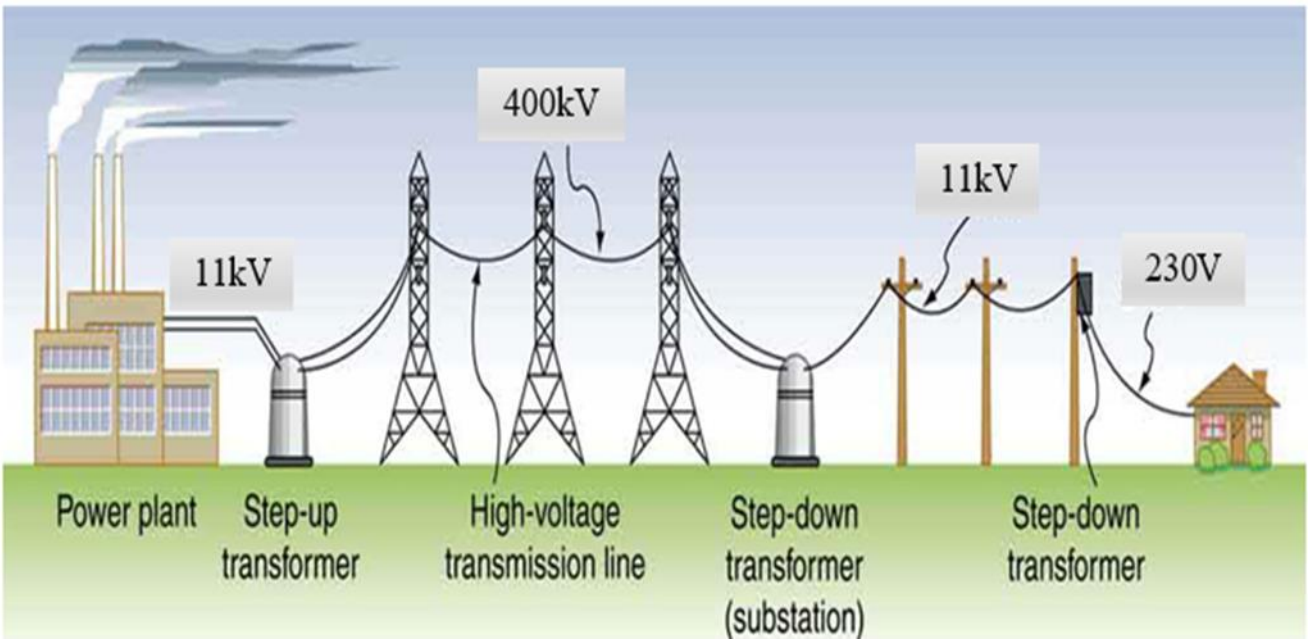

Figure 3.1: Typical power system [61].

The fundamental objective of distribution systems is to provide electricity to consumers. However, the integration of DG units, particularly renewable energy-based DGs, alters the operational characteristics of distribution networks due to bidirectional power flows. If improperly sized or located, DGs can introduce power losses, voltage fluctuations, and stability issues. Therefore, effective DG planning, sizing, and placement are crucial to ensuring a stable, efficient, and reliable power distribution system [61].

The global demand for electrical power is rapidly increasing, whereas generation capacity is expanding at a slower pace. One approach to bridging this gap is the deployment of DGs near load centres. The integration of DGs provides multiple benefits, including loss reduction, voltage profile enhancement, and improved system reliability. Additionally, DGs help reduce operational costs, are easier to install, and have lower capital investment requirements compared to conventional power plants [60]. Despite these benefits, the high penetration of DGs introduces challenges such as reverse power flow, voltage rise and increased operational complexity. To maintain system stability and reliability, it is essential to perform reliability assessments and adopt optimal DG placement strategies that minimize power losses, improve voltage stability, and enhance overall grid performance.

3.2 Reliability Indices

Reliability assessment is fundamental to evaluating power system performance. Power supply interruptions occur due to component failures, and reliability indices are used to quantify the frequency, duration, and severity of these interruptions [62]. Reliability indices are categorized into Load Point Reliability Indices and System Reliability Indices.

3.2.1 Load Point Reliability Indices

These indices assess reliability at specific load points in the distribution network. The commonly used indices include:

- **Failure rate (λ):** Probability of a component failing over a specific period.

  The reliability index is assessed as the probability of failure occurrence during a specific period for load point [62]. This index is the load point average interruptions caused by system components failure in a period, and is evaluated with (3.1) [62]:

$$\lambda = \sum_{i=1}^{N} \lambda_i \tag{3.1}$$

Where,

λ is the failure rate of the series components from the source point to load point and λ_i is the failure rate of the i^{th} component.

- **Average outage time** *(U)*: The expected total outage time per load point per year.

  This index is the average interruption time of load point in a specific period [63]. This index reflects average customer interruption hours in a period. The higher this value, the less reliable the system supplies power to this load point. The average interruption time of a network composed of *N* components with series structure can be given by (3.2) [63].

$$U = \sum_{i=1}^{N} \lambda_i r_i \tag{3.2}$$

Where,

r_i is average restoration time of network component i^{th} and *U* is the corresponding repair time.

- **Average interruption duration time** (r): The mean time required to restore service after an outage. For a network composed of N components with series structure, the average interruption duration time can be evaluated with (3.3) [63]:

$$r = \frac{U}{\lambda} \frac{\sum_{i=1}^{N} \lambda_i r_i}{\sum_{i=1}^{N} \lambda_i} \tag{3.3}$$

3.2.2 System Reliability Indices

System reliability indices quantify the overall power supply reliability of a distribution system. These indices are widely used, primarily focusing on customer satisfaction. Some indices are presented in pairs, where the "System" (S) variant represents an average across all customers, while the "Customer" (C) variant applies only to affected customers, those who experienced at least one interruption [64] . These indices are typically calculated over a defined period, usually a year. Common reliability indices include the System Average Interruption Frequency Index (SAIFI), System Average Interruption Duration Index (SAIDI), Customer Average Interruption Frequency Index (CAIFI), Customer Average Interruption Duration Index (CAIDI), and Average Service Availability Index (ASAI).

- **The System Average Interruption Duration Index** (SAIDI) is a widely used metric for assessing the average duration of power interruptions experienced by customers. It

quantifies the total duration of sustained interruptions per customer over a one-year period [64]. SAIDI is calculated using (3.4) [63]:

$$\text{SAIDI} = \frac{Sum\ of\ customers\ interrpted\ duration}{Total\ number\ of\ customer\ served}$$

$$SAIDI = \frac{\sum_{i=1}^{N} U_i N_i}{\sum_{i=1}^{N} N_i} \tag{3.4}$$

- **System Average Interruption Frequency Index** (SAIFI) represents the average number of power interruptions per customer. It quantifies the frequency of sustained interruptions that customers experience over a one-year period [63]. SAIFI is calculated (3.5) [63]:

$$\text{SAIFI} = \frac{Total\ number\ of\ customers\ interrpted.}{Total\ number\ of\ customer\ served}$$

$$SAIFI = \frac{\sum_{i=1}^{N} \lambda_i N_i}{\sum_{i=1}^{N} N_i} \tag{3.5}$$

Where,

N_i is number of customers per load point.

- **The Customer Average Interruption Frequency Index (CAIFI)** represents the average number of interruptions experienced by customers who encountered at least one interruption during the analysis period. It is calculated by dividing the total number of interruptions by the total number of affected customers within the analysed system as indicated in (3.6) [63]. This index provides insight into the reliability of service for impacted customers.

$$\text{CAIFI} = \frac{Number\ of\ customers\ interrpted.}{Total\ number\ of\ customer\ served\ who\ had\ at\ least\ one\ interruption}$$

$$CAIFI = \frac{\sum_{i=1}^{N} N}{N_T} \tag{3.6}$$

- **The Customer Average Interruption Duration Index** (CAIDI) represents the average duration of power outages experienced by affected customers. It indicates the

typical time required to restore service after an interruption. CAIDI is calculated using (3.7) [63].

$$\text{CAIDI} = \frac{Sum\ of\ customers\ interrpted\ duration}{Total\ number\ of\ customer\ interrupted.}$$

$$CAIDI = \frac{\sum_{i=1}^{N} U_i N_i}{\sum_{i=1}^{N} \lambda_i N_i} = \frac{SAIDI}{SAIFI} \tag{3.7}$$

- **The Average Service Availability Index** (ASAI) measures the percentage of time an electric power system successfully supplies service compared to the total requested hours. It reflects the probability of all loads being served within a given period and is calculated with (3.8) [63].

$$\text{ASAI} = \frac{Customer\ hours\ of\ available\ service}{Customer\ hours\ demand}$$

$$ASAI = \frac{\sum_{i=1}^{N} N_i \times 8760 - \sum_{i=1}^{N} U_i N_I}{\sum_{i=1}^{N} N_i \times 8760} \tag{3.8}$$

- **Expected Energy Not Supplied (EENS)** quantifies the total amount of energy expected to be undelivered to loads due to interruptions, using (3.9) [63].

$$\text{EENS} = \frac{Total\ energy\ not\ supplied}{Total\ number\ of\ customer\ served.}$$

$$EENS = \frac{\sum_{i=1}^{N} L_i U_i}{\sum_{i=1}^{N} N_i} \tag{3.9}$$

3.3 Reliability Evaluation Techniques

This section outlines commonly used reliability evaluation methodologies for power distribution systems. Reliability can be assessed using two main techniques: analytical and simulation methods:

Analytical methods involve mathematical models and probabilistic calculations to estimate system reliability indices. These models provide approximate solutions, particularly in

complex networks, by evaluating failure probabilities, repair rates, and load distribution. While computationally efficient, analytical techniques may be less accurate for large, non-linear systems where uncertainties play a significant role [65].

Simulation-based methods offer a more realistic approach by replicating the random behaviour of power system components under different operational conditions. These methods allow system operators to analyze various failure scenarios, system responses, and corrective actions. Although simulation approaches require higher computational effort, they provide detailed insights into system reliability [66].

3.3.1 Reliability Evaluation Techniques: Analytical

3.3.1.1 Markov Models

Markov models are widely used in quantitative reliability analysis, as they effectively model system states and transitions between failure and repair conditions. These models represent the dynamic evolution of system components over time and enable the estimation of failure probabilities, repair times, and system downtime [67]. The classification of Markov-based models depends on the degree of observability and whether the system operates autonomously or requires control adjustments. Table 3.1 presents the classification of Markov models based on these factors.

Table 3.1: Markov model approach

	System state is fully observable	**System state is partially observable**
System is autonomous	Markov chain	Hidden Markov model
System is controlled	Markov decision process	Partially observable Markov decision process

The common Markov-based models include:

- **Markov Chains:** A fundamental model where the current state depends only on the previous state and not on past events.
- **Hidden Markov Models**: Used when system states are not fully observable but can be inferred from available data.
- **Markov Decision Processes:** Applied in scenarios where control decisions influence system transitions.

- **Partially Observable Markov Decision Processes (POMDPs):** Suitable for systems where both control actions and uncertainty in state observations exist

3.3.2 Reliability Evaluation Techniques: Simulation

3.3.2.1 Monte Carlo Simulation

Monte Carlo simulation is one of the most widely used techniques in power system reliability analysis. This method randomly samples possible system states and evaluates performance over multiple iterations to generate probabilistic reliability indices. It is useful for modeling complex systems with multiple failure modes and uncertainties [65**]**. The technique provides accurate estimates for failure rates, downtime, and energy not supplied (EENS).

There are two types of Monte Carlo simulation methods: Non-Sequential Methods and Sequential Methods.

Non-Sequential Methods

The non-sequential Monte Carlo method simulates system states randomly over its lifespan without considering time progression. The service period is reproduced multiple times to obtain statistically reliable averages. System states depend on the combination of component states, determined probabilistically. Two main non-sequential techniques are used in power system reliability evaluation [65]:

State Sampling Approach

- System states are obtained by randomly sampling component states without considering event chronology.
- A random number generator determines component states (up/down) based on forced unavailability.
- If an abnormal state occurs, load curtailment is assessed.
- The process is repeated until statistical variation falls below a threshold.
- This method cannot accurately determine frequency indices.

State Transition Sampling Approach

- System indices are calculated based on system state transitions rather than component states.
- The initial state assumes all components are operational (up state).
- Component state transitions trigger system state transitions assessed using random number generation.

- A long sequence of transitions is required for accurate index evaluation.
- The process stops when statistical variation meets a predefined criterion.
- This method is more time-consuming but provides accurate frequency indices.

Sequential Monte Carlo Simulation

In this method, chronological state transitions are generated for all components based on their state duration distribution functions. Unlike non-sequential techniques, sequential Monte Carlo considers the time-dependent behaviour of components. Any type of distribution function can be applied. The procedure for Reliability Evaluation follows [66]:

- The initial state of each component (up/down) is assumed.
- Chronological state sequences for each component are determined.
- The system state sequence is obtained by combining individual component states.
- Reliability indices are computed based on the system state transitions.
- Steps (1–4) are repeated until the coefficient of variation for a specified index meets the criterion.

This method provides accurate frequency indices but requires significant computational time and memory. It also depends on detailed component state duration distributions. In this study, the Monte Carlo simulation algorithm was applied to the test distribution network using the sequential Monte Carlo method.

3.4 Failure Mode and Effect Analysis (FMEA)

Failure Mode and Effect Analysis (FMEA) is a structured approach for identifying potential failure modes in a system and evaluating their consequences. This technique allows engineers to prioritize failure modes based on severity, frequency, and detectability [67].

3.4.1 Classes of FMEA analysis

- Design Failure Mode and Effects Analysis (DFMEA): Focuses on potential failures in system design before implementation.
- Process Failure Mode and Effects Analysis (PFMEA): Evaluates potential risks associated with operational processes.
- Functional Failure Mode and Effects Analysis (FFMEA): Assesses failure modes in terms of system functionality and performance.

3.5 Load Flow Analysis: Newton-Rapson Technique

Load flow analysis is essential for evaluating voltage profiles, power losses, and system stability. Among various techniques shown in Table 3.2, the Newton-Raphson (NR) method is widely preferred due to its high accuracy and fast convergence . Unlike other methods, the NR method effectively handles non-linear load flow equations with fewer iterations, making it suitable for large-scale power systems [68].

Table: 3.2 Comparison of the Load Flow Methods

Load flow method	Speed	Accuracy	Solution Robustness
Gauss-Seidel	Very Slow	Approximate	Robust
Newton Raphson	Slow	Accurate	Robust
Fast Decoupled	Fast	Accurate	Less Robust

The NR method transforms non-linear equations into linear ones, solving them efficiently using iterative techniques. Its convergence is independent of the number of buses, requiring fewer iterations for power flow calculations [69]. NR's characteristic graph is shown in Figure 3.3.

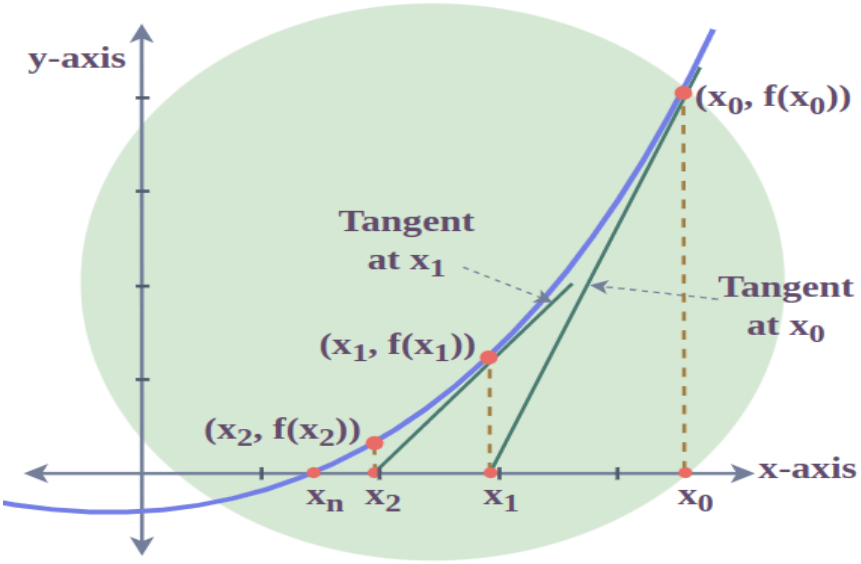

Figure 3.3: Newton-Raphson characteristic graph [70] .

The NR method applies Taylor series expansion to approximate solutions iteratively. Given a non-linear function $f(x)$, the iterative solution follows [70]:

$$f(x) = 0 \tag{3.10}$$

Since $f(x)$ is non-linear direct solutions are not possible, requiring an iterative approach (3.11) [71].

$$x = x^0 + \Delta x^0 \tag{3.11}$$

The function is rewritten as shown in (3.12) and expanded using the Taylor series (3.13)-(3.14).

$$f(x^0 + \Delta x^0) = 0 \tag{3.12}$$

$$f(x^0) + f'(x^0)\Delta x^0 + f''(x^0)\frac{(\Delta x^0)^2}{2!} + \ldots\ldots\ldots + \tag{3.13}$$

$$f^n(x^n)\frac{(\Delta x^0)^2}{n!} + \ldots\ldots\ldots = 0 \tag{3.14}$$

Where,

$f'(x^0), \ldots\ldots\ldots f^n(x^0)$ are the derivatives of $f(x)$

If the difference between iterations is small, higher-order terms are neglected, resulting in a linearized form (3.15) [72].

$$f(x^0) + f'(x^0)\Delta x^0 = 0 \tag{3.15}$$

The initial solution is derived using (3.16), and the new solution is obtained iteratively as shown in (3.17).

$$\Delta x^0 = -\frac{f(x^0)}{f'(x^0)} \tag{3.16}$$

$$x^1 = x^0 + \Delta x^0 \tag{3.17}$$

$$x^1 = x^0 - \frac{f(x^0)}{f'(x^0)}$$

The iterative equation follows (3.18), and this process continues until the error is within a predetermined tolerance.

$$x^{k+1} = x^k + \Delta x^k \tag{3.18}$$

$$= x^k - \frac{f(x^k)}{f'(x^k)}$$

For a set of non-linear equations, the general solution is given by (3.19) [73].

$F(X^K) = -J^K \Delta X^K$, and $X^{K+1} = X^K + \Delta X^K$ (3.19)

Where,

J is the Jacobian matrix, containing all derivative elements.

The NR method can be implemented using either rectangular or polar coordinates for load flow analysis.

Rectangular Coordinates:

The general power flow equation, along with voltage, active, and reactive power equations, is given by (3.20)-(3.22) [74].

$$V_i^* = e_i + jf_i \tag{3.20}$$

$$P_i = e_i \sum_{j=1}^{n} (G_{ij} e_j - B_{ij} f_j) + f_i \sum_{j=1}^{n} (G_{ij} f_j + B_{ij} e_j) \tag{3.21}$$

$$Q_i = f_i \sum_{j=1}^{n} (G_{ij} e_j - B_{ij} f_j) - e_i \sum_{j=1}^{n} (G_{ij} f_j + B_{ij} e_j) \tag{3.22}$$

Where,

G_{ij} and B_{ij} refers to conductance and susceptance of the bus system.

The correction equation for power mismatch is formulated as (3.23).

$$\Delta F = -J \Delta V \tag{3.23}$$

Where,

ΔF is a matrix containing real powers $\Delta P_{i's}$, $\Delta Q_{i's}$ and $\Delta V_{i's}$.ΔV is the matrix containing $\Delta e_{i's}$ and $\Delta f_{i's}$ and The *Jacobian* matrix consists of partial derivatives of real and reactive powers with respect to voltage magnitude and phase angle [73].

Polar Coordinates:

The voltage magnitude equation and real/reactive power equations are represented in (3.24)-(3.26).

$$V_i^* = V_i(\cos\theta + j \sin\theta) \tag{3.24}$$

$$P_i = V_i \sum_{j=1}^{n} V_j (G_{ij} \cos\theta_{ij} + B_{ij} \sin\theta_{ij}) \tag{3.25}$$

$$Q_i = V_i \sum_{j=1}^{n} V_j (B_{ij} \cos\theta_{ij} + G_{ij} \sin\theta_{ij}) \tag{3.26}$$

Where,

$\theta_{ij} = \theta_i - \theta_j$ and is the angle difference between bus i and bus j.

Jacobian Matrix Formation

The phase angle difference between buses is shown in (3.27) and the *Jacobian* matrix is structured as shown in (3.28)-(3.32).

$$\begin{bmatrix}\Delta P\\ \Delta Q\end{bmatrix}=-J\begin{bmatrix}\Delta\theta\\ \Delta V/V\end{bmatrix}\text{ or }\begin{bmatrix}\Delta P\\ \Delta Q\end{bmatrix}=-J\begin{bmatrix}H & N\\ K & L\end{bmatrix}\begin{bmatrix}\Delta\theta\\ V_D^{-1}\Delta V\end{bmatrix} \tag{3.27}$$

$$\begin{bmatrix}\Delta P\\ \Delta Q\end{bmatrix}=\begin{bmatrix}J_1 & J_2\\ J_3 & J_4\end{bmatrix}\text{where }\Delta P=\begin{bmatrix}\Delta P_1\\ \Delta P_2\\ .....\\ .....\\ .....\\ \Delta P_{n-1}\end{bmatrix},\Delta Q=\begin{bmatrix}\Delta Q_1\\ \Delta Q_2\\ .....\\ .....\\ .....\\ \Delta Q_m\end{bmatrix},\Delta\theta=\begin{bmatrix}\Delta\theta_1\\ \Delta\theta_2\\ .....\\ .....\\ .....\\ \Delta\theta_{n-1}\end{bmatrix},\Delta V=\begin{bmatrix}\Delta V_1\\ \Delta V_2\\ .....\\ .....\\ .....\\ \Delta V_m\end{bmatrix}\text{ and} \tag{3.28}$$

$$V_D=\begin{bmatrix}V_1 & . & .\\ . & V_2 & .\\ . & . & V_m\end{bmatrix} \tag{3.29}$$

H is a $(n-1)\times(n-1)$ matrix, and its element is $H_{ij}=\dfrac{\partial\Delta P_i}{\partial\theta_j}$

N is a $(n-1)\times m$ matrix, and its element is $N_{ij}=V_j\dfrac{\partial\Delta P_i}{\partial V_j}$ (3.30)

K is a $m\times(n-1)$ matrix, and its element is $K_{ij}=\dfrac{\partial\Delta Q_i}{\partial\theta_j}$ (3.31)

L is a $m\times m$ matrix, and its element is $L_{ij}=V_j\dfrac{\partial\Delta Q_i}{\partial V_j}$ (3.32)

These parameters are the defining one in forming Jacobian matrix and hence to perform load flow solution. Calculation of P_{cal} and Q_{cal}. The real and reactive powers can be calculated using the following equations:

$$P_{i,cal}=P_i=\sum_{j=1}^{n}|V_i||V_j|(G_{ij}\cos\theta_{ij}+B_{ij}\sin\theta_{ij}) \tag{3.33}$$

$$P_i=G_{ii}|V_i^2|+\sum_{j=1}^{n}|V_i||V_j|(G_{ij}\cos\theta_{ij}+B_{ij}\sin\theta_{ij})\text{ and} \tag{3.34}$$

$$Q_{i,cal}=Q_i=\sum_{j=1}^{n}|V_i||V_j|(G_{ij}\sin\theta_{ij}+B_{ij}\cos\theta_{ij}) \tag{3.35}$$

$$P_i = -B_{ii}\left|V_i^2\right| + \sum_{j=1}^{n}|V_i|\left|V_j\right|(G_{ij}\sin\theta_{ij} + B_{ij}\cos\theta_{ij}) \tag{3.36}$$

The powers are computed at any $(r+1)^{th}$ iteration by using the voltages available from previous iteration. The elements of the Jacobian are found using the above equations as:

Elements of J_1

$$\frac{\partial P_i}{\partial \theta_i} = \sum_{\substack{j=1 \\ j\neq i}}^{n}|V_i|\left|V_j\right|\left\{G_{ij}(-\sin\theta_{ij}) + B_{ij}\cos\theta_{ij}\right\} \tag{3.37}$$

$$= -Q_i - B_{ii}\left|V_i\right|^2$$

Elements of J_3

$$\frac{\partial Q_i}{\partial \theta_i} = \sum_{\substack{j=1 \\ j\neq i}}^{n}|V_i|\left|V_j\right|(G_{ij}\cos\theta_{ij} + B_{ij}\sin\theta_{ij}) \tag{3.38}$$

$$= P_i - G_{ii}\left|V_i\right|^2$$

$$\frac{\partial Q_i}{\partial \theta_i} = -|V_i|\left|V_j\right|\left(G_{ij}\cos\theta_{ij} + B_{ij}\sin\theta_{ij}\right) \tag{3.39}$$

Elements of J_4

$$\frac{\partial P_i}{\partial |V_j|}|V_i| = -2|V_i|^2 B_{ii} + \sum_{\substack{j=1 \\ j\neq i}}^{n}|V_i|\left|V_j\right|\left(G_{ij}\sin\theta_{ij} + B_{ij}\cos\theta_{ij}\right) \tag{3.40}$$

$$= Q_i - B_{ii}\left|V_i\right|^2$$

$$\frac{\partial Q_i}{\partial |V_j|} = |V_i|\left|V_j\right|\left(G_{ij}\sin\theta_{ij} - B_{ij}\cos\theta_{ij}\right) \tag{3.41}$$

Elements of J_2

$$\frac{\partial P_i}{\partial |V_j|}|V_i| = 2|V_i|^2 G_{ii} + |V_i|\sum_{\substack{j=1 \\ j\neq i}}^{n}\left|V_j\right|\left(G_{ij}\cos\theta_{ij} + B_{ij}\sin\theta_{ij}\right) \tag{3.42}$$

$$= P_i + G_{ii}\left|V_i\right|^2$$

$$\frac{\partial P_i}{\partial |V_j|}|V_j| = |V_i|\left|V_j\right|\left(G_{ij}\cos\theta_{ij} + B_{ij}\sin\theta_{ij}\right) \tag{3.43}$$

Thus, the linearized load flow equation can be rewritten as:

$$\begin{bmatrix} \Delta P \\ \Delta Q \end{bmatrix} = \begin{bmatrix} H & N \\ K & L \end{bmatrix} \begin{bmatrix} \Delta \theta \\ \frac{\Delta V}{V} \end{bmatrix} \tag{3.44}$$

3.6 Modelling Distribution Generations

The various forms of DG were discussed in Chapter 2. In this study, solar PV and wind energy conversion systems (WECS) are considered as the renewable energy sources for DG. These sources are integrated into the system as solar farms and wind farms, respectively. Solar energy operates only during daylight hours, making it less erratic, whereas wind energy functions both day and night but is highly variable. The objective is to assess whether these renewable sources, integrated at a specific bus, can supply power to the distribution system while operating in parallel with the utility supply.

The following subsections present the mathematical models used to simulate the power input from solar PV and wind energy conversion systems.

3.6.1 Solar PV System Modelling

The PV module topology is illustrated in Figure 3.4, where multiple arrays are arranged in series and parallel configurations to achieve the desired voltage and current output. The parallel connections increase current output, while the series connections increase voltage output.

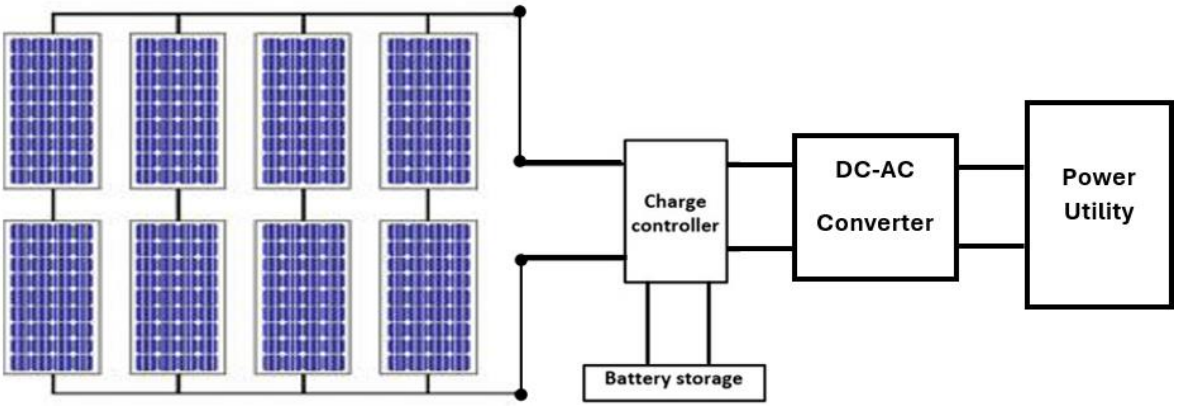

Figure 3.4: Utility connected Solar PV systems.

A solar cell equivalent circuit is shown in Figure 3.5, where a real diode is modelled in parallel with an ideal current source. The current output is proportional to solar irradiance, as expressed in (3.45).

$$I = I_{SC} - I_d - \frac{V}{R_p} \tag{3.45}$$

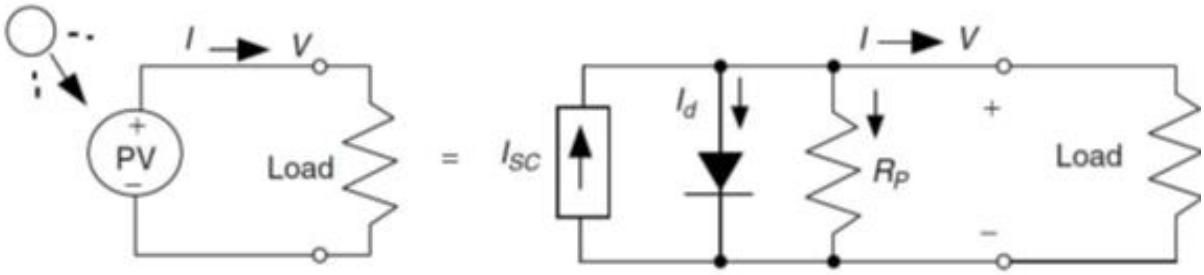

Figure 3.5: Equivalent circuit of the solar cell with the load connected [75].

The current-voltage characteristics of a real PV cell are mathematically represented by (3.46)-(3.47), defining its electrical behavior.

$$I = I_{SC} - I_O(e^{38.9Vd} - 1) - \left(\frac{V_d}{R_p}\right) \tag{3.46}$$

$$I = I_{SC} - I_O(e^{q\left(\frac{V+IR_S}{AkT}\right)} - 1) - \left(\frac{V + IR_S}{R_p}\right) \tag{3.47}$$

3.6.2 Wind Energy Conversion System (WECS) Modelling

Figure 3.6 shows the diagram of a utility-scale wind energy conversion system (WECS). A typical WECS consists of the following subsystem:

- Rotor (consist of blades and hub)
- Drive-train (shaft, gearbox, coupling, mechanical brakes, and electrical generator)
- Nacelle and main frame (housing, bedplate, and yaw)
- Tower and foundation
- Electrical system (cables, switchgear, transformer, and power electronics converters)

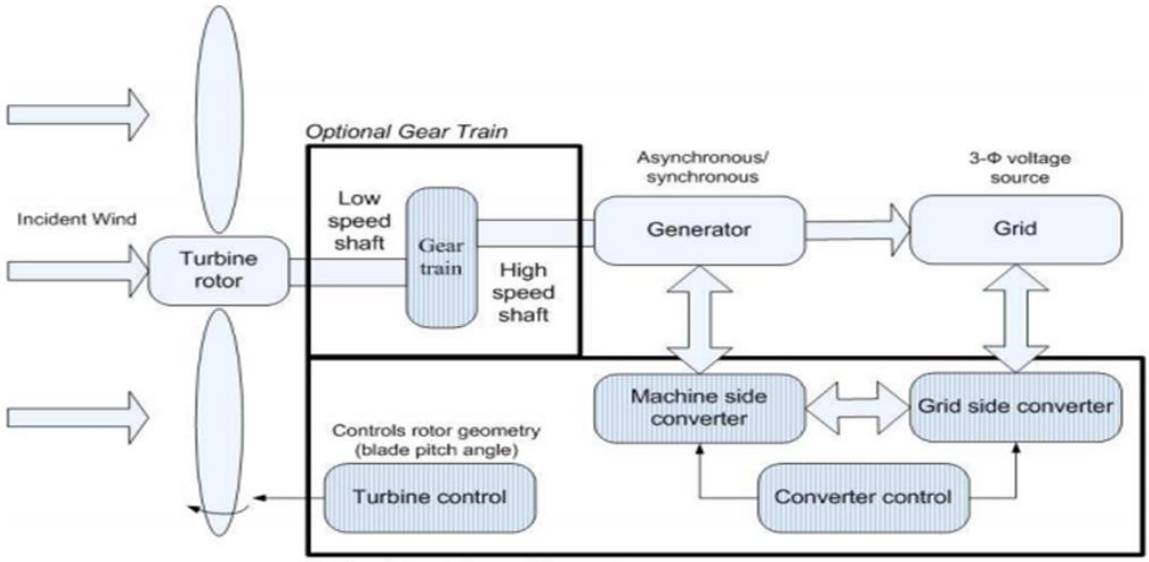

Figure 3.6: Modern utility-scale wind diagram [76].

Power is extracted from the kinetic energy of wind and converted to mechanical energy as the rotor spins. The kinetic energy in the wind is given by (3.48)

$$E = \frac{1}{2} \times m \times V_w^2 \tag{3.48}$$

Where,

m is air mass and V_w is the velocity of the wind.

The mass of air passing through the rotor blades over time is derived using (3.49), considering air density ρ, rotor radius R, and wind speed [80].

$$m = \rho \times v = \rho \times V_w \times A \times t = \rho \times V_w \times \pi \times R^2 \times t \tag{3.49}$$

Where,

ρ is the air density in (Kg/m^3) , t is the time, R is the radius of circular area in (meters) swiped by the wind turbine blade.

Substituting (3.48) into (3.49) results in (3.50), which expresses energy conversion efficiency.

$$E = \frac{1}{2} \times \rho \times V_w^3 \times \pi \times R^2 \times t \tag{3.50}$$

Then the stream power of the wind P_W through a cross-sectional area normal to the wind is calculated using (3.51).

$$P_W = \frac{1}{2} \times \rho \times \pi \times R^2 \times V_w^3 \tag{3.51}$$

The power coefficient (Cp) represents the efficiency of capturing wind energy, defined as the ratio of mechanical power output P_M to available wind power (3.52)-(3.53).

$$C_p = \frac{P_M}{P_W} = \frac{P_M}{\frac{1}{2}\rho A v^3} \tag{3.52}$$

$$C_P(\lambda,\beta) = C_1(C_2\frac{1}{\gamma} - C_3\beta - C_4\beta^x - C_5)e^{-C_6\frac{1}{\gamma}} \tag{3.53}$$

Where,

$C_1 = 0.5, C_2 = 116, C_3 = 0.4, C_4 = 0, C_5 = 5$ and $C_6 = 21$

The maximum theoretical efficiency is determined by (3.54)-(3.55).

With γ defined as $\frac{1}{\gamma} = \frac{1}{\lambda + 0.08\beta} - \frac{0.035}{1+\beta^3}$ (3.54)

Hence,

$$P_M = \frac{1}{2}\rho A V^3 C_P \tag{3.55}$$

Due to aerodynamic losses (blade-tip, rotation, and blade root losses), the actual power coefficient ranges between 30-45% [77]. The tip-speed ratio (λ), which influences power output, is defined in (3.56). The power coefficient curve is given in Figure 3.7.

$$P_M = \frac{1}{2}\rho\pi R^2 V^3 C_p(\lambda,\beta) \tag{3.56}$$

The rotor blade speed is calculated using (3.57) and the mechanical torque on the rotor is given by (3.58).

$$T_M = \frac{P_M}{\omega_M} = \frac{\pi C_P(\lambda,\beta)\rho R^2 A V^3}{2\omega_M} \tag{3.57}$$

$$T_M = \frac{1}{2}C_T\rho\pi R^3 V^2 \tag{3.58}$$

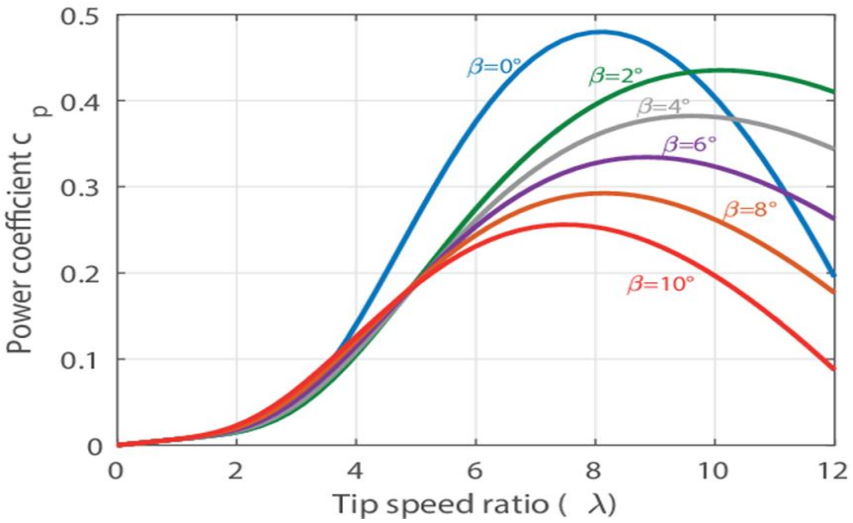

Figure 3.7: Power coefficient curve [78].

The tip-speed ratio can be calculated using (3.59)

$$\lambda = \frac{\omega_{rotor} R_{rotor}}{V_{wind}} \tag{3.59}$$

Where,

ω_{rotor} is the angular velocity of the motor, R_{rotor} is the length of the rotor blade and V_{wind} is the wind speed.

At steady-state, rotor power (P_m) equals the electrical power output (P_e), expressed in (3.60).

$$P_M = P_e \tag{3.60}$$

Where,

P_e is power used to drive the generator (3.61):

$$P_e = T_g \omega_g \tag{3.61}$$

Where,

T_g is the torque of the generator and ω_g is the generator speed.

A Permanent Magnet Synchronous Generator (PMSG) is used to convert mechanical energy into electrical energy. The d-q axis equivalent circuits for the generator are shown in Figure 3.8. The d-axis and q-axis dynamic equations are represented by (3.62)-(3.63) [79].

$$V_{ds} = -R_s i_{ds} - L_s \frac{di_{ds}}{dt} + \omega_r L_s i_{qs} \tag{3.62}$$

$$V_q = -R_s i_{qs} - L_s \frac{di_{qs}}{dt} - \omega_r L_s i_{ds} + \omega_r \lambda_r \tag{3.63}$$

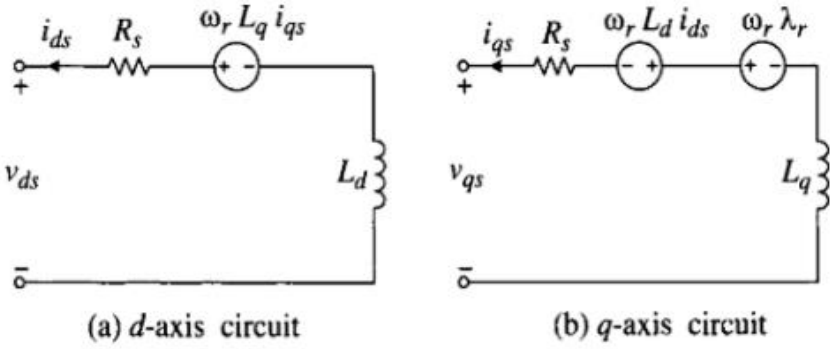

Figure 3.8: The equivalent d-axis and q-axis circuits of the PMSG [80].

The mechanical equation governing PMSG operation is given by (3.64).

$$J \frac{d\omega_r}{dt} = T_e - T_m - B\omega_r \tag{3.64}$$

Through mathematical rearrangement, the mechanical torque and angular velocity of the rotor influence the electromagnetic torque, as defined in (3.65) [79].

$$T_e = J \frac{d\omega_r}{dt} + T_m + B\omega_r \tag{3.65}$$

Where,

J represents the moment of inertia, $\frac{d\omega_r}{dt}$ represents the rate of change of angular velocity over time, T_m represents the mechanical torque, B represents the friction coefficient, ω_r represents the angular or rotational velocity of the turbine rotor and T_e represents the electromagnetic torque.

Through mathematical rearrangement, the mechanical torque and angular velocity of the rotor influence the electromagnetic torque, is defined in (3.65) [79].

$$T_e = \frac{3}{2}.\frac{P}{2}\left[\lambda_r i_{qs} - \left(L_d - L_q\right) i_{ds} i_{qs}\right] \tag{3.66}$$

Where,

P represents the number of poles, λ_r represents the magnetic flux of the rotor, i_q and i_d represent the currents in the *dq*-axis, and L_q and L_d represent the inductance in the *dq*-axis.

For non-salient pole PMSGs, $L_d = L_q$. leading to the simplified torque equation in (3.67).

$$T_e = \frac{3P}{4}\left(\phi_r i_{qs}\right) \tag{3.67}$$

Through mathematical rearrangement, the final expression for q-axis current (i_q) is given in (3.68).

$$i_q = \frac{4T_e}{3P\lambda_r} \tag{3.68}$$

3.7 Distribution Network: IEEE 30 Bus System

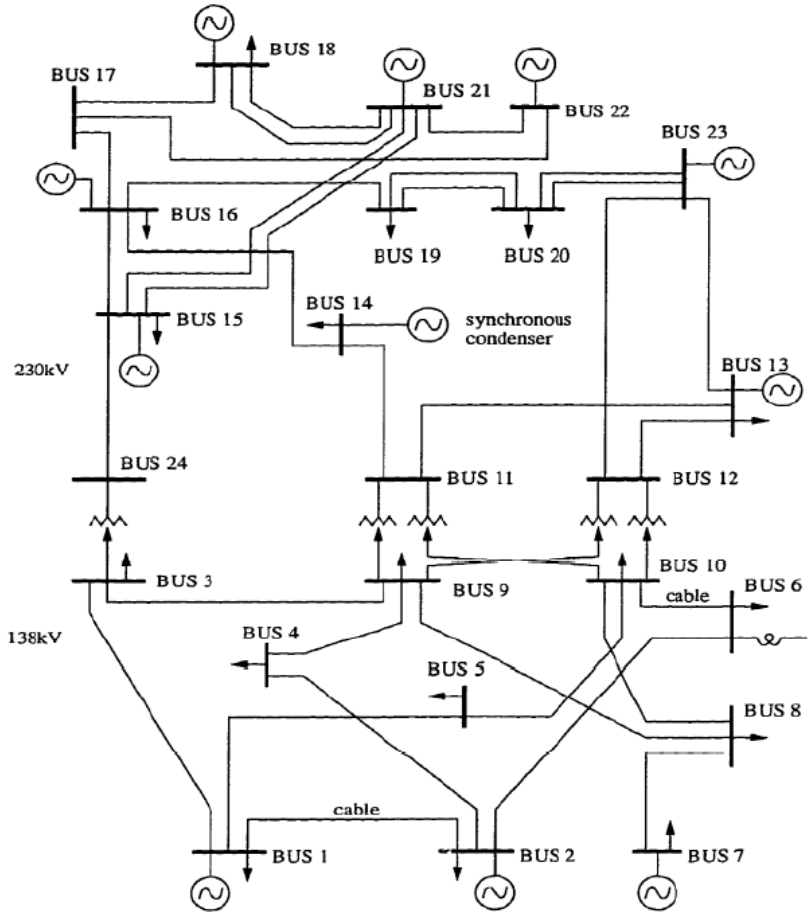

Figure 3.9: The IEEE 30 bus system

To model the distribution network for this study, the IEEE 30-bus system is used, as shown in Figure 3.9. This system consists of 30 buses, 32 generators, and 38 transmission lines, providing a standardized test network for power system analysis. The IEEE 30-bus system is widely used for load flow analysis, stability studies, and distributed generation integration due to its well-defined structure and industry relevance. The parameter for this configuration and the generation data are presented in Chapter 4. The results from Chapter 4 will compare system performance with and

without DG integration, highlighting improvements in power quality, voltage stability, and reliability.

3.8 Reliability Evaluation of Distribution Networks with Distributed Generation

This section presents the reliability evaluation of a distribution network integrated with DG. Various DERs exist, such as wind, solar, and geothermal. In this study, the distribution network incorporates PV and WECS, which contribute to supplying part of the load during grid-connected mode. Given the stochastic nature of solar and wind resources, probabilistic models are employed to simulate their random variations and assess their impact on system reliability.

A well-planned DG placement is essential for minimizing its adverse effects on utility networks. Optimal placement and sizing require a thorough understanding of the network characteristics where DG will be integrated. This process relies on optimization techniques during the grid integration planning stage to ensure efficient system operation. Commonly used methods for determining the optimal DG location and size include Particle Swarm Optimization (PSO) and Genetic Algorithm (GA) [81]. Effective DG integration planning involves optimizing multiple factors, including the type of DG technology, number and capacity of DG units, location, and network connection type [81]. Additionally, the impact of DG integration on power quality, power losses, stability, and reliability must be carefully assessed. Among available optimization techniques, PSO is selected for this study due to its fast convergence and ability to handle complex non-linear problems, making it well-suited for DG allocation.

3.8.1 Particle Swarm Optimization Method

Particle Swarm Optimization (PSO) is a population-based heuristic optimization technique, first introduced by Kennedy and Eberhart in 1995, inspired by the social behaviour of bird flocking and fish schooling [81]. It is widely used to solve optimization problems, including the optimal placement of Distributed Generation (DG) in power distribution systems. In PSO, a swarm of particles represents potential solutions. Each particle moves through the solution space, adjusting its position based on both its personal best solution and the global best solution found by the swarm. The primary objective in DG allocation is to minimize total real power loss by adjusting the particle positions iteratively. The fitness function evaluates the

performance of each particle, guiding the optimization process. The main parameters used to model the PSO are [82]:

- $S(n) = \{S_1, S_2, ..., S_n\}$: a swarm of n particles
- S_i : an individual in the swarm with a position p_i and velocity $v_i, i \in 1, n$
- p_i : the position of a particle S_i
- V_i : the velocity of a particle p_i
- $pbest_i$: the best solution of a particle
- $gbest$: the best solution of the swarm
- f : fitness function
- c_1, c_2 : acceleration constants
- r_1, r_2 : random numbers between 0 and 1
- t : the iteration numbers.

PSO is modelled using key parameters, including a swarm of particles, each with a position and velocity that evolve over iterations [82]. The velocity of each particle is updated using (3.69) [82], which incorporates cognitive and social components influenced by acceleration constants and random factors.

$$v_i^{t+1} = v_i^t + c_1 r_1 (pbest_i^t - p_i^t) + c_2 r_2 (gbest^t - p_i^t) \tag{3.69}$$

Where,

c_1 and c_2 are acceleration factor coefficients of related to the individual and social aspects, as trust parameters.

r_1 and r_2, are random numbers that define the stochastic effect of cognitive and social behaviors of the swarm.

The new particle position is then determined using (3.70) [82]. The relationship between velocity and position is interdependent, ensuring particles move toward optimal solutions dynamically.

$$p_i^{t+1} = p_i^t + v_i^{t+1} \tag{3.70}$$

Figure 3.10 illustrates the motion of a particle in the optimization process, demonstrating how particles adjust their velocity and position based on individual and collective experiences.

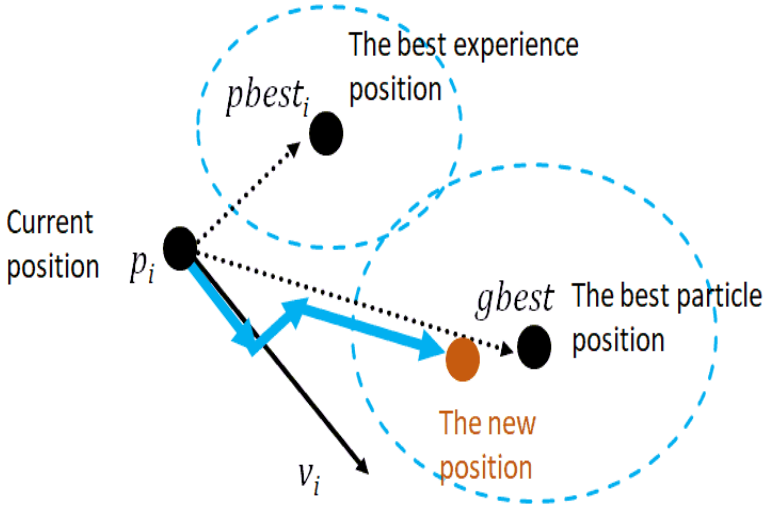

Figure 3.10: PSO moving particle diagram [83].

The PSO-based approach for solving the Optimal Placement of Distributed Generation (OPDG) problem follows these steps [83]:

1. Input line and bus data along with bus voltage limits.
2. Compute initial power loss using load flow analysis via the backward-forward sweep method.
3. Generate an initial population of particles with random positions and velocities within the solution space.
4. Evaluate each particle's fitness value, ensuring voltage limits are met; infeasible particles are discarded.
5. Compare each particle's objective value with its individual best (P_{best}) and update accordingly.
6. Identify the global best (G_{best}) among all particles, which corresponds to the best overall solution.
7. Update each particle's velocity and position using (3.69)-(3.70).
8. Repeat steps 4-7 until the maximum number of iterations is reached.
9. Output the optimal DG locations and sizes, ensuring minimum total real power loss.

Figure 3.11 provides a flowchart representation of the PSO algorithm, detailing its iterative execution.

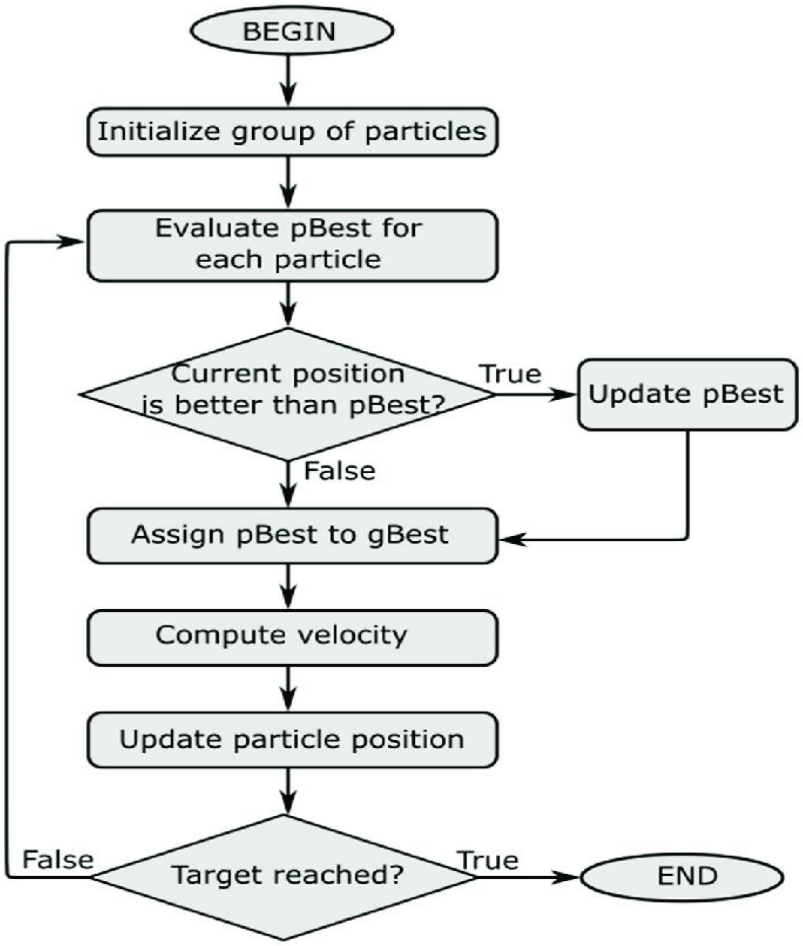

Figure 3.11: PSO flowchart [83].

Advantages of PSO in DG Allocation

PSO offers several advantages in optimizing DG placement and sizing [83]:

- Determines the optimal DG location and size to minimize power loss.
- Reduces overall system costs by optimizing DG parameters.
- Enhances the voltage profile of the distribution system.
- Increases power transfer capacity, improving grid performance.
- Minimizes total harmonic distortion, ensuring better power quality.

Due to its fast convergence and efficiency in handling non-linear optimization problems, PSO is selected for this study to achieve an optimal DG integration strategy in the distribution network.

3.9 System Configuration and Simulation Model

To effectively evaluate the impact of DG integration on the reliability and performance of power distribution networks, a simulation model was developed based on the IEEE 30-bus system. The configuration of this model was designed to incorporate renewable energy-based DGs, specifically PV systems and wind energy conversion systems WECS. This section provides a detailed description of the system configuration, including the power flow model, integration of DG units, and simulation methodology.

A modified version of this IEEE 30-bus system was adopted in this study, incorporating two DG sources at strategic locations to assess their impact on the system's reliability and operational efficiency. Figure 3.12 presents a schematic representation of the IEEE 30-bus distribution system with integrated DGs. The parameters and characteristics of the IEEE 30-bus system, including bus voltage levels, generator capacities, and transmission line data, are documented in Chapter 4, where the simulation results are analysed.

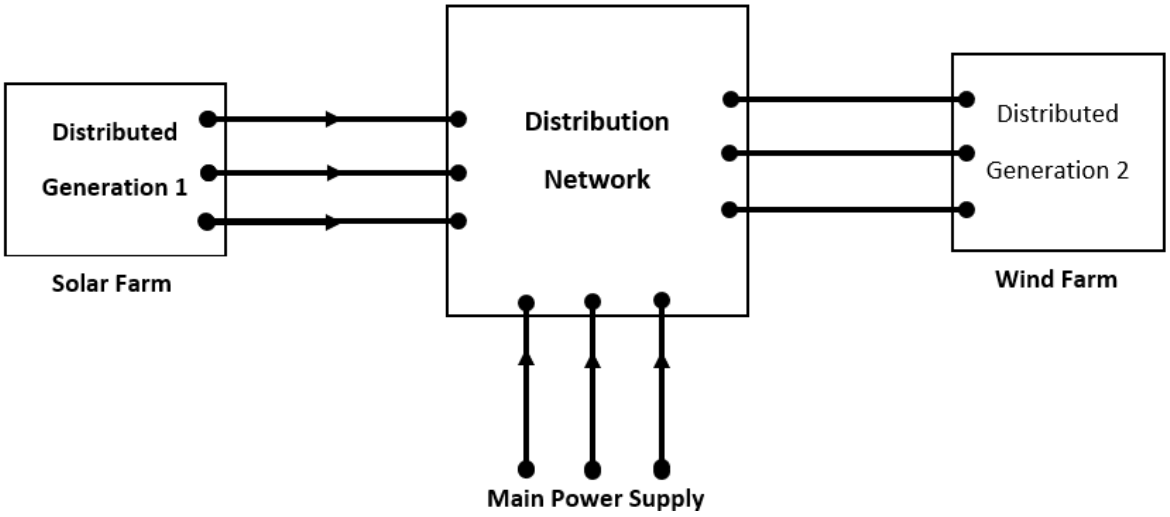

Figure 3.12: The designed simulation model.

Each DG unit was integrated into a selected bus in the network, ensuring that their operation closely resembles real-world conditions. The selection of the DG locations was based on optimal placement strategies to minimize power losses, enhance voltage profiles, and improve reliability indices.

The solar PV system was modelled as a grid-connected photovoltaic array, providing active power injection into the system during daylight hours. The behaviour of the PV system was simulated based on irradiance levels and temperature variations. The WECS was integrated

into the network as a variable-speed wind turbine coupled with a permanent magnet synchronous generator (PMSG). A wind speed dataset was used to simulate the fluctuations in wind power output, ensuring that the DG model captured the intermittent nature of wind energy.

The Newton-Raphson method is used for power flow analysis to assess the impact of DG integration on:

- **Voltage Stability** – Evaluating voltage deviations at different buses.
- **Power Losses** – Quantifying reductions in active and reactive power losses.
- **Load Balancing** – Assessing the impact of DG units on system-wide power distribution.

To quantify the effect of DGs on system reliability, various reliability indices are evaluated before and after DG integration. The reliability indices are computed using historical failure rate data and Monte Carlo simulations, ensuring realistic representation of grid disturbances and DG contributions.

The simulation model is implemented in MATLAB/Simulink, integrating:

- IEEE 30-bus system model
- Power flow solver using Newton-Raphson method
- Renewable DG models (Solar PV and Wind Turbine)
- Reliability assessment algorithms (Monte Carlo simulations)

The implementation model in MATLAB/Simulink environment is provided in Appendix A. The MATLAB simulation framework allow for:

- Dynamic power flow analysis under varying load and generation conditions
- Evaluation of voltage profiles, system losses, and reliability indices
- Comparison of system performance with and without DG integration

The designed simulation model serves as the foundation for the analyses presented in Chapter 4, where the simulation results and findings are discussed in detail.

Chapter 4

Simulations, Results and Analysis

4.1 Computer Simulations

Reliable power distribution is a key priority for utilities, necessitating ongoing assessments to enhance system performance and meet regulatory standards while ensuring customer satisfaction. Power system reliability assessments help identify areas of improvement, allowing utilities to implement strategic enhancements for sustained power quality. One of the most effective tools in this endeavour is computer-based simulations, which facilitate planning, design, and performance evaluation. This chapter presents the simulation models, results, and analysis conducted to assess the reliability and performance of a distribution network integrated with DG sources. The simulations were developed using MATLAB/Simulink, incorporating PV and WECS. The computational model allowed for detailed load flow analysis, DG integration, and reliability assessments based on key indices. The obtained results are systematically analysed to derive meaningful conclusions regarding DG deployment.

4.2 System Specifications

The first distributed generation unit (DG1) is a solar PV farm. The specifications of the solar panels used in this simulation are outlined in Table 4.1.

Table 4.1: The solar PV specifications

Module STC: irradiance level 1000W/m^2, spectrum AM 1.5 and cell temperature 25°C		
Parameter	Symbol	Value
Rated power	P_R	355W
Peak power	P_{mmp}	355W
Module efficiency	η	13.4%
Maximum system voltage	V_{sys}	1000V(UL); 1015V (TUV)
Peak power voltage	V_{mmp}	43.40V
Peak power current	I_{mmp}	8.18A
Open circuit voltage	V_{OC}	51.90V
Short circuit current	I_{SC}	8.68A
Nominal voltage	V	12
The abbreviation ‘mpp’ stands for Maximum Power Point		

Similarly, DG2 represents a wind farm modelled with a WECS, whose specifications are detailed in Table 4.2.

Table 4.2: The Specifications for the WECS

Parameter	Value	Unit
Blade Radius	36	m
Rated Power	1.5	MW
Rated Apparent Power	1.67	MVA
Number of Pole Pairs	4	
Rated Stator Flux Linkage	1.2748	Wb (rms)
Rated Stator Flux Linkage	1.2096	Wb (rms)
Stator Winding Resistance, R_s	0.180	$m\Omega$
Rotor Winding Resistance R_r	1.397	$m\Omega$
Stator Leakage Inductance L_{is}	0.323	mH
Rotor Leakage Inductance L_{ir}	0.323	mH
Magnetizing Inductance L_m	1.935	mH

The IEEE 30-bus system is adopted as the test network model for this study. While a local municipal network with DG integration would have been ideal, confidentiality constraints necessitated using the standardized IEEE 30-bus model. The network specifications include generator data, transmission line parameters, and power limits, as detailed in Tables 4.3 and 4.4.

The MATLAB/Simulink environment was used to develop simulation models for the power system, incorporating the solar PV farm, wind energy system, and distribution network. These models were designed to analyse load flow, DG integration, and network reliability. Figure 4.1 presents the MATLAB/Simulink model developed for the solar PV system, integrating a PV array, MPPT controller, and boost converter. The system was designed to deliver 8 MW of power to the grid. The wind energy simulation model, shown in Figure 4.2, consists of a rotor blade system, PMSG generator, and power electronic converters. The wind farm operates at a constant speed of 12 m/s and generates 6.5 MW. The distribution network simulation model was built using MATLAB script functions, implementing the Newton-Raphson method for load flow analysis.

Table 4.3: The line parameters for IEEE 30-Bus System [84]

Line Number	From Bus	To Bus	Line impedance		Half Line Charging Susceptance per unit
			Resistance/unit	Reactance/ unit	
1	1	2	0.0192	0.0575	0.0528
2	1	3	0.0452	0.1652	0.0408
3	2	4	0.0570	0.1737	0.0368
4	3	4	0.0132	0.0379	0.0084
5	2	5	0.0472	0.1983	0.0418
6	2	6	0.0581	0.1763	0.0374
7	4	6	0.0119	0.0414	0.0090
8	5	7	0.0460	0.1160	0.0204
9	6	7	0.0267	0.0820	0.0170
10	6	8	0.0120	0.0420	0.0090
11	6	9	0.0	0.2080	0.0
12	6	10	0.0	0.5560	0.0
13	9	10	0.0	0.1100	0.0
14	4	12	0.0	0.2560	0.0
15	12	14	0.1231	0.2559	0.0
16	12	15	0.0662	0.1304	0.0
17	12	16	0.0945	0.1987	0.0
18	14	15	0.2210	0.1997	0.0
19	16	17	0.0524	0.1923	0.0
20	15	18	0.1073	0.2185	0.0
21	18	19	0.0639	0.1292	0.0
22	19	20	0.0340	0.0680	0.0
23	10	20	0.0936	0.2090	0.0
24	10	17	0.0324	0.0845	0.0
25	10	21	0.0348	0.0749	0.0
26	10	22	0.0727	0.1499	0.0
27	21	22	0.0116	0.0236	0.0
28	15	23	0.1000	0.2020	0.0
29	22	24	0.1150	0.1790	0.0
30	23	24	0.1320	0.2700	0.0
31	24	25	0.1885	0.3292	0.0
32	25	27	0.1093	0.2087	0.0
33	28	27	0.0	0.3960	0.0
34	27	29	0.2198	0.4153	0.0
35	27	30	0.3202	0.6027	0.0
36	29	30	0.2399	0.4533	0.0
37	8	28	0.0636	0.2000	0.4028
38	6	28	0.0169	0.0599	0.0130
39	9	11	0.0	0.2080	0.0
40	12	13	0.0	0.1400	0.0
41	25	26	0.2544	0.3800	0.0

Table 4.4: The power (MW) Limits for Branches in IEEE 30-Bus System [84]

From Line	To Line	MW Limit (pu)
1 – 2	2	1.0400
1 – 3	3	1.0400
2 – 4	4	0.5200
3 – 4	4	1.0400
2 – 5	5	1.0400
2 – 6	6	0.5200
4 – 6	6	0.7200
5 – 7	7	0.5600
6 – 7	7	1.0400
6 – 8	8	0.2560
6 – 9	9	0.5200
6 – 10	10	0.2560
9 – 10	10	0.5200
4 – 12	12	0.5200
12 – 14	14	0.2560
12 – 15	15	0.2560
12 – 16	16	0.2560
14 – 15	15	0.1280
16 – 17	17	0.1280
15 – 18	18	0.1280
18 – 19	19	0.1280
19 – 20	20	0.2560
10 – 20	20	0.2560
10 – 17	17	0.2560
10 – 21	21	0.2560
10 – 22	22	0.2560
21 – 22	22	0.2560
15 – 23	23	0.1280
22 – 24	24	0.1280
23 – 24	24	0.1280
24 – 25	25	0.4800
25 – 27	27	0.1280
28 – 27	27	0.5200
27 – 29	29	0.1280
27 – 30	30	0.1280
29 – 30	30	0.1280
8 – 28	28	0.2560
6 – 28	28	0.2560
9 – 11	11	0.5200
12 – 13	13	0.5200
25 – 26	26	0.1280

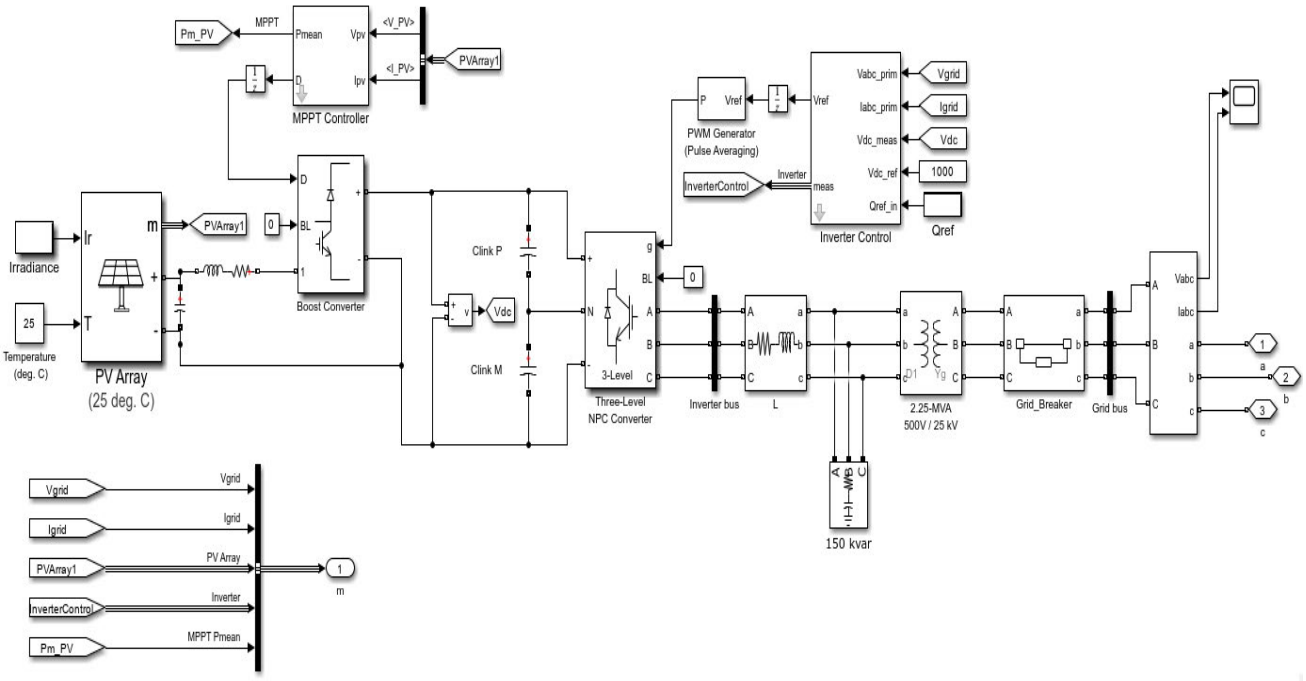

Figure 4.1: MATLAB/Simulink simulation model for Solar PV.

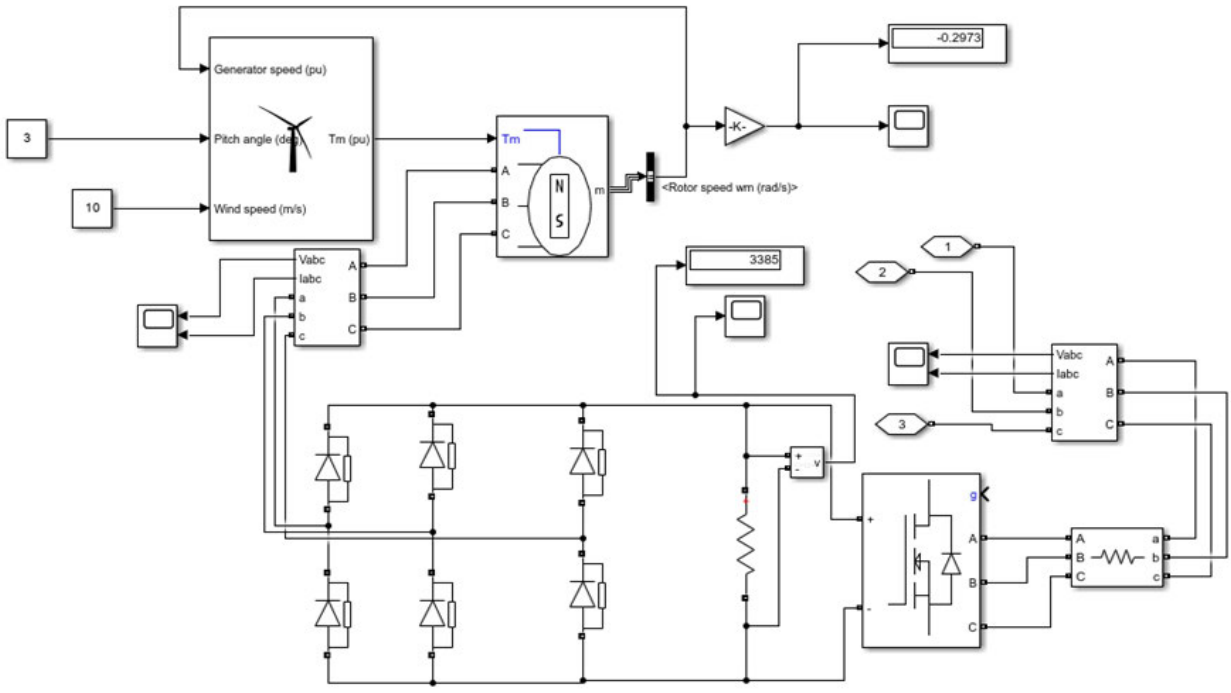

Figure 4.2: MATLAB/Simulink simulation model for WECS.

4.3 Simulation Results

This section presents the simulation results and subsequent analysis conducted to evaluate the performance of the distribution network under various conditions. The simulations focused on evaluating the performance of the network with and without DG integration, employing solar

PV and wind energy conversion systems WECS as the primary distributed generation sources. The results obtained are analysed to determine the impact of DG integration on power quality, system losses, and reliability improvements.

4.5 Simulation Result for Solar PV System

The PV array comprises of interconnected cells that are arranged to form an integrated structure The solar farm was constructed with a total of 282 parallel strings, each consisting of 15 series connected modules and the PV array consists of 83 cells per module. The results presented are derived from the specifications as documented in Table 4.1 of the photovoltaic system and configurations as shown in Figure 4.1. A crucial part of PV system performance analysis involves understanding the current-voltage (I-V) and power-voltage (P-V) characteristics under different irradiance levels. Figure 4.3 presents the I-V characteristics of the simulated PV array, showing the relationship between output current and voltage.

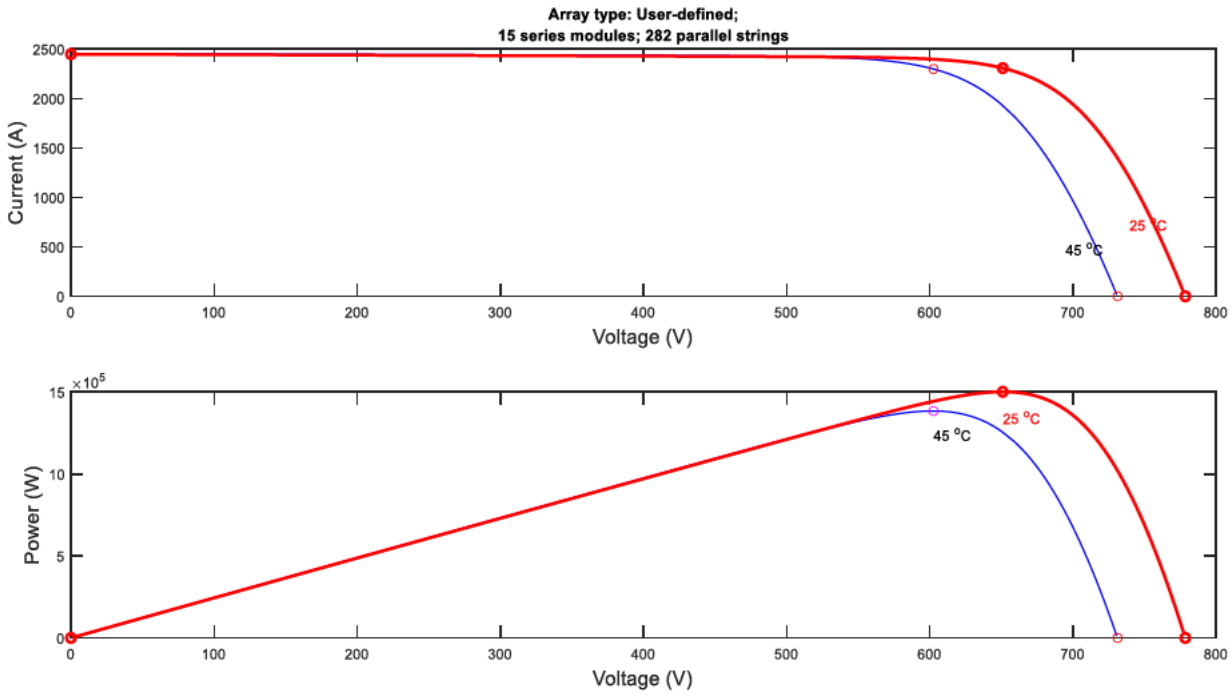

Figure 4.3: The I-V characteristic for the solar PV array

The maximum power point (MPP) was tracked using the Maximum Power Point Tracking (MPPT) algorithm, ensuring that the PV system operates at its optimal efficiency despite variations in solar irradiance. The PV system produces a DC voltage of 778.5 V, which is then boosted to 1000 V using a DC-DC boost converter before being fed into the inverter. The inverter converts the DC power into AC power suitable for grid integration. Figure 4.4 and Figure 4.5 show the output voltage and current waveforms from the inverter.

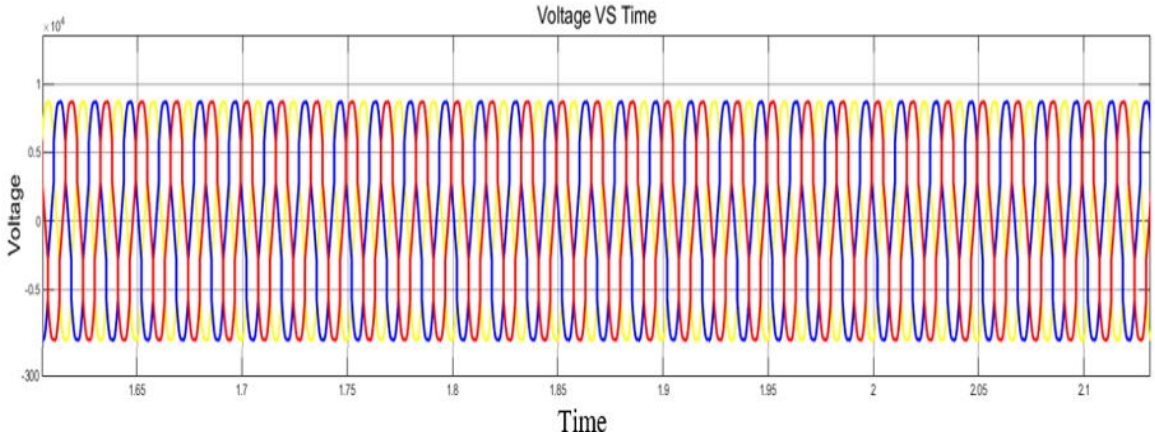

Figure 4.4: The inverter output voltage from the solar PV system

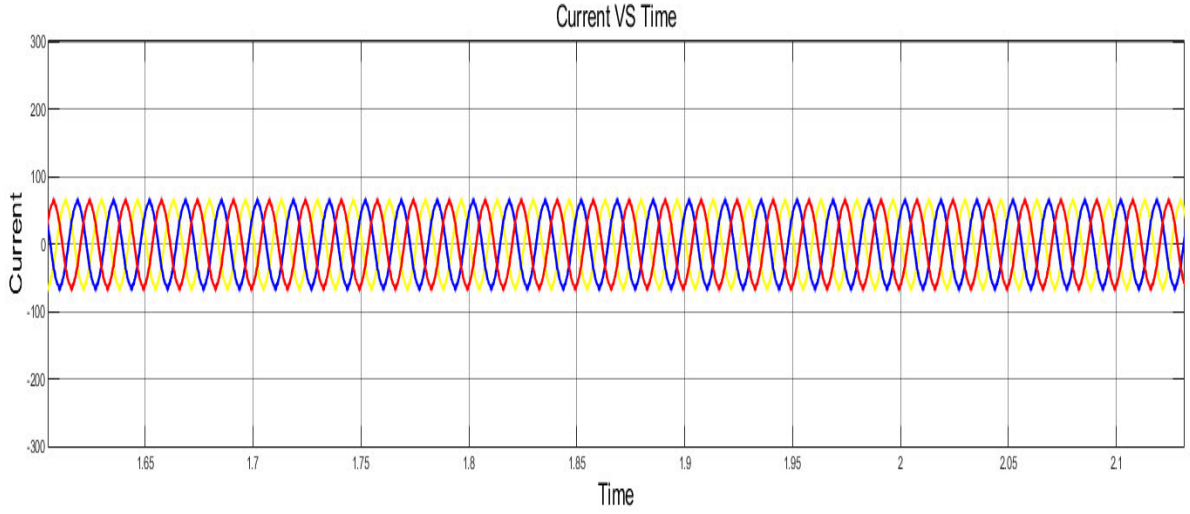

Figure 4.5: The inverter output current from the solar PV system

These waveforms indicate a stable sinusoidal output, confirming that the solar farm can effectively contribute to the distribution network without introducing harmonic distortions.

4.6 Simulation Result for WECS

The wind farm (DG2) was modelled in MATLAB/Simulink using a three-blade wind turbine, a gearbox, a Permanent Magnet Synchronous Generator (PMSG), and a power converter system. The wind turbine was simulated at a constant wind speed of 12 m/s, generating an output power of 6.5 MW.

The efficiency of the WECS is determined by the power coefficient (Cp), which quantifies how effectively kinetic energy is converted into mechanical energy. The turbine power coefficient curve, shown in Figure 4.6, illustrates the relationship between wind speed, power coefficient, and turbine output power.

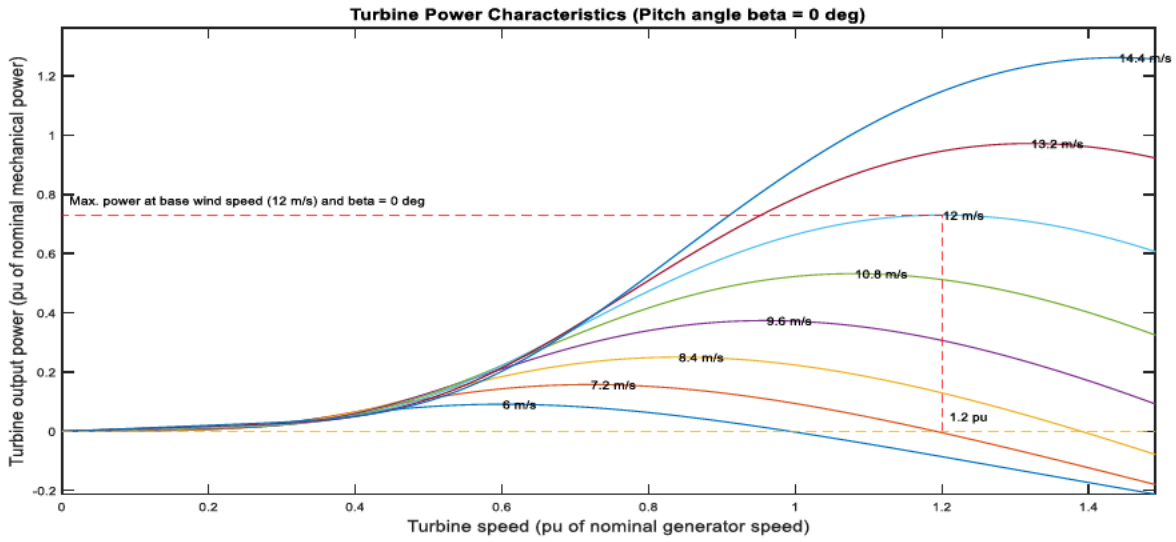

Figure 4.6: The diagram of the turbine power characteristics

The wind turbine used in the simulation had a blade radius of 36 m, and the power converted from the wind amounted to 1.732 MW at the rotor. The rotor was coupled to the PMSG, and its performance was analyzed during steady-state operation. At a wind speed of 12 m/s, the turbine operated at 1.2 per unit (pu) of generator synchronous speed. The PMSG produced a regulated DC voltage of 1150 V, which was converted into AC power for grid integration using an inverter. The reactive power was maintained at 0 MVar, ensuring a stable operation. The inverter output voltage and current waveforms before being fed into the distribution network are shown in Figure 4.7 and Figure 4.8, respectively. These results demonstrate the steady-state performance of the PMSG and the power conversion process.

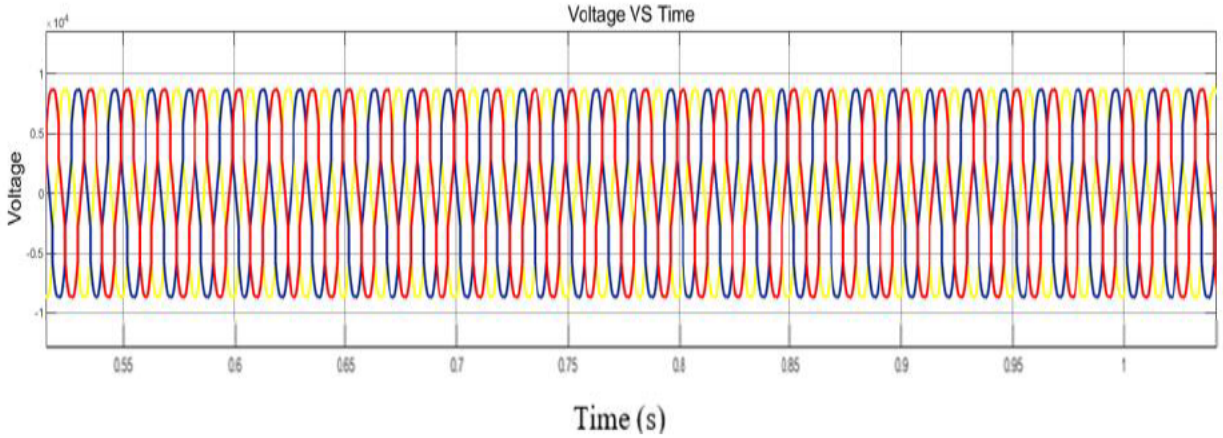

Figure 4.7: The inverter output voltage from the WECS

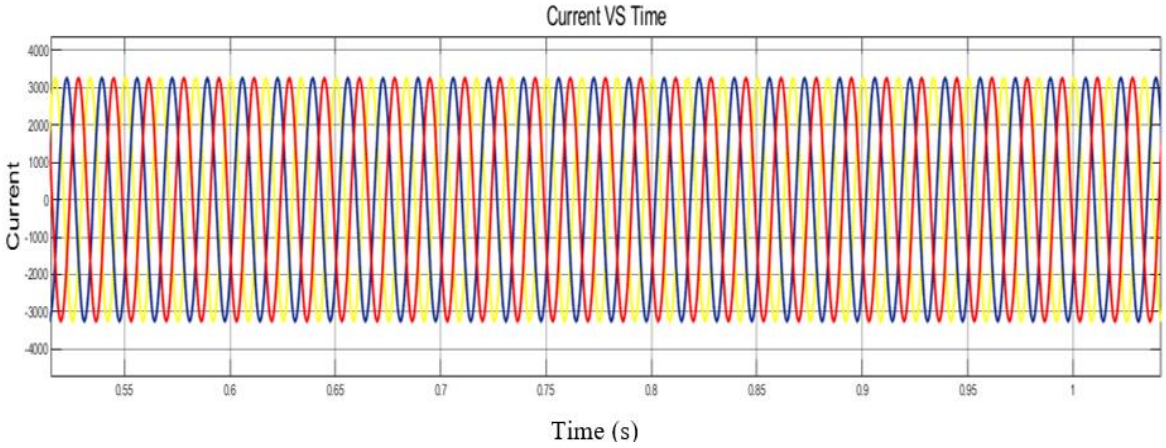

Figure 4.8: The inverter output current from the WECS

The wind farm was expected to produce 6.5 MW, and the simulation confirmed the system's ability to achieve this target under steady-state conditions. The results validate the feasibility of integrating the WECS into the distribution network, ensuring efficient power generation and stability.

4.7 Computer Simulation Result for Load Flow

Load-flow studies play a crucial role in power system planning and operation, providing insights into voltage stability, power losses, and network efficiency. These studies are essential for future system expansion and optimizing the operation of existing power grids. The key outcomes of a power flow study include the voltage magnitude and phase angle at each bus and the real and reactive power flow in each transmission line.

For this study, the Newton-Raphson method was implemented in MATLAB to conduct a load flow analysis of the IEEE 30-bus system. The analysis involved:

- Bus admittance matrix formation
- Conversion of polar to rectangular coordinates
- Solving power flow equations

The results of the Newton-Raphson load flow analysis provide valuable insights into the electrical behaviour of the IEEE 30-bus system, particularly concerning voltage regulation, phase angle variations, and power distribution. The findings reveal how increasing reactance loading affects system stability, voltage performance, and power losses. Below is a detailed discussion of the key findings presented in Tables 4.5 and 4.6.

Voltage Profile and System Stability

The voltage magnitude across the 30-bus system varies from 1.0600 p.u. (Bus 1) to 0.9953 p.u. (Bus 30). However, some buses, particularly Buses 18, 19, 29, and 30, experience voltage magnitudes below the acceptable limit of 0.95 p.u., which raises concerns regarding voltage instability. The presence of low voltage levels at Buses 18, 19, 29, and 30 indicates that these buses are located far from the main power sources (generators) and are affected by high impedance in the transmission network. These buses represent weak points in the system where voltage drops occur due to high reactance and insufficient reactive power support. The low voltage levels suggest poor voltage regulation, which can lead to issues such as equipment malfunction, reduced power quality, and system instability.

As reactance loading increases, voltage levels tend to drop due to the greater impedance of the system, which restricts power transfer. The voltage profile indicates that buses located further from the slack bus experience significant voltage drops. The lack of reactive power compensation in weak areas further exacerbates voltage instability. Without DG integration, voltage regulation relies heavily on the main grid's voltage control mechanisms (tap changers, capacitor banks, and synchronous condensers). The analysis suggests that placing DGs at weak voltage buses (such as Buses 18, 19, 29, and 30) can significantly improve voltage stability by injecting active and reactive power locally.

Table 4.5: Results for load flow

Newton Raphson Load Flow Analysis								
Bus No.	**V (pu)**	**Angle degree**	**Injection**		**Generation**		**Load**	
			MW	**MVar**	**MW**	**MVar**	**MW**	**MVar**
1	1.0600	0.0000	260.93	-17.12	260.93	-17.12	0.00	0.00
2	1.0430	-5.3474	18.30	35.07	40.00	47.77	21.70	12.70
3	1.0217	-7.5448	-2.40	-1.20	-0.00	0.00	2.40	1.20
4	1.0129	-9.2989	-7.60	-1.60	0.00	0.00	7.60	1.60
5	1.0100	-14.1542	-9420	16.97	-0.00	35.97	94.20	19.00
6	1.0121	-11.0880	0.00	-0.00	0.00	-0.00	0.00	0.00
7	1.0035	-12.8734	-22.80	-10.90	-0.00	0.00	22.80	10.90
8	1.0100	-11.8039	-30.00	0.69	0.00	30.69	30.00	30.00
9	1.0507	-14.1363	0.00	-0.00	0.00	-0.00	0.00	0.00
10	1.0438	-15.7341	-5.80	17.00	0.00	19.00	5.80	2.00
11	1.0820	-14.1363	-0.00	16.27	-0.00	16.27	0.00	0.00

12	1.0576	-14.9416	-11.20	-7.50	0.00	0.00	11.20	7.50
13	1.0710	-14.9416	0.00	10.25	0.00	10.25	0.00	0.00
14	1.0429	-15.8244	-6.20	-1.60	-0.00	-0.00	6.20	1.60
15	1.0384	-15.9101	-8.20	-2.50	-0.00	0.00	8.20	2.50
16	1.0445	-15.5487	-3.50	-1.80	-0.00	0.00	3.50	1.80
17	1.0387	-15.8856	-9.00	-5.80	0.00	0.00	9.00	5.80
18	1.0282	-16.5425	-3.20	-0.90	-0.00	-0.00	3.20	0.90
19	1.0252	-16.7273	-9.50	-3.40	-0.00	0.00	9.50	3.40
20	1.0291	-16.5363	-2.20	-0.70	0.00	-0.00	2.20	0.70
21	1.0293	-16.2462	-17.50	-11.20	-0.00	0.00	17.50	11.20
22	1.0353	-16.0738	-0.00	-0.00	-0.00	-0.00	0.00	0.00
23	1.0291	-16.2528	-3.20	-1.60	-0.00	0.00	3.20	1.60
24	1.0237	-16.4409	-8.70	-2.40	-0.00	4.30	8.70	6.70
25	1.0202	-16.0539	-0.00	-0.00	-0.00	0.00	0.00	0.00
26	1.0025	-16.4712	-3.50	-2.30	0.00	0.00	3.50	2.30
27	1.0265	-15.558	0.00	0.00	0.00	0.00	0.00	0.00
28	1.0109	-11.7436	0.00	-0.00	0.00	-0.00	0.00	0.00
29	1.0067	-16.7777	-2.40	-0.90	-0.00	0.00	2.40	0.90
30	0.9953	-17.6546	-10.60	-1.90	0.00	0.00	10.60	1.90
Total			**17.528**	**20.921**	**300.928**	**147.121**	**283.400**	**126.200**

Table 4.6: Results for load flow in terms line flow and losses

Line Flow and Losses									
From Bus	**To Bus**	**P(W)**	**Q (MVar)**	**From Bus**	**To Bus**	**P(W)**	**Q (MVar)**	**Line loss**	
								MW	**MVar**
1	2	176.11	-18.11	2	1	-165.09	33.62	11.20	15.51
1	3	90.08	6.25	3	1	-82.54	5.14	7.54	11.39
2	4	45.62	5.19	4	2	-40.72	-2.11	4.90	3.08
3	4	82.17	3.77	4	3	-80.98	6.23	1.73	2.46
2	5	84.57	4.03	5	2	-77.22	8.34	7.35	12.37
2	6	62.39	1.40	6	2	-56.49	4.50	5.90	5.91
4	6	72.73	-17.52	6	4	-71.17	19.75	1.56	2.23
5	7	-13.81	11.80	7	5	16.04	-11.39	2.23	0.41
6	7	39.07	-1.20	7	6	-36.96	2.37	2.11	1.17
6	8	29.95	-3.21	8	6	-28.93	3.57	1.02	0.36
6	9	29.06	-19.33	9	6	-28.42	8.96	0.64	-10.37
9	10	27.80	7.04	10	9	-27.80	-6.22	0.00	0.82
4	12	50.82	-19.33	12	4	-47.37	-10.62	3.46	-29.95
12	13	-0.00	-10.12	13	12	0.00	10.25	0.00	0.13

12	14	7.79	2.39	14	12	-7.72	-2.24	0.07	0.15
14	15	1.52	0.64	15	14	-1.51	-0.63	0.01	0.00
16	17	3.96	1.50	17	16	-3.95	-1.47	0.01	0.03
15	18	6.29	1.83	18	15	-6.25	-1.74	0.04	0.09
18	19	3.05	0.84	19	18	-3.04	-0.83	0.01	0.01
19	20	-6.46	-2.57	20	19	6.47	2.60	0.02	0.03
10	20	8.75	3.47	20	10	-8.67	-3.30	0.08	0.17
10	17	5.07	4.37	17	10	-5.05	-4.33	0.01	0.03
10	21	18.29	11.76	21	10	-18.13	-11.44	0.15	0.33
10	22	5.78	3.11	22	10	-5.75	-3.05	0.03	0.06
21	23	0.63	0.24	23	21	-0.63	-0.24	0.00	0.00
15	23	4.45	2.59	23	15	-4.42	-2.54	0.02	0.05
22	24	4.75	3.05	24	22	-5.71	-2.98	0.05	0.07
23	24	1.89	1.18	24	23	-1.85	-1.17	0.01	0.01
24	25	-1.14	1.75	25	24	1.15	-1.73	0.01	0.01
25	26	3.54	2.37	26	25	-3.50	-2.30	0.04	0.07
25	27	-4.69	-0.63	27	25	4.72	0.68	0.02	0.04
28	27	18.59	5.46	27	28	-18.59	-4.14	-0.00	1.32
27	29	6.19	1.67	29	27	-6.10	-1.51	0.09	0.16
27	30	7.09	1.66	30	27	-6.93	-1.36	0.16	0.30
29	30	3.70	0.61	30	29	-3.67	-0.54	0.03	0.06
8	28	1.57	-0.24	28	8	2.80	0.24	4.37	0.00
6	28	25.33	-3.09	28	6	-11.97	3.30	13.36	0.21
Total Loss								**68.828**	**14.624**

Phase Angle Variations and Reactive Power Demand

Phase angles provide crucial insights into the power flow direction and reactive power demands within the network. As expected, Bus 1 (slack bus) is set at 0°, serving as the reference point for all voltage angles. This bus acts as the primary generator bus, supplying both real and reactive power to balance network demand. Bus 30 has the most negative phase angle (-17.6546°), which suggests that this bus is experiencing high reactive power demand and is at the receiving end of significant power flows. A large negative phase angle generally indicates that a bus is far from the main power generation sources and requires additional reactive power support to maintain stability. This suggests the need for voltage-supporting devices such as DGs and capacitor banks, at Bus 30.

Power Injection and Load Distribution

The power flow results reveal how active and reactive power is distributed across the network and how different buses contribute to power balance. Bus 1 is the primary power source, supplying 260.93 MW and -17.12 MVar to the system. The high-power supply indicates that

the grid relies heavily on centralized generation, leading to high transmission losses. This centralized dependency highlights the potential benefits of DG integration, which can reduce power flow stress on transmission lines. High power demand at buses 2, 5, 7, and 8; these buses draw significant real and reactive power, making them critical load centres. The demand at these buses impacts the system's overall performance, particularly in terms of voltage stability and reactive power requirements. If power demand continues to grow, the network might require additional voltage support mechanisms such as reactive power compensation or local generation through DGs. Certain buses exhibit negative reactive power injections, which indicates the presence of inductive loads (such as motors and transformers) that consume reactive power or components supplying reactive power to improve voltage stability. This suggests that the system is attempting to self-compensate for reactive power imbalances, but DGs could enhance system performance.

The findings also demonstrate that increasing reactance loading influences voltage regulation and stability:

1. Voltage Regulation Challenges

As reactance increases, the system becomes more resistive to power transfer, resulting in greater voltage drops across transmission lines. Buses at the periphery (such as Buses 18, 19, 29, and 30) experience the most significant voltage degradation, reinforcing the need for reactive power compensation in those areas.

2. Losses in the System

Increased reactance loading leads to higher transmission losses, which reduces overall system efficiency. Table 4.6 confirms that lines experiencing the highest power losses correspond to those with significant reactance loading and phase angle differences.

3. Reactive Power Compensation is Necessary

To maintain a stable voltage profile, the system requires reactive power support through capacitor banks or DG integration. Optimally placed solar PV and wind DGs can supply both active and reactive power, mitigating the adverse effects of reactance loading.

The results from Tables 4.5 and 4.6 illustrate that reactance loading negatively impacts voltage regulation, increases power losses, and causes significant phase angle variations across the network.

4.8 Simulation Results for Placement and Sizing of DGs Using PSO

This section presents the results of the Particle Swarm Optimization (PSO) algorithm applied to determine the optimal placement and sizing of distributed generation (DG) units within the IEEE 30-bus system. The primary objective of this optimization was to enhance voltage stability, minimize power losses, and improve overall system reliability. A MATLAB-based numerical model was used to analyze three key scenarios: a base case without DGs, a case with a single solar PV system (DG1) integrated at an optimal bus location, and a case with both solar PV (DG1) and a wind energy conversion system (DG2) integrated into the network.

The PSO-based simulation iterated through different DG placement possibilities to identify optimal locations and sizes that would maximize power quality and minimize system losses. The comparative analysis of the three cases focused on evaluating voltage profiles, system power losses, and overall network stability.

4.8.2 Simulation Results for the Base Case (Without DGs)

The first scenario represents the base case, where the IEEE 30-bus system operates without any distributed generation. This scenario serves as a baseline for comparison with cases involving DG integration. After executing the Newton-Raphson power flow analysis in MATLAB/Simulink, the voltage magnitudes at various buses were obtained.

The results indicate that the voltage magnitudes across the system ranged between 0.9953 p.u. and 1.0600 p.u., with some buses experiencing voltage drops below the acceptable lower limit of 0.95 p.u. Notably, buses 18, 19, 29, and 30 exhibited the lowest voltage levels, identifying them as weak points within the network where voltage instability is most likely to occur. Overall, only 50% of the buses were within the acceptable voltage range, while the remaining buses operated near their lower voltage limits.

Power losses in the system were significant, with high active power losses contributing to inefficiencies in power delivery. Additionally, reactive power demand was high, placing stress on the system's voltage regulation capability. Buses at the farthest ends of the network, particularly Bus 30, exhibited noticeable voltage drops, reinforcing the need for localized power generation or voltage support.

The poor voltage regulation in this scenario suggests that without DGs, the system is susceptible to instability, especially at buses with high reactive power demand and long

transmission distances. These findings highlight the necessity of DG integration to improve voltage stability and reduce transmission losses. Figure 4.9 illustrates the voltage profile for the IEEE 30-bus system without DGs, visually demonstrating the weak voltage conditions in certain parts of the network.

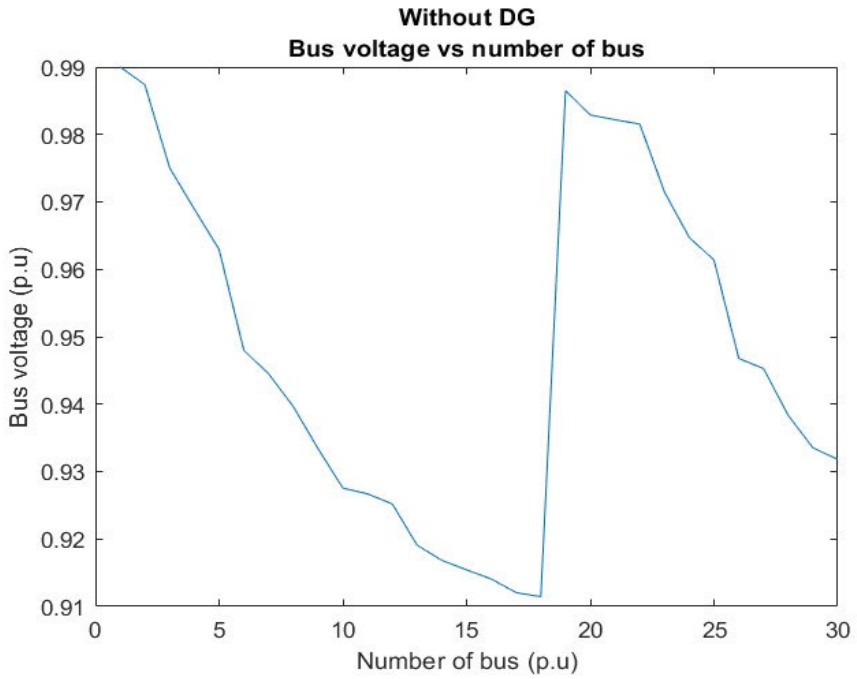

Figure 4.9: Result showing the voltage profile for the IEEE 30-bus without DGs.

4.8.2 Simulation Results with DG1 (Solar PV Only)

In the second scenario, a single distributed generation unit (DG1), represented by a solar farm, was integrated into the network. The PSO algorithm determined that Bus 26 was the most optimal location for DG1 in terms of voltage stability and power loss reduction. The optimal size of DG1 was found to be 9.0863 kVA. The results reveal a significant improvement in voltage levels across the network, particularly in buses 19 to 30, where most buses achieved the acceptable voltage threshold of 0.95 p.u. The overall voltage stability of the system improved, increasing from 50% in the base case to 64% after the integration of DG1. Moreover, the voltage at Bus 18, which was previously one of the weakest buses, improved from 0.9114 p.u. to 0.9315 p.u., indicating a substantial enhancement in power quality.

A considerable reduction in both active and reactive power losses was also observed, further improving the system's efficiency. The presence of the solar PV system provided localized power injection, reducing the reliance on long-distance power transmission from the main grid. However, while voltage stability improved, buses 10 to 18 still exhibited voltage levels below

the required threshold, suggesting that a single DG unit may not be sufficient to fully enhance system stability. This result underscores the potential need for additional DG integration to further improve voltage support. Figure 4.10 presents the improved voltage profile resulting from the integration of DG1 (solar PV), showcasing the enhanced performance in previously weak areas of the network.

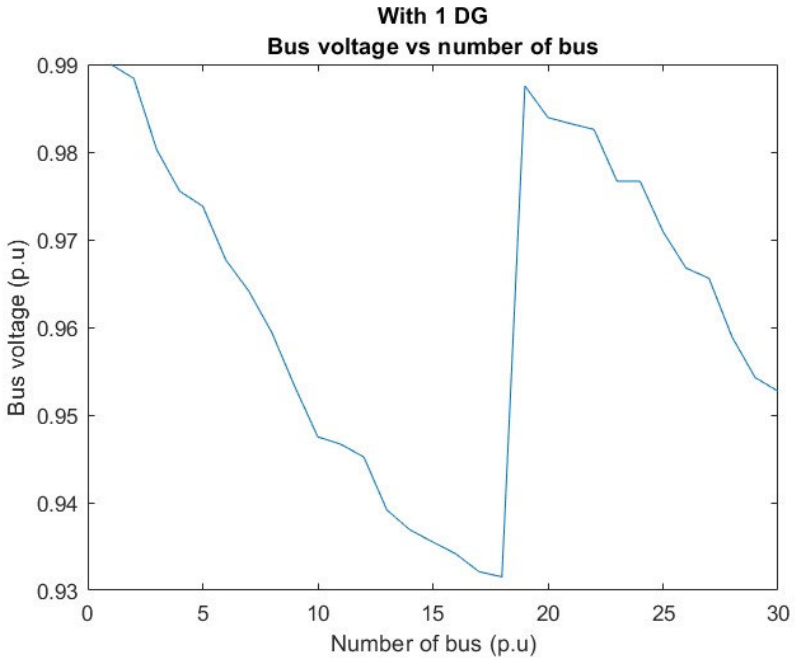

Figure 4.10: Result showing the voltage profile for the IEEE 30-bus with DG1

4.8.3 Simulation Results with Both DG1 (Solar PV) and DG2 (WECS)

The third scenario evaluates the combined effect of two DG units, DG1 (solar PV) and DG2 (WECS), on voltage regulation and power loss reduction. Figure 4.11 illustrates the improved voltage profile across the IEEE 30-bus system, demonstrating the system-wide benefits of optimized DG placement.

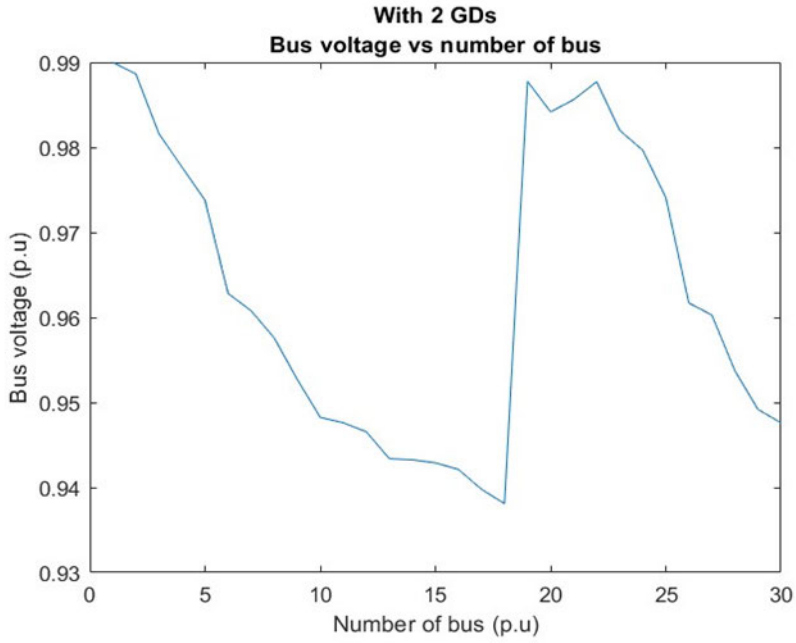

Figure 4.11: Result showing the voltage profile for the IEEE 30-bus with DG1 and DG2.

Using PSO, the optimal placement for DG1 was determined to be Bus 18, with a size of 9.3407 kVA, while DG2 was best placed at Bus 26, with a size of 7.215 kVA. The results indicate a substantial enhancement in voltage stability, with most buses achieving the acceptable voltage level of 0.95 p.u. The previously weak buses (10, 11, 12, 13, 29, and 30) still exhibited slightly lower voltages, but overall, they experienced marked improvements. Bus 18's voltage increased further to 0.9381 p.u., proving that the integration of both solar PV and wind energy provided better voltage support compared to a single DG unit.

The combined DG operation also led to a notable reduction in active power losses, significantly improving grid efficiency. By distributing power generation between two sources, the system achieved better load balancing, reduced line losses, and enhanced power quality. Additionally, integrating both solar PV and wind energy sources ensured power availability under varying weather conditions, as the wind system continued to generate power at night when solar PV was inactive.

Overall, the introduction of both DG1 and DG2 resulted in a fully optimized voltage profile, reduced transmission losses, and an overall enhancement of the system's performance.

The comparative analysis of the three scenarios provides critical insights into the impact of DG placement and sizing on power system performance. The introduction of DGs significantly

improved voltage stability, reduced power losses, and enhanced overall network efficiency. Voltage stability improved considerably with DG1, but the integration of both DG1 and DG2 yielded the best results, with almost all buses reaching stable voltage levels. Power loss reduction was also significantly more effective in the dual DG scenario, demonstrating the advantage of integrating multiple distributed generation sources. The placement of DGs at Buses 18 and 26 proved to be the most effective, reinforcing the importance of strategic DG positioning in weak areas of the network. These findings suggest that future DG installations should prioritize locations where voltage support is most needed.

4.9 Simulation Results for Reliability Analysis: Monte-Carlo Simulation

This section presents the results of the reliability analysis of the IEEE 30-bus system, evaluating the impact of DG integration using the sequential Monte Carlo simulation (MCS) technique. The reliability assessment was performed for three scenarios: the base case without DGs, a system with DG1 (solar PV), and a system with both DG1 (solar PV) and DG2 (WECS). The objective of this analysis is to quantify how DG placement and size influence system reliability, measured using key reliability indices such as the System Average Interruption Frequency Index (SAIFI), System Average Interruption Duration Index (SAIDI), Customer Average Interruption Duration Index (CAIDI), Expected Energy Not Supplied (EENS), and the Availability Indices (ASAI and ASUI). These indices provide insight into the frequency, duration, and impact of system interruptions, allowing for an assessment of the potential reliability improvements offered by DG integration.

The MCS method was chosen due to its ability to simulate random failure events, incorporating historical failure data, customer demand, and component outage rates to estimate the system's performance under varying operating conditions. The results of the simulation for the three cases are summarized in Table 4.7, which presents the calculated SAIFI, SAIDI, CAIDI, EENS, ASAI, ASUI, and AENS values for each scenario.

Table 4.7: Reliability indices values for IEEE 30 bus without and with DGs

Network Configuration	SAIFI	SAIDI	CAIDI	EENS	ASAI	ASUI	AENS
IEEE 30-bus System without DG	1.752	6.908	0.4226	26.436	0.9992	0.00091	0.1024
IEEE 30-bus System with DG 1	0.513	4.282	0.4511	15.147	0.9996	0.00043	0.0714
IEEE 30-bus System with DG 1 and DG 2	0.427	2.629	0.4776	9.211	0.9997	0.00032	0.0521

The results in Table 4.7 demonstrate significant improvements in system reliability following the integration of DG, particularly when both solar PV and WECS are deployed. The MCS effectively captured the impact of DG placement and sizing on key reliability indices, including SAIFI, SAIDI, CAIDI, EENS, ASAI, ASUI, and AENS. The findings underscore the crucial role of DGs in reducing outage frequency and duration while enhancing overall system availability and stability. One of the most notable improvements is the reduction in the System Average Interruption Frequency Index (SAIFI), which measures the average number of service interruptions per customer. In the base case, SAIFI was recorded at 1.752, indicating frequent interruptions across the IEEE 30-bus system. With the integration of DG1, the SAIFI value dropped significantly to 0.513, reflecting a 71% reduction in the frequency of power outages. When both DG1 (solar PV) and DG2 (WECS) were incorporated, SAIFI further decreased to 0.427, marking a 76% overall improvement. This decline highlights the role of localized power generation in reducing dependency on the main grid, thereby minimizing the likelihood of cascading failures and ensuring a more resilient distribution network.

Similarly, the System Average Interruption Duration Index (SAIDI) and the Customer Average Interruption Duration Index (CAIDI) exhibited substantial improvements. SAIDI, which represents the total duration of interruptions per customer per year, was initially measured at 6.908 hours. With the integration of DG1, SAIDI decreased to 4.282 hours, and with both DGs, it further dropped to 2.629 hours. This 62% reduction in outage duration underscores the ability of DGs to provide continuous power supply during grid failures, effectively reducing customer downtime. While CAIDI, which measures the average restoration time per outage, experienced a slight increase with DG1 (from 0.4226 to 0.4511 hours per outage), it later improved to 0.4776 hours per outage with the dual DG setup. This indicates that DGs facilitate quicker

restoration times, as they allow for an immediate transition to local power sources during outages. The Expected Energy Not Supplied (EENS) metric further reinforces the reliability benefits of DGs. In the base case, EENS was measured at 26.436MWh, indicating a significant amount of energy unavailability due to system interruptions. With the integration of DG1, this value decreased to 15.147MWh, signifying a 43% reduction in unserved energy. When both DG1 and DG2 were implemented, EENS was further reduced to 9.211MWh, amounting to a 65% improvement. This substantial decrease in EENS illustrates the critical role of DGs in maintaining supply adequacy, particularly in mitigating the impact of grid disturbances.

The system availability indices also demonstrated marked improvements. The Average System Availability Index (ASAI), which measures the fraction of time the system is operational, increased from 0.9992 in the base case to 0.9997 with both DG1 and DG2. Conversely, the Average System Unavailability Index (ASUI), which quantifies the proportion of time the system is unavailable, decreased from 0.00091 to 0.00032. These results indicate that DG integration significantly enhances long-term system reliability, reducing the probability of extended service disruptions. A similar trend was observed for the Average Energy Not Supplied (AENS) index, which measures the average amount of unserved energy per customer. Without DGs, AENS was recorded at 0.1025 MWh. Following the integration of DG1, this value dropped to 0.0714 MWh, and with both DG1 and DG2, it was further reduced to 0.0501 MWh. The 51% improvement in AENS highlights the effectiveness of DGs in ensuring energy availability, particularly in areas prone to frequent supply interruptions. The impact of DG integration on voltage stability was analyzed through the comparative results presented in Table 4.8. The weakest buses in the network, particularly Buses 18, 19, 29, and 30, demonstrated substantial voltage improvements following DG deployment. In the base case, Bus 18 had a voltage magnitude of 0.9114 p.u., which increased to 0.9315 p.u. with DG1 and further to 0.9381 p.u. with both DG1 and DG2. The phase angles across the network also indicated enhanced stability, as evidenced by a more balanced distribution of voltage magnitudes across buses.

Table 4.8: Comparison of outcomes for three scenarios: with no DG, DG1, and DG2

No. bus	***Voltage (p.u)***			***Phase angle (radians)***
	With no DG	DG1	DG2	
1	0.99	0.99	0.99	0
2	0.987361909	0.98839807	0.988611889	0.000259999
3	0.975047766	0.980258249	0.981602667	0.001723388
4	0.968912347	0.975515549	0.97767822	0.002898754
5	0.962919297	0.973814949	0.973773792	0.004087408
6	0.947959626	0.967687694	0.962815453	0.003372353
7	0.944492279	0.964136759	0.960780389	-0.000684543
8	0.939635765	0.959410824	0.957598401	-9.10549E-05
9	0,933367898	0.953228921	0.952726771	-0.001435431
10	0.927554391	0.947498811	0.948243171	-0.002594905
11	0.926691852	0.946660206	0.947602431	-0.002477978
12	0.925187881	0.945197191	0.946550691	-0.002295255
13	0.919083595	0.93916242	0.943385882	-0.003976928
14	0.916829931	0.936902712	0.943252123	-0.005387571
15	0.915423765	0.93550073	0.942895563	-0.006070008
16	0.914059096	0.934149475	0.942123821	-0.006499961
17	0.912048192	0.932127806	0.939782028	-0.007888792
18	0.911442577	0.931528629	0.938098905	-0.008067504
19	0.986498788	0.987535396	0.98775415	-6.3108E-05
20	0.982888405	0.983927092	0.984169944	-0.001267872
21	0.982177912	0.983216849	0.985607795	-0.001615271
22	0.98153538	0.982574469	0.987711846	-0.001980301
23	0.971433069	0.976675192	0.981991667	0.001169746
24	0.964709026	0.976675192	0.979663428	-0.000415639
25	0.961358169	0.970914579	0.974090527	-0.001199393
26	0.946782416	0.966755587	0.961702795	0.00408639
27	0.945271737	0.965582454	0.960276474	0.005098908
28	0.938319093	0.958895136	0.953721933	0.00790662
29	0.933500816	0.954276466	0.949181626	0.01026565
30	0.931822618	0.952707205	0.947599249	0.012123006

Figure 4.12 graphically illustrates these voltage improvements, reinforcing the importance of strategic DG placement in enhancing system reliability. The results confirm that the presence of DGs improves voltage profiles and mitigates the risks associated with voltage fluctuations, particularly in regions with high reactive power demand. The MCS reliability analysis confirms the substantial benefits of DG integration in modern power distribution systems. The presence of both solar PV and wind energy sources reduced outage frequency by 78% and outage

duration by 62%, reinforcing the importance of multi-DG integration. Additionally, the significant 62% improvement in EENS and AENS highlights the role of DGs in maintaining continuous energy supply, especially in mitigating the impact of unplanned outages. The enhanced voltage stability and improved availability indices further validate the effectiveness of DG placement in increasing overall system resilience.

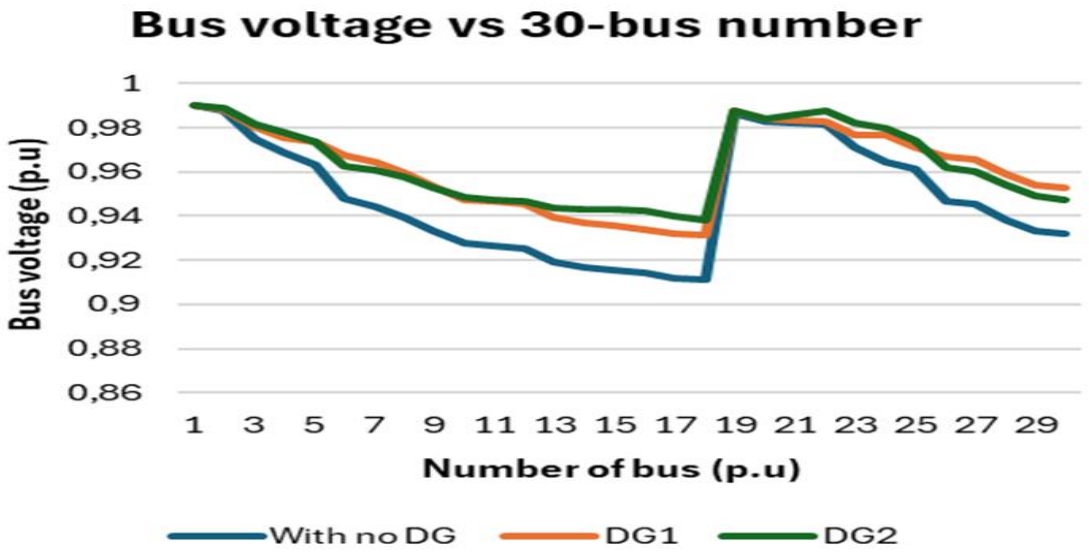

Figure 4.12: Comparison graph of DG systems.

These findings emphasise the need for optimised DG placement and sizing strategies to maximise power system reliability. The MCS provides valuable insights into how DGs can be leveraged to enhance grid resilience and minimise disruptions, proving that hybrid renewable energy integration is a key strategy for modern power distribution networks.

4.11 Conclusion

This chapter analysed the impact of distributed generation (DG) integration on the IEEE 30-bus system using MATLAB/Simulink simulations. The results demonstrated that incorporating DGs significantly improved voltage stability, reduced power losses, and enhanced overall system reliability.

The PSO-based optimisation effectively identified optimal DG placement and sizing, leading to substantial voltage improvements at weak buses and a notable reduction in system losses. The Monte Carlo simulation reliability assessment confirmed that DGs decrease outage

frequency and duration while increasing system availability. Overall, the findings validate the effectiveness of DG integration in improving power distribution performance. The combination of solar PV and wind energy sources provided the best results, highlighting the potential of hybrid renewable energy in modern power systems.

Chapter 5

Conclusion and Recommendations

This study analysed the impact of distributed generation (DG) integration on power system reliability, voltage stability, and power loss reduction within the IEEE 30-bus distribution network. The research leveraged advanced simulation techniques, including load flow analysis, Particle Swarm Optimization (PSO) for optimal DG placement and sizing, and Monte Carlo Simulation (MCS) for reliability assessment. The results demonstrate that integrating solar photovoltaic (PV) and wind energy conversion systems (WECS) significantly enhances system performance, reduces power losses, and improves voltage stability.

5.1 Summary of Key Findings

- **Voltage Stability:** Including DGs significantly improved the voltage profile across weak buses. Without DGs, certain buses experienced voltage drops below the acceptable 0.95 p.u. Threshold. DG1 (solar PV) integration improved stability, and the combined operation of DG1 and DG2 (WECS) resulted in the best voltage regulation across the network.
- **Power Loss Reduction**: The IEEE 30-bus system, without DGs, exhibited significant active power losses due to high transmission distances and reactive power demands. The PSO algorithm determined that optimal DG placement at Bus 18 and Bus 26 substantially reduced power losses, thereby improving overall system efficiency.
- **Reliability Enhancement:** The Monte Carlo Simulation results indicated that DG integration led to a drastic improvement in reliability indices:
    - SAIFI (System Average Interruption Frequency Index) was reduced by 78%, indicating fewer service interruptions.
    - SAIDI (System Average Interruption Duration Index) decreased by 62%, reflecting shorter outage durations.
    - EENS (Expected Energy Not Supplied) improved by 62%, ensuring better energy availability for consumers.
    - ASAI (Average System Availability Index) increased, demonstrating greater system resilience.

- **Optimized DG Placement is Crucial**: The PSO-based optimisation identified Buses 18 and 26 as the most effective DG placement locations, showing that proper DG siting is essential for maximising system benefits.
- **Hybrid DG Integration is Superior**: The combined operation of solar PV and wind energy provided the best overall improvements in voltage profile, power loss reduction, and reliability, proving the effectiveness of hybrid renewable energy systems in modern distribution networks.

5.2 Contributions of the Study

This research makes several significant contributions to the field of power system reliability and distributed generation planning:

1. Development of an Optimized DG Integration Framework

By employing PSO for optimal DG placement and sizing, this study provides an efficient method for improving power system performance, which can be applied to real-world networks.

2. Reliability Assessment Using Monte Carlo Simulation

The study utilises sequential Monte Carlo Simulation (MCS) to quantify the impact of DGs on power system reliability, offering data-driven insights into outage frequency, duration, and energy availability.

4. Enhancement of Voltage Stability and Loss Reduction

The findings confirm that strategic DG placement improves voltage stability and minimises system losses, contributing to better grid efficiency.

5. Validation of Hybrid Renewable Energy Integration

The research proves that a hybrid approach combining solar PV and wind energy provides superior grid performance compared to a single DG unit.

5.3 Limitations of the Study

While the findings of this research are impactful, the following limitations must be acknowledged:

- **Use of a Standard Test System**

The study was conducted on the IEEE 30-bus test system rather than a real-world power network. Although this system is widely used for research, real-world networks may exhibit

additional complexities, such as dynamic load variations, unbalanced loads, and network reconfiguration.

- **Weather-Dependent Renewable Energy Sources**

The study assumes constant solar and wind energy availability, but these resources are intermittent. Future work should incorporate probabilistic models for solar irradiation and wind speed variations.

- **Limited DG Types Considered**

The research focuses on solar PV and wind energy conversion systems, whereas other DG technologies, such as fuel cells, microturbines, and biomass generators, were not explored.

- **Computational Complexity of PSO Optimization**

While PSO provided excellent results, its computational time increases with network size. More advanced hybrid optimisation techniques (such as Genetic Algorithms (GA) combined with PSO) could be explored to improve efficiency.

5.4 Recommendations for Future Work

Given the promising results of this study, the following areas are identified for further investigation:

1. **Application of the Proposed Framework to Real-world Networks**

Future research should apply the PSO-based DG placement methodology to actual power distribution networks, considering real-time load variations, dynamic power flows, and operational constraints.

2. **Integration of Advanced Energy Storage Systems**

The variability of renewable energy sources could be mitigated by incorporating battery energy storage systems (BESS) to store excess energy during peak generation periods and supply power during shortages.

3. **Incorporation of Demand-Side Management (DSM) Techniques**

A demand-response model could be integrated to optimise energy consumption patterns, further enhancing system reliability and efficiency.

4. **Comparison of PSO with Other Optimization Algorithms**

Future studies could compare PSO with other metaheuristic algorithms such as Genetic Algorithms (GA), Artificial Bee Colony (ABC), and Differential Evolution (DE) to determine the most effective method for DG placement.

5. **Economic and Environmental Impact Assessment**

Future research should evaluate the economic feasibility of DG integration, considering installation costs, return on investment (ROI), and environmental benefits such as carbon emission reduction.

6. Hybrid Microgrid Development

The concept of hybrid microgrids, where DGs operate autonomously or in grid-connected mode, should be explored to enhance system resilience and energy security.

This research has demonstrated that optimally placed distributed generation can drastically improve power system reliability, voltage stability, and efficiency. By leveraging PSO for DG placement and Monte Carlo Simulation for reliability assessment, the study provides a robust framework for enhancing modern power distribution networks. The findings underscore the importance of hybrid renewable energy integration as a sustainable solution for addressing power quality challenges in contemporary electrical grids. As power systems evolve towards decentralised and renewable-based networks, this study contributes to making electricity more reliable, efficient, and resilient. The research findings serve as a foundation for future advancements in DG planning, supporting the transition toward smart grids and sustainable energy solutions.

References

[1] M. Mauri, L. Frosio, and G. Marchegiani, "Integration of Hybrid Distributed Generation Units in Power Grid," *Electrical Generation and Distribution Systems and Power Quality Disturbances*, pp. 3-30, 2016.

[2] F. V. Bekun, F. Emir, and S. A. Sarkodie, "Another look at the relationship between energy consumption, carbon dioxide emissions, and economic growth in South Africa," *Science of the Total Environment*, vol. 655, pp. 759-765, 2019.

[3] L. I. Dulău, M. Abrudean, and D. Bică, "Effects of distributed generation on electric power systems," *Procedia Technology*, vol. 12, pp. 681-686, 2014.

[4] R. J. Heffron, D. McCauley, and B. K. Sovacool, "Resolving society's energy trilemma through the Energy Justice Metric," *Energy Policy*, vol. 87, pp. 168-176, 2015.

[5] A. O. Aluko, R. P. Carpanen, D. G. Dorrell, and E. E. Ojo, "Robust state estimation method for adaptive load frequency control of interconnected power system in a restructured environment," *IEEE Systems Journal*, vol. 15, no. 4, pp. 5046-5056, 2020.

[6] S. E. Manahan, *Water chemistry: green science and technology of nature's most renewable resource*. CRC Press, 2010.

[7] L. Baker, "Governing electricity in South Africa: wind, coal and power struggles," 2011.

[8] T. Güney, "Renewable energy, non-renewable energy and sustainable development," *International Journal of Sustainable Development & World Ecology*, vol. 26, no. 5, pp. 389-397, 2019.

[9] G. E. Azuela and L. A. Barroso, *Design and performance of policy instruments to promote the development of renewable energy: emerging experience in selected developing countries*. World Bank Publications, 2012.

[10] W. Tong, *Wind power generation and wind turbine design*. WIT press, 2010.

[11] F. Iov and F. Blaabjerg, "Power electronics and control for wind power systems," in *2009 IEEE Power Electronics and Machines in Wind Applications*, 2009: IEEE, pp. 1-16.

[12] M. Iqbal, *An introduction to solar radiation*. Elsevier, 2012.

[13] S. Baljit, H.-Y. Chan, and K. Sopian, "Review of building integrated applications of photovoltaic and solar thermal systems," *Journal of Cleaner Production*, vol. 137, pp. 677-689, 2016.

[14] K. Mertens, *Photovoltaics: fundamentals, technology, and practice*. John Wiley & Sons, 2018.

[15] L. A. Weinstein, J. Loomis, B. Bhatia, D. M. Bierman, E. N. Wang, and G. Chen, "Concentrating solar power," *Chemical reviews*, vol. 115, no. 23, pp. 12797-12838, 2015.

[16] S. A. Kalogirou, S. Karellas, V. Badescu, and K. Braimakis, "Exergy analysis on solar thermal systems: a better understanding of their sustainability," *Renewable Energy*, vol. 85, pp. 1328-1333, 2016.

[17] S. Yao, Y. Wei, Z. Lu, S. Guo, J. Chen, and Z. Yu, "Review of Research Progress on Concentrated Solar Energy Utilization System," *Renewables*, vol. 1, no. 4, pp. 397-414, 2023.

[18] S. Sheth and M. Shahidehpour, "Tidal energy in electric power systems," in *IEEE Power Engineering Society General Meeting, 2005*, 2005: IEEE, pp. 630-635.

[19] E. Segura, R. Morales, J. Somolinos, and A. López, "Techno-economic challenges of tidal energy conversion systems: Current status and trends," *Renewable and Sustainable Energy Reviews*, vol. 77, pp. 536-550, 2017.

[20] G. Hagerman, B. Polagye, R. Bedard, and M. Previsic, "Methodology for estimating tidal current energy resources and power production by tidal in-stream energy conversion (TISEC) devices," *EPRI North American tidal in stream power feasibility demonstration project*, vol. 1, 2006.
[21] S. Singer, *The energy report: 100% renewable energy by 2050*. 2010.
[22] C. B. Field, J. E. Campbell, and D. B. Lobell, "Biomass energy: the scale of the potential resource," *Trends in ecology & evolution*, vol. 23, no. 2, pp. 65-72, 2008.
[23] Y. Zeng, Y. Cai, G. Huang, and J. Dai, "A review on optimization modeling of energy systems planning and GHG emission mitigation under uncertainty," *Energies*, vol. 4, no. 10, pp. 1624-1656, 2011.
[24] I. E. Agency, *Key world energy statistics: 2013*. OECD/IEA, 2013.
[25] N. Kishor, R. Saini, and S. Singh, "A review on hydropower plant models and control," *Renewable and Sustainable Energy Reviews*, vol. 11, no. 5, pp. 776-796, 2007.
[26] S. F. Singer, *Nature, not human activity, rules the climate*. Heartland Institute Chicago, 2008.
[27] E. Barbier, "Geothermal energy technology and current status: an overview," *Renewable and sustainable energy reviews*, vol. 6, no. 1-2, pp. 3-65, 2002.
[28] C. Ginn, "Energy pick n'mix: Are hybrid systems the next big thing?"," *CSIROscope. https://blog. csiro. au/energy-pick-n-mix-hybrid-systems-next-big-thing*, 2016.
[29] D. P. Kaundinya, P. Balachandra, and N. H. Ravindranath, "Grid-connected versus stand-alone energy systems for decentralized power—A review of literature," *Renewable and sustainable energy reviews*, vol. 13, no. 8, pp. 2041-2050, 2009.
[30] N. Priyadarshi, S. Padmanaban, M. S. Bhaskar, F. Blaabjerg, and A. Sharma, "A fuzzy SVPWM based inverter control realization of grid integrated PV-wind system with FPSO MPPT algorithm for a grid-connected PV/wind power generation system: hardware implementation," *IET Electric Power Appl*, vol. 12, no. 7, pp. 962-971, 2018.
[31] H. L. Willis, *Power distribution planning reference book*. CRC press, 1997.
[32] T. Ackermann, G. Andersson, and L. Söder, "Distributed generation: a definition," *Electric power systems research*, vol. 57, no. 3, pp. 195-204, 2001.
[33] T. J. Modise, "Local loop unbundling implementation model in South Africa's information communication and technology sector," North-West University, 2009.
[34] K. Nakayama, C. Zhao, L. F. Bic, M. B. Dillencourt, and J. Brouwer, "Distributed power flow loss minimization control for future grid," *International Journal of Circuit Theory and Applications*, vol. 43, no. 9, pp. 1209-1225, 2015.
[35] A. Baggini, *Handbook of power quality*. John Wiley & Sons, 2008.
[36] W. El-Khattam and M. M. Salama, "Distributed generation technologies, definitions and benefits," *Electric power systems research*, vol. 71, no. 2, pp. 119-128, 2004.
[37] J. Driesen and R. Belmans, "Distributed generation: challenges and possible solutions," in *2006 IEEE power engineering society general meeting*, 2006: IEEE, p. 8 pp.
[38] C. D. Iweh, S. Gyamfi, E. Tanyi, and E. Effah-Donyina, "Distributed generation and renewable energy integration into the grid: Prerequisites, push factors, practical options, issues and merits," *Energies*, vol. 14, no. 17, p. 5375, 2021.
[39] G. Allan, I. Eromenko, M. Gilmartin, I. Kockar, and P. McGregor, "The economics of distributed energy generation: A literature review," *Renewable and Sustainable Energy Reviews*, vol. 42, pp. 543-556, 2015.
[40] T. Matlokotsi, "Power quality enhancement in electricity networks using grid-connected solar and wind based DGs," 2017.
[41] J. Paska, P. Biczel, and M. Kłos, "Hybrid power systems–An effective way of utilising primary energy sources," *Renewable energy*, vol. 34, no. 11, pp. 2414-2421, 2009.

[42] S. Chowdhury and T. Matlokotsi, "Role of grid integration of distributed generation in power quality enhancement: A review," *2016 IEEE PES PowerAfrica*, pp. 164-168, 2016.
[43] C. Sankaran, *Power quality*. CRC press, 2017.
[44] S. Khalid and B. Dwivedi, "Power quality issues, problems, standards & their effects in industry with corrective means," *International Journal of Advances in Engineering & Technology*, vol. 1, no. 2, pp. 1-11, 2011.
[45] A. de Almeida, L. Moreira, and J. Delgado, "Power quality problems and new solutions," *RE&PQJ*, vol. 1, no. 1, 2003.
[46] H. Khan, "Power Quality Improvement of Distribution System with Dispersed Generation Using Novel Algorithm for Detection and Control of Islanding Process‖," *University of Engineering and Technology Taxila*, 2009.
[47] D. G. Photovoltaics and E. Storage, "IEEE Application Guide for IEEE Std 1547™, IEEE Standard for Interconnecting Distributed Resources with Electric Power Systems," 2009.
[48] S. Std, "Grid connection code for renewable power plants (RPPs) connected to the electricity transmission and distribution systems in South Africa," 2014.
[49] A. Polycarpou, "Power quality and voltage sag indices in electrical power systems," *Electrical Generation and Distribution Systems and Power Quality Disturbances*, pp. 139-160, 2011.
[50] S. Chattopadhyay, M. Mitra, S. Sengupta, S. Chattopadhyay, M. Mitra, and S. Sengupta, *Electric power quality*. Springer, 2011.
[51] Y. Zhao, "Electrical power systems quality," *University Of Buffalo*, 2016.
[52] S. Sewchurran and I. E. Davidson, "Guiding principles for grid code compliance of large utility scale renewable power plant intergration onto South Africa's transmission/distribution networks," in *2016 IEEE International Conference on Renewable Energy Research and Applications (ICRERA)*, 2016: IEEE, pp. 528-537.
[53] T. Adefarati and R. Bansal, "Reliability assessment of distribution system with the integration of renewable distributed generation," *Applied energy*, vol. 185, pp. 158-171, 2017.
[54] R. N. Allan, *Reliability evaluation of power systems*. Springer Science & Business Media, 2013.
[55] E. Pohl and K. McKenna, "Interconnection of Distributed Energy Resources in the Indian Context: IEEE 1547-2018 Adaptation for Locally-Appropriate Grid Code Development," National Renewable Energy Laboratory (NREL), Golden, CO (United States), 2024.
[56] Z. Zhang, L. F. Ochoa, and G. Valverde, "A novel voltage sensitivity approach for the decentralized control of DG plants," *IEEE Transactions on Power Systems*, vol. 33, no. 2, pp. 1566-1576, 2017.
[57] S. A. Almohaimeed and M. Abdel-Akher, "Power quality issues and mitigation for electric grids with wind power penetration," *Applied Sciences*, vol. 10, no. 24, p. 8852, 2020.
[58] M. M. Islam *et al.*, "Improving reliability and stability of the power systems: A comprehensive review on the role of energy storage systems to enhance flexibility," *IEEE Access*, 2024.
[59] M. Bilal, M. Rizwan, I. Alsaidan, and F. M. Almasoudi, "AI-based approach for optimal placement of EVCS and DG with reliability analysis," *IEEE Access*, vol. 9, pp. 154204-154224, 2021.

[60] A. S. Ghanim and A. N. B. Alsammak, "DQ Model of PMSG with The Most Proficient Dynamic Analysis in Standalone Grid," *Journal of Optimization and Decision Making,* vol. 2, no. 1, pp. 199-206, 2023.
[61] A. N. Huda and R. Živanović, "Large-scale integration of distributed generation into distribution networks: Study objectives, review of models and computational tools," *Renewable and Sustainable Energy Reviews,* vol. 76, pp. 974-988, 2017.
[62] S. Garip, Ş. Özdemir, and N. Altın, "Power System Reliability Assessment—A Review on Analysis and Evaluation Methods," *Journal of Energy Systems,* vol. 6, no. 3, pp. 401-419, 2022.
[63] R. Arya, "Estimation of distribution system reliability indices neglecting random interruption duration incorporating effect of distribution generation in standby mode," *International Journal of Electrical Power & Energy Systems,* vol. 63, pp. 270-275, 2014.
[64] P. C. Sekhar, R. Deshpande, and V. Sankar, "Evaluation and improvement of reliability indices of electrical power distribution system," in *2016 National Power Systems Conference (NPSC)*, 2016: IEEE, pp. 1-6.
[65] G. Lian, "The application of the Monte Carlo simulation method to terminal stations," University of Saskatchewan, 1990.
[66] R. Billinton, W. Li, R. Billinton, and W. Li, "Reliability Cost/Worth Assessment," *Reliability Assessment of Electric Power Systems Using Monte Carlo Methods*, pp. 255-297, 1994.
[67] C. Hwang, F. A. Tillman, and M. Lee, "System-Reliability Evaluation Techniques for Complex/Large SystemsнA Review," *IEEE Transactions on Reliability,* vol. 30, no. 5, pp. 416-423, 1981.
[68] U. Thongkrajay, N. Poolsawat, T. Ratniyomchai, and T. Kulworawanichpong, "Alternative Newton-Raphson power flow calculation in unbalanced three-phase power distribution systems," in *5th WSEAS International Conference on Applications of Electrical Engineering*, 2006: Citeseer, pp. 24-29.
[69] W.-T. Huang and W.-C. Yang, "Power flow analysis of a grid-connected high-voltage microgrid with various distributed resources," in *2011 Second International Conference on Mechanic Automation and Control Engineering*, 2011: IEEE, pp. 1471-1474.
[70] T. J. Ypma, "Historical development of the Newton–Raphson method," *SIAM review,* vol. 37, no. 4, pp. 531-551, 1995.
[71] R. Idema, D. Lahaye, K. Vuik, and L. Van der Sluis, "Fast Newton load flow," in *IEEE PES T&D 2010*, 2010: IEEE, pp. 1-7.
[72] V. K. Shukla and A. Bhadoria, "Understanding Load Flow Studies by Using PSAT," *International Journal for enhanced Research in Science Technology & Engineering,* vol. 2, no. 6, pp. 50-57, 2013.
[73] S. Iwamoto and Y. Tamura, "A load flow calculation method for ill-conditioned power systems," *IEEE transactions on power apparatus and systems*, no. 4, pp. 1736-1743, 1981.
[74] N. Nayak and A. Wadhwani, "Performance of Newton-Raphson Techniques in Load Flow Analysis using MATLAB," in *National Conference on Synergetic Trends in engineering and Technology*, 2014, pp. 177-180.
[75] M. M. Gilbert, *Renewable and efficient electric power systems*. John Wiley & Sons, 2004.
[76] M. R. Milligan, "Modelling utility-scale wind power plants. Part 2: Capacity credit," *Wind Energy: An International Journal for Progress and Applications in Wind Power Conversion Technology,* vol. 3, no. 4, pp. 167-206, 2000.

[77] Y. Xia, K. H. Ahmed, and B. W. Williams, "Wind turbine power coefficient analysis of a new maximum power point tracking technique," *IEEE transactions on industrial electronics*, vol. 60, no. 3, pp. 1122-1132, 2012.

[78] A. A. Teyabeen, F. R. Akkari, and A. E. Jwaid, "Power curve modelling for wind turbines," in *2017 UKSim-AMSS 19th International Conference on Computer Modelling & Simulation (UKSim)*, 2017: IEEE, pp. 179-184.

[79] C. Rat, C. Ichim-Burlacu, and C. Panoiu, "Modeling the synchronous permanent magnet generator with RLC load," in *Journal of Physics: Conference Series*, 2022, vol. 2212, no. 1: IOP Publishing, p. 012019.

[80] S. Tao, L. Zhao, Y. Liu, and K. Liao, "Impedance network model of D-PMSG based wind power generation system considering wind speed variation for sub-synchronous oscillation analysis," *IEEE Access*, vol. 8, pp. 114784-114794, 2020.

[81] M. H. Moradi and M. Abedini, "A combination of genetic algorithm and particle swarm optimization for optimal DG location and sizing in distribution systems," *International Journal of Electrical Power & Energy Systems*, vol. 34, no. 1, pp. 66-74, 2012.

[82] A. El-Zonkoly, "Optimal placement of multi-distributed generation units including different load models using particle swarm optimisation," *IET generation, transmission & distribution*, vol. 5, no. 7, pp. 760-771, 2011.

[83] F. H. Zhou and Z. Z. Liao, "A particle swarm optimization algorithm," *Applied Mechanics and Materials*, vol. 303, pp. 1369-1372, 2013.

[84] M. Shahidehpour; Y. Wang, "Appendix C: IEEE30 Bus System Data," in *Communication and Control in Electric Power Systems: Applications of Parallel and Distributed Processing* , IEEE, 2003, pp.493-495, doi: 10.1002/0471462926.app3

Appendices

Appendix A: The intergration of wind network, solar network and the distribution generator which forms the system on MATLAB/SIMULINK Model.

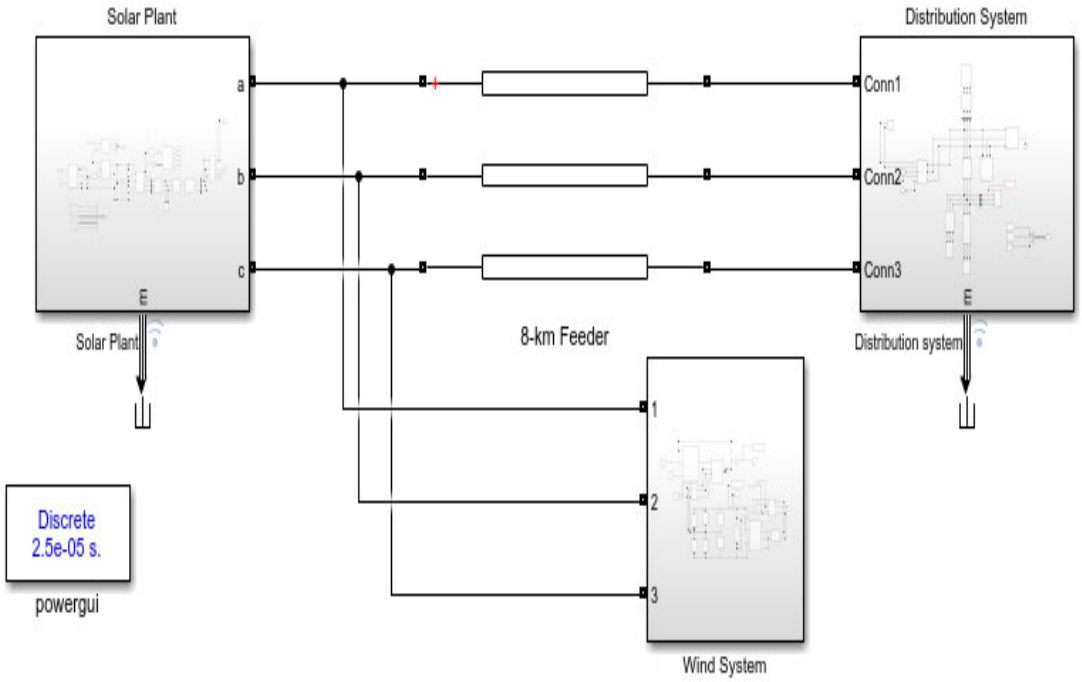

Appendix B: The interconnection of the distribution network model integrated on MATLAB/SIMULINK.